Funktionsanalyse des *Vezf1* Gens während der Embryonalentwicklung der Maus

Dissertation

zur Erlangung des akademischen Grades
Doctor rerum naturalium
(Dr. rer. nat.)

vorgelegt der

Mathematisch-Naturwissenschaftlich-Technischen Fakultät der Martin-Luther-Universität Halle-Wittenberg

von Herrn Frank Kuhnert
geboren am 01.04.1969 in Hovestadt

Gutachter:

1. Prof. Dr. Dr. Thomas Braun, Halle
2. Prof. Dr. Elmar Wahle, Halle
3. Prof. Dr. Heidi Stuhlmann, San Diego

Tag der Verteidigung: 9. Januar 2003

urn:nbn:de:gbv:3-000005384
[http://nbn-resolving.de/urn/resolver.pl?urn=nbn%3Ade%3Agbv%3A3-000005384]

Hiermit versichere ich, daß die vorliegende Dissertation eigenständig verfasst und keine anderen als die angegebenen Hilfsmittel verwendet wurden. Die Passagen der Arbeit, die anderen Schriften entnommen sind, wurden unter Angabe der Quelle kenntlich gemacht.

Frank Kuhnert

Palo Alto, 17 Juli 2002

TABLE OF CONTENT

Acknowledgements

I am indebted to many people for collaboration and support. First and foremost, I would like to express my gratitude to my thesis advisor, Dr. Heidi Stuhlmann, for professional guidance and her unflagging enthusiasm, support and encouragement. Furthermore, I would like to thank all members of the Stuhlmann laboratory, past and present, for their support and for creating a stimulating work environment.

I am especially grateful to Prof. Thomas Braun and Prof. Elmar Wahle for their willingness to serve as reviewer for this thesis. I would also like to thank Prof. Gordon Keller and all members of his laboratory for teaching me ES cell differentiation and making this enterprise such an enjoyable experience, and Dr. Humphrey Gardener for helping with the histological analysis of the embryos.

Finally, I would like to thank my family and friends for their encouragement and patience, which has been instrumental for the success of this endeavour.

1. INTRODUCTION

1.1 Embryonic vascular development

The cardiovascular system consists of the heart, the blood vasculature and the lymphatics. During vertebrate embryogenesis, it is the first functional organ system to develop, as embryonic growth and differentiation is critically dependent on the transport of oxygen, nutrients and waste products through the early vasculature. The blood circulatory system forms via distinct cellular processes in the embryo (Fig. 1). Initially, mesodermal cells differentiate into endothelial precursor cells, the angioblasts. Differentiation *in situ* of these angioblasts into endothelial cells (EC) and their subsequent coalescence into primitive blood vessels to form a primary vascular plexus is referred to as vasculogenesis. The term angiogenesis describes the subsequent growth, remodeling and maturation processes, which will ultimately lead to the formation of the mature blood vasculature. In a parallel process, lymphangiogenesis, the lymphatic system develops. The origin of the lymphatic vessels is still unresolved. Based on descriptive studies, the prevailing theory postulates that it originates through a sprouting mechanism from the venous endothelium.

In recent years, substantial progress has been made in identifying signaling systems and molecules that define the different stages of blood vascular development. An emerging theme in vascular development is the concept of vascular polarity and heterogeneity (arterial versus venous specification, left-right asymmetry, vascular bed-specific molecules). With respect to the development of the lymphatic system, the recent identification of highly specific markers for lymphatic endothelium has triggered the reinvestigation of the embryonic origin of the lymphatics. In the following part of the introduction the present understanding of the molecular mechanisms by which the vascular system forms in the vertebrate embryo will be summarized.

1.1.1 Endothelial lineage specification and vasculogenesis

The initial step of blood vessel formation is the differentiation of endothelial precursor cells, angioblasts, from mesoderm. During gastrulation, a process of highly integrated cell and tissue movements, mesoderm and endoderm are derived from the embryonic epiblast and thus the multilayered body plan of the vertebrate embryo is established. T-box transcription factors, fibroblast growth factor (FGF), transforming growth factor (TGF-

) and Wnt signaling pathways play crucial roles in the initial induction of the mesendoderm (for reviews, (Kimelman and Griffin, 2000), (Harland and Gerhardt, 1997). Embryonic mesoderm, formed in the primitive streak, migrates anteriorly and is divided along the mediolateral axis into distinct populations including axial, paraxial (somitic), intermediate and lateral plate mesoderm. The antagonistic activities of BMP-4 and noggin control mediolateral differentiation of the mesoderm, with BMP-4 promoting lateral plate formation (Tonegawa *et al.*, 1997). The lateral plate is further subdivided into somatopleure and splanchnopleure by a split in the mesoderm, which creates the coelum. It has been shown by means of quail/chick transplantation experiments that two subsets of mesoderm, somitic and splanchnopleuric, have the potential to give rise to endothelial progenitors (Pardanaud, 1999), (Coffin, 1988).

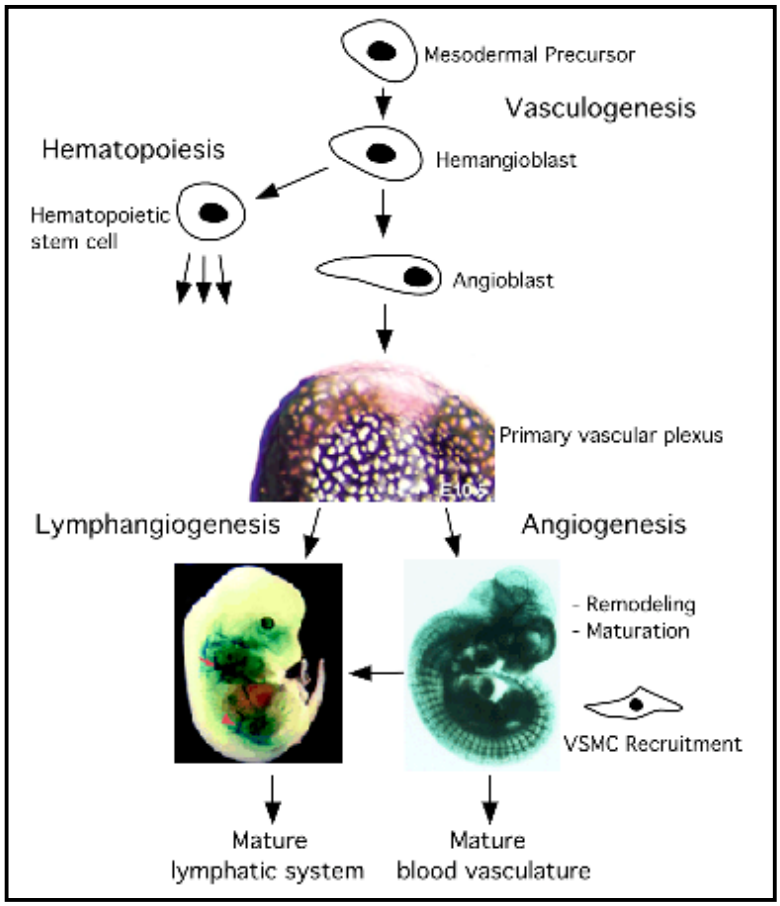

Figure 1. Vascular development during mouse embryogenesis.
A schematic representation of the processes involved in vascular development is depicted. Primary vascular plexus: Indian ink staining of an early yolk sac (Urness, 2000); angiogenesis: -galactosidase staining of an E11.5 Tie2-lacZ embryo (Schlaeger, 1997); lymphangiogenesis: -galactosidase staining of an E13.5 VEGFR-3 lacZ knock-in embryo (Dumont, 1998); VSMC, vascular smooth muscle cells.

The formation of blood islands in the extraembryonic yolk sac marks the onset of vasculogenesis (and hematopoiesis) in the developing mouse embryo (Risau, 1997). The mammalian yolk sac consists of an endodermal and a mesodermal layer and is continuous with the splanchnopleure of the embryo proper. Blood islands develop from aggregates of

mesodermal cells at approximately 7 days post-coitum (dpc) of mouse development. They consist of an inner layer of primitive hematopoietic cells and a peripheral population of angioblasts. These angioblasts differentiate into endothelial cells, form a lumen, migrate and interconnect to form a primary vascular plexus (Risau and Flamme, 1995).

The close developmental association of the hematopoietic and endothelial lineages within the blood islands has led to the hypothesis that they arise from a common precursor, the hemangioblast (Murray, 1932). Although the hemangioblast remains elusive *in vivo,* support for its existence comes from several observations. First, in the quail/chick transplantation system two distinct endothelial lineages were identified. One of them, derived from the splanchnopleural mesoderm, has the potential to give rise to endothelial and hematopoietic precursors, the other, of somitic origin, has purely angiogenic potential (Pardanaud *et al.*, 1996). Second, the fact that both lineages share expression of a number of different genes such as CD34 (Fina *et al.*, 1990), Tie2 (Yano *et al.*, 1997) and SCL/tal-1 (Kallianpur *et al.*, 1994). Moreover, targeted inactivation of Flk-1, encoding VEGF receptor 2 (VEGFR-2), (Shalaby *et al.*, 1995) and SCL/tal-1 (Shivdasani *et al.*, 1995) (Visvader *et al.*, 1998) in mice lead to deficiencies in both the endothelial and hematopoietic compartment. Similarly, the zebrafish *cloch*e mutation results in defects in blood cells and blood vessels. (Liao *et al.*, 1997). The most compelling evidence for the presence of the hemangioblast comes from studies utilizing the *in vitro* differentiation system of mouse embryonic stem (ES) cells. ES cells differentiate efficiently *in vitro* and give rise to three-dimensional structures, embryoid bodies (EBs), that contain precursors of multiple lineages (Keller, 1995). Several studies have shown that the development of the endothelial and hematopoietic lineages in EBs recapitulate the events that take place *in vivo* in the yolk sac blood islands (Vittet *et al.*, 1996; Wiles and Keller, 1991) (Wang *et al.*, 1992) (Doetschman *et al.*, 1985). Using this model system, Choi et al. isolated a transient population of cells which expresses markers common to both cell lineages (SCL/tal-1, CD34 and Flk-1) and, more importantly, can give rise to both hematopoietic and endothelial cells in clonogenic progenitor assays (Choi *et al.*, 1998), (Kennedy *et al.*, 1997). The same hemangiogenic progenitor was identified via cell sorting as a VEGFR-2^{+}, VE-cadherin^{+}, CD45^{-} cell population in a two-dimensional ES cell differentiation protocol (Nishikawa *et al.*, 1998a). More recently, this protocol has led to the isolation of a new type of blood vessel precursor, designated the common vascular precursor, from which both endothelial and smooth muscle cells develop (Yamashita *et al.*, 2000).

Intraembryonic vasculogenesis is initiated in the cranial region of 7.5 dpc embryos with the emergence of endocardial progenitor cells. Concomitantly, the aortic primordia first become discernable (Drake and Fleming, 2000). The larger vessels of the embryo and the primary vascular plexus in the lung, the pancreas, the spleen and the heart are formed via vasculogenesis in the embryo (Wilting and Christ, 1996). Angioblast differentiation in the embryo proper does not occur in close association with hematopoietic cells, except for the floor of the aorta (paraaortic clusters) (Jaffredo *et al.*, 1998), (Tavian *et al.*, 1999). Here, hematopoietic precursor cells appear to be budding from underlying epithelium, indicating that a diverse set of endothelial cells is generated during early embryogenesis (Nishikawa *et al.*, 2000; Nishikawa *et al.*, 1998b).

Despite great interest in understanding the signals and factors governing the initiation of endothelial cell differentiation in the developing embryo, little knowledge exists regarding the mechanisms of endothelial lineage specification. It seems conceivable that some of the molecules that specify mesoderm also control endothelial commitment (Zhong *et al.*, 2000). Moreover, the fact that angioblast and hematopoietic differentiation occurs in regions where mesoderm is in contact with endoderm suggests that an inducing signal is produced by the latter. In quail/chick transplantation experiments this hemangiopoietic induction potential of the endoderm could be mimicked by administration of vascular endothelial growth factor (VEGF), basic fibroblast growth factor (bFGF) and transforming growth factor (TGF) (Pardanaud, 1999). Similarly, ES cell *in vitro* differentiation studies suggest that bFGF signaling is critical for the proliferation of the hemangioblast (Faloon *et al.*, 2000), whereas the importance of TGF signaling for the development of the early vascular plexus is illustrated by the fact that embryos lacking TGF or its receptors, TRI and TRII, exhibit severe defects in yolk sac vasculogenesis (Dickson *et al.*, 1995; Larsson *et al.*, 2001; Oshima *et al.*, 1996).

1.1.1.1 The VEGF signaling system

Gene inactivation studies in mice demonstrated that VEGF signaling is critical for the process of vasculogenesis (for reviews (Carmeliet, 2000; Yancopoulos *et al.*, 2000)). VEGF (now referred to as VEGF-A) was the first growth factor described to be specific and critical for blood vessel formation. It was initially defined, characterized and purified

for its ability to induce vascular permeability and to promote endothelial cell proliferation. There are five characterized VEGF relatives in mammals (VEGF-A through VEGF-D, as well as placental growth factor, PlGF), and they display differential interaction with three related receptor tyrosine kinases (VEGFR-1/VEGFR-1, VEGFR-2/Flk-1, and VEGFR-3/Flt-4) and a number of ancillary receptor components, such as the neuropilins (Soker *et al.*, 1998). VEGF-A signals through binding to VEGFR-1 and VEGFR-2, which are restricted largely to vascular endothelium in their expression, accounting for the specificity of VEGF-A signaling. In embryos lacking either VEGF or VEGFR-2 blood islands, endothelial cells, and major vessels fail to develop in appreciable numbers, showing their critical importance for these early stages of vasculogenesis (Carmeliet *et al.*, 1996a; Ferrara *et al.*, 1996; Shalaby *et al.*, 1995). Remarkably, even loss of a single VEGF allele results in embryonic lethality, demonstrating a strict dose-dependence of VEGF during development. In contrast, inactivation of VEGFR-1 leads to the formation of abnormally organized vessels due to the excess formation of endothelial cells (Fong *et al.*, 1995; Fong *et al.*, 1999). Thus, while VEGFR-1 suppresses, VEGFR-2 seems to promote endothelial differentiation. However, subsequent *in vitro* studies demonstrate that endothelial cells develop normally within VEGFR-2 mutant EBs, indicating that VEGFR-2 is not a determinant for endothelial cell lineage commitment, but rather plays a role in regulating the migration of early mesodermally derived precursor into a microenvironment that is permissive for vasculogenesis and hematopoiesis (Schuh *et al.*, 1999; Shalaby *et al.*, 1997).

1.1.3 Angiogenic remodeling and maturation

Historically, the term angiogenesis described the growth of endothelial sprouts from preexisting vessels. More recently, it has been used to generally denote the growth, remodeling and maturation processes that transform the primitive vascular plexus into a complex network. Angiogenesis leads to the vascularization of intersomitic spaces and initially avascular organs, such as kidney, brain and limb buds. This involves the enlargement of vessels by sprouting or intussusception (non-sprouting angiogenesis) and the pruning of the developing vascular network to form the interconnecting branching patterns characteristic of the mature vasculature (Risau, 1997). Non-sprouting angiogenesis is the process of splitting pre-existing vessels by transcapillary pillars of periendothelial cells or extracellular matrix into individual capillaries. Non-sprouting

angiogenesis predominates in the lung, for example, which contains intrinsic endothelial precursors and is initially vascularized by vasculogenesis (Risau, 1997). Sprouting angiogenesis occurs both in the yolk sac and in the embryo (most frequently during later organogenesis). Sprouting angiogenesis is prevalent in the vascularization of the brain and retina, which do not contain endothelial progenitor cells, and is also responsible for most new vessel formation in the adult. The mechanisms regulating the latter process are of particular interest as targets for the therapeutic control of angiogenesis in pathological settings such as tumor development and myocardial or limb ischemias (Carmeliet and Jain, 2000).

Concomitant to the angiogenic remodeling processes, the nascent vasculature matures through the investment of vessels with mural cells. Depending on morphology and density, the latter cells are referred to as either pericytes (PC) or vascular smooth muscle cells (VSMC). Pericytes are solitary VSMC-like cells associated with the finest diameter blood vessels, i.e. arterioles, capillaries and venules (Sims, 1986). VSMC, in contrast, form concentric layers around larger blood vessels. The recruitment of pericytes and vascular smooth muscle cells (VSMC) leads to the stabilization of nascent vessels by inhibiting endothelial proliferation and migration, and by stimulating the production of extracellular matrix (Darland and D'Amore, 1999). Mural cells thereby provide hemostatic control and protect new endothelium-lined vessels against rupture and regression.

VEGF-A, angiopoietin, transforming growth factor (TGF), platelet-derived growth factor (PDGF) and, more recently also ephrin and Notch signaling have all been implicated in angiogenic remodeling and vascular maturation processes (Krebs *et al.*, 2000), (Yancopoulos *et al.*, 2000) (Carmeliet, 2000; Liu *et al.*, 2000). VEGF-A, interacting with VEGFR-1 and 2, and promoting proliferation and survival of endothelial cells, is a key regulator of embryonic and adult angiogenesis (see above). VEGFR-3, in addition to its function in lymphangiogenic development (see below), appears to be critical for the angiogenic remodeling process, as VEGF-R3 null embryos display defective blood vessel development before the emergence of lymphatic vessels (Dumont *et al.*, 1998).

1.1.3.1 The Angiopoietin signaling system

The angiopoietins, a second family of growth factors specific for the vascular endothelium, have been shown to have important functions during angiogenesis. Similar to VEGF-A, the specificity of the angiopoietins for the vascular endothelium stems form the restricted distribution of their tyrosine kinase receptor Tie2. Transgenic overexpression of angiopoietin1 (Ang1) leads to striking hypervascularization by promoting vascular remodeling events and inhibiting normal vascular pruning (Suri *et al.*, 1998). In mouse embryos lacking either Ang1 or Tie2, the early stages of VEGF dependent vascular development appear to occur rather normally. However, remodeling and stabilization of the primitive vascular plexus is severely perturbed, leading to embryonic lethality (Sato *et al.*, 1995; Suri *et al.*, 1996). These defects are thought to be a result of disruptions in Ang1-mediated interactions between endothelial cells and supporting smooth muscle cells and pericytes. Interestingly, angiopoietin 2 (Ang2) acts as a natural antagonist for the Ang1/Tie2 interaction. Transgenic overexpression results in a phenotype reminiscent of that seen in embryos lacking either Ang1 or Tie2 (Maisonpierre *et al.*, 1997). Ang2 is highly expressed at sites of vascular remodeling and is hypothesized to destabilize mature vessels, thus rendering them more amenable to vascular remodeling (Yancopoulos *et al.*, 2000).

Tie1 is an orphan receptor tyrosine kinase that is primarily expressed in vascular endothelial cells and is closely related to Tie2 (Sato *et al.*, 1993). Based on the knockout phenotype Tie1 is superficially defined as a regulator of angiogenesis (Puri *et al.*, 1995). Double-knockouts for Tie1 and Ang1 display specific defects in the formation of the right-hand side of the venous system (Loughna and Sato, 2001). This finding provides the first evidence for the presence of distinct genetic program for the left-right asymmetrical development of the vascular system.

1.1.3.2 The Ephrin signaling system

As a third growth factor system that acts via endothelial cell-specific receptor tyrosine kinases, the ephrins have been implicated in vascular development. The Eph receptor tyrosine kinases constitute the largest known family of growth factor receptors, and use the equally numerous membrane-bound ephrins as their ligands (Gale and Yancopoulos, 1999). Although initially characterized in the nervous system, recent knockout studies have suggested key roles for the ephrins and the Eph receptors in vascular development.

Targeted inactivation of *ephrinB2*, *EphB4,* or *EphB2* and *B3* lead to remodeling and endothelial cell/mural cell interaction defects similar to those seen in Ang1 and Tie2 mutant embryos (Adams *et al.*, 1999; Gerety *et al.*, 1999; Wang *et al.*, 1998). Moreover, expression analysis in the early embryo revealed that ephrinB2 marks arterial endothelial cells, whereas its receptor, EphB4, specifically and reciprocally is only expressed in venous endothelium (Gerety *et al.*, 1999; Wang *et al.*, 1998), indicating that endothelial tubes are specified as arteries and veins at the earliest stages of vascular development, even before the onset of circulation. Interestingly, embryos lacking the activin receptor-like-kinase-1 gene (Acvrl1), which encodes a type I receptor for the TGF superfamily of growth factors, show downregulation of ephrinB2 in arterial endothelium and arteriovenous malformations in form of fusion of the major arteries and veins (Urness *et al.*, 2000), suggesting that ephrin signaling acts downstream of Acvrl1 mediated TGF signaling.

1.1.3.3 The Notch Signaling system

More recently, Notch signaling has been shown to be involved in vascular morphogenesis. The Notch signaling pathway is an evolutionary conserved intercellular signaling mechanism that controls cell fate specification in a variety of tissues, for example during primary neurogenesis or T-cell development (Chitnis *et al.*, 1995; Robey, 1999). Notch1, Notch4 and the Notch ligand Delta-like 4 (Dll4) are all expressed in vascular endothelial cells during early embryogenesis in mice (Krebs *et al.*, 2000; Shirayoshi *et al.*, 1997; Uyttendaele *et al.*, 1996). Notch1 and Notch1/Notch4 double mutant embryos display severe defects in angiogenic vascular remodeling (Krebs *et al.*, 2000; Swiatek *et al.*, 1994). In addition, the expression of an activated Notch4 in embryonic endothelium leads to disorganized vascular development and a reduction of the number of small vessels, resulting in embryonic lethality at E10.5 (Uyttendaele *et al.*, 2001). Moreover, inactivation studies of genes encoding Notch ligands have shown that both *Jag1* and *Dll1* homozygous mutant embryos die from vascular defects and hemorrhaging at around E10.5 (Hrabe de Angelis *et al.*, 1997; Xue *et al.*, 1999). In the zebrafish model, the Notch pathway has been implicated in arterial versus venous specification. Notch signaling has been demonstrated to regulate the expression of *gridlock* (*grl*) (Zhong *et al.*, 2001). The *gridlock* gene encodes a transcriptional repressor that belongs to the family of hairy-related transcription factors and is required for the formation of the embryonic aorta

(Nakagawa *et al.*, 1999; Zhong *et al.*, 2000). Moreover, *grl* represses the venous marker *EphB4*, while it enhances expression of the reciprocal arterial gene*ephrinB2*, thereby adjudicating an arterial versus venous cell fate decision (Zhong *et al.*, 2001).

1.1.3.4 TGF and PDGF signaling

The TGF and PDGF signaling pathways have been demonstrated to regulate the interaction between endothelial and mesenchymal cells. (Dickson *et al.*, 1995; Lindahl *et al.*, 1997). *In vitro* studies have shown that endothelial cells recruit mural cells via the secretion of PDGF-B (Hirschi *et al.*, 1999). Consistent with this model, mice null for PDGF-B or the PDGFR- display VSMC hypoplasia of larger vessels and pericyte deficiencies in capillaries due to reduced VSMC and pericyte proliferation and migration (Hellstrom *et al.*, 1999; Lindahl *et al.*, 1997). Mural cells, in turn, have been shown to inhibit proliferation and migration of endothelial cells *in vitro* (Orlidge and D'Amore, 1987). Furthermore, coculture studies reveal that endothelial-mural cell contacts lead to the activation of TGF (Hirschi *et al.*, 1999). In the context of microvasculature, TGF appears to function at multiple steps leading to vessel stabilization, including inhibition of endothelial cell proliferation and migration, as well as induction of pericyte and smooth muscle cell differentiation (Hirschi *et al.*, 1999). Consistently, embryos deficient for the TGF binding protein, endoglin, and its downstream signaling molecule, SMAD5, display defects in VSMC differentiation and lack VSMC around major vessels (Li *et al.*, 1999; Yang *et al.*, 1999).

1.1.4 Development of the lymphatic system

The lymphatic system is a vascular network of thin-walled capillaries and larger vessels lined by a continuous layer of endothelial cells that transport tissue fluid, macromolecules and cells from the tissue spaces of most organs back into the venous circulation. Several theories regarding the origin of the lymphatic system exist. The most widely accepted view is that isolated primitive lymph sacs originate through endothelial sprouting from veins, a model first described by Florence Sabin almost a hundred years ago (Sabin, 1909). Based on ink injection experiments in chick embryos, she postulates that the two jugular lymph sacs develop from the anterior cardinal veins by endothelial budding. Later in development, the iliac and retroperitoneal sacs and the cisterna chyli originate from the mesonephric vein and the veins in the dorsomedial edge of the Wolffian bodies (Gray,

1985). The peripheral lymphatic vessels subsequently form by centrifugal sprouting from these primary lymph sacs. According to Huntington and Kampmeier, mesenchymal lymphangioblast-like cells are the source of lymphatic vessels, meaning that lymphatics develop independently of veins (Huntington, 1908; Kampmeier, 1912). Van der Jagt, on the other hand, finds both mechanisms, venous sprouting and lymphangioblast differentiation, to be operative during lymphatic development (van der Jagt, 1932).
The latter two theories are supported by the recent identification of lymphangioblastic cells in avian embryos by quail/chick grafting experiments (Schneider *et al.*, 1999; Wilting *et al.*, 2001).

The expression of VEGFR-3 (Flt-4) in developing mouse embryos coincides with Sabin's model of lymphatic development. VEGFR-3 is expressed in venous endothelium during early embryonic development but becomes restricted to the lymphatic vessels after their formation (Kaipainen *et al.*, 1995). Recent studies have demonstrated that signaling via VEGFR-3 is sufficient to induce lymphangiogenesis in transgenic mice, suggesting an essential role for the VEGFR-3 signaling pathway in the development of the lymphatic system (Jeltsch *et al.*, 1997; Veikkola *et al.*, 2001). Moreover, expression of a dominant-negative VEGFR-3 in the skin of transgenic mice blocks lymphangiogenesis and induces the regression of already formed lymphatic vessels, demonstrating that VEGFR-3 signaling is required for formation and maintenance of the lymphatic vasculature (Makinen *et al.*, 2001).
Further support for Sabin's model is derived from the analysis of expression pattern and function of the homeobox gene *Prox1*. *Prox1*, although broadly expressed during embryonic development, has been identified as a specific marker of a subpopulation of endothelilal cells that give rise to the lymphatic system (Oliver *et al.*, 1993; Wigle and Oliver, 1999). As early as E10.5, Prox1-positive cells were detected in the wall of the anterior cardinal vein. As development proceeded, these Prox1-positive cells appeared to be budding from the anterior cardinal vein and migrating dorsoanteriorly to form the lymphatic jugular sacs. Interestingly, the inactivation of *Prox1* in mice leads to a complete arrest of lymphatic system development (Wigle and Oliver, 1999). Vasculogenesis and angiogenesis, in contrast, were unaffected, demonstrating that *Prox1* activity is specifically required for normal development of the lymphatic system.

1.2 Cloning and Characterization of *Vezf1*

Vezf1 was identified in a genetic screen for genes involved in the formation of the circulatory system by Dr. Jing-Wei Xiong in Dr. Heidi Stuhlmann's laboratory (Xiong *et al.*, 1998; Xiong *et al.*, 1999). In this screen, retroviral entrapment vectors were used to infect ES cells, and candidate genes were identified by virtue of the expression pattern of an alkaline phosphatase (AP) reporter gene upon *in vitro* differentiation of infected ES cell clones into embryoid bodies (EBs). One insertion, 1-13, displayed regulated expression of the AP reporter gene in EBs and embryos, which co-localized with the expression of the endothelial cell-specific marker *VEGFR-2* (Leahy *et al.*, 1999). In order to isolate the corresponding endogenous gene, flanking host genomic DNA 3' of the retroviral insertion was cloned by *supF* complementation (Xiong *et al.*, 1998). The resulting 0.9 kb genomic fragment was used to screen an E7.5 mouse embryonic cDNA library. Two overlapping cDNA clones, 10-1 and 10-2, were isolated (Fig. 4). One of them (10-1) shared significant homology to the 3' end of the previously identified human gene ZNF161 (DB1) (Koyano-Nakagawa *et al.*, 1994). The 5' portion of the mouse cDNA was obtained by RT-PCR using primers corresponding to 5' UTR sequences of ZNF161 and the 5' end of 10-1. A 3681 bp full-length coding mouse cDNA was obtained by these two complementary approaches. An in-frame ATG initiation codon was found at position 40 within a Kozak consensus sequence (Kozak, 1987) and a termination codon at position 1593. The 1554 bp coding sequence of the cDNA is flanked at the 5' end by 39 bp of GC-rich sequence and at the 3' end by 2080 bp of untranslated sequences that contained a consensus poly(A) signal 11bp upstream of the poly(A) strech. Based on its specific expression pattern in the embryo and its structural hallmarks, the identified mouse gene was named *Vezf1* for Vascular endothelial zinc finger 1 (Xiong *et al.*, 1999). Alignment of the genomic sequences at the entrapment vector insertion with the *Vezf1* cDNA sequence indicated that the retroviral insertion in ES cell clone 1-13 had occurred in the 3' untranslated region of the gene. Consistently, no mutant phenotype was detected in transgenic embryos or adult mice derived from the 1-13 ES cell clone.

Vezf1 encodes a 518 amino acid protein with a predicted molecular mass of 56 kDa, which contains six putative zinc finger motifs of the C2H2 (Krüppel-like) type, a glutamine stretch, and a proline-rich region at its C-terminus (Fig. 2). VEZF1 shows 98% amino acid sequence identity to the human transcription factor ZNF161, which was cloned as a binding activity to the human interleukin-3 (IL-3) promoter (Koyano-Nakagawa *et al.*,

1994). Database analysis and low stringency Southern blot analysis identified *Pur-1* (Kennedy and Rutter, 1992) as the only related mouse gene with significant homology. PUR-1 shares 76% amino acid sequence over the zinc fingers region with VEZF1 (Fig. 2), but no significant homology outside the zinc finger domains, and shows widespread expression during embryonic development (Xiong *et al.*, 1999).

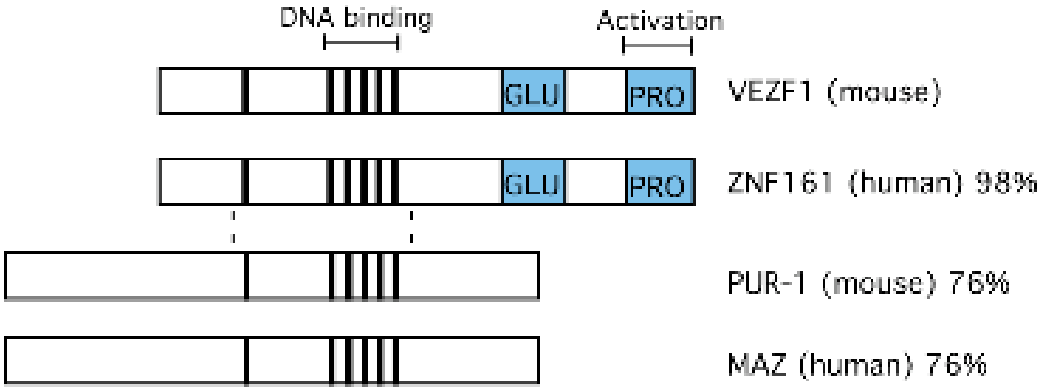

Figure 2. VEZF1 and related proteins. GLU, glutamine stretch; PRO, proline-rich region. The 76% amino acid identity between VEZF1 and PUR-1 is confined to the zinc finger region.

Recent studies in Dr. Stuhlmann's laboratory have shown that VEZF1 displays characteristics of a bona fide transcription factor (Sun *et al.*, 2001). In GAL4-fusion transactivation studies, the C-terminal proline-rich region of VEZF1 was identified as a strong transcriptional activation domain. Furthermore, VEZF1 was shown to be localized to the nuclear and perinuclear compartments in endothelial cells by immunostaining with polyclonal anti-VEZF1 antibodies. In electromobility shift assays, binding of VEZF1 to a CT/GC core region in the human IL-3 as well as the murine *VEGFR-2* and *VEGFR-1* promoters was demonstrated. In an independent study, the ability of human ZNF161 to bind and transactivate the human *endothelin-1* promoter *in vitro* was shown recently (Aitsebaomo *et al.*, 2001).

A DNA interspecies backcross panel from The Jackson Laboratory was used to map the chromosomal localization of the *Vezf1* gene (Xiong *et al.*, 1999). A single-strand confirmation polymorphism (SSCP) between the two parental strains was detected by PCR using a primer pair spanning intronic sequences in the flanking genomic DNA. Analysis of the backcross panel data placed *Vezf1* onto the end of mouse Chromosome 2, a region that has extensive homology to human Chromosome 9q.

1.2.1 Expression of *Vezf1* during murine embryonic development

The expression pattern of *Vezf1* during mouse embryonic development, as reported by (Xiong *et al.*, 1999), was analyzed by RNA *in situ* hybridization. The cDNA clones 10-1 and 10-2 were used as probes for this analysis and both fragments yielded identical results. Thus, expression of *Vezf1* during embryogenesis was found to be restricted to endothelial cells and their precursors. This is consistent with *Vezf1* specifically marking the earliest progenitors of the endothelial and hematopoietic lineage, the hemangioblasts, as well as endothelial cells arising during both vasculogenesis and angiogenesis. The onset of *Vezf1* expression was detected at the primitive streak stage (E7.25) in the extraembryonic mesoderm of the visceral yolk sac. During neural plate formation (E7.5), *Vezf1* expression domains expanded throughout the yolk sac and extended into the embryo proper. Expression was strongest in clusters of visceral mesoderm cells of the yolk sac, which constitute the precursors of the yolk sac blood islands. At E8.5 (early vasculogenesis), *Vezf1* expression was detected in intra- and extraembryonic regions of angioblast differentiation, i.e. in capillary structures of the cephalic mesenchyme and the first branchial arch, the inner lining of the dorsal aorta, the endocardium and the yolk sac blood islands. Between E8.5 and E9.5 *Vezf1* expression in the blood islands became restricted to the vascular endothelial cells lining the perimeter of the blood islands. In embryos between day 10.5 and 13.5 of gestation (during angiogenesis), *Vezf1* was detected in virtually all vascular structures arising by both vasculogenesis and angiogenesis and appeared to be restricted to a single cell layer of presumptive endothelium. At later stages of embryogenesis, continued but overall reduced expression of *Vezf1* was observed throughout the vascular system. Highest expression in late stage embryos was found in the capillaries and lower expression in the large vessels.

In adult mice, *Vezf1* was found to be a marker for quiescent endothelial cells. Thus, it is expressed predominantly in the endothelium of the capillaries, and less in mature blood vessels, of adult tissues, including heart, liver, spleen, kidney and brain (Leahy *et al.*, 2001). *Vezf1* expression is very low in quiescent endothelium, but is upregulated during arterial injury and tumor angiogenesis. As a second site of expression, *Vezf1* is also detected in megakaryocytes in bone marrow (Leahy *et al.*, 2001).

Northern blot analysis of staged embryos detected a major *Vezf1*-specific 4.2 kb transcript and a lower abundance 1.7 kb transcript in all sources of RNA by using a 5' *Vezf1* probe (nucleotides 3-776 of the published cDNA sequence, GeneBank accession# AF104410)

(Xiong *et al.*, 1999). In adult tissues an additional 4.5 kb mRNA species was observed with the relative abundance of the various transcripts differing for every organ.

1.3 Significance and Specific Aims

VEZF1 displays the hallmarks of a classical C2H2 zinc finger transcription factor. The C2H2 zinc finger proteins form the largest family of transcriptional regulators. It is estimated that there are 900 members encoded in the mammalian genome (Tupler *et al.*, 2001). Zinc fingers are known as DNA binding motifs. The sequential arrays of zinc fingers arranged in different combinations can recognize a huge range of DNA, but also RNA and DNA-RNA hybrid sequences (for review, see Mackay and Crossley, 1998). Furthermore, more recent reports suggest that zinc fingers can also mediate protein-protein interactions (Morgan *et al.*, 1997; Sun *et al.*, 1996).

Several zinc finger transcription factors have been shown to be important regulators of hematopoietic and blood vessel development. The hematopoietic-specific zinc finger protein Ikaros is a central regulator of lymphocyte differentiation (Georgopoulos *et al.*, 1997). The inactivation of erythroid Krüppel-like factor (EKLF) leads to fetal anemia during embryonic liver erythropoiesis due to beta-globin deficiency (Perkins *et al.*, 1995). Lung Krüppel-like factor (LKLF) is required for the stabilization of embryonic blood vessels and for T cell activation (Kuo *et al.*, 1997).

Several other known transcription factors, including Ets and bHLH-PAS family members, SCL/tal-1, LKLF, MEF2C, and LMO2 have been implicated in the development of the vasculature through gene targeting studies (Table 1). In addition, promoter analysis of several endothelial-specific genes, including *VEGFR-2*, *Tie2*, *Pecam-1*, and *endothelin-1* revealed binding sites for known transcription factors, such as HIF-1□, HIF-2□, SCL/tal-1, GATA, and Ets-like factors (Table 1). Strikingly, none of these factors show endothelial-restricted expression. Thus, *Vezf1* would be the first transcription factor whose expression during embryonic development is restricted to endothelial cells and their precursors (Xiong *et al.*, 1999).

However, towards the end of the practical part of this thesis I accumulated evidence (described in detail in Chapter 1 of the Results section) that suggested that the published *Vezf1* cDNA represents a chimeric cDNA clone, containing two open reading frames corresponding to two independent genes, *Vezf1* and *Zneu1*. Subsequent experimental

analysis confirmed this notion and furthermore suggested that the reported endothelial cell-restricted expression pattern corresponds to the *Zneu1* gene. In contrast, *Vezf1* appeared to be expressed in a widespread fashion during mouse embryonic development (see Results section, Chapter 1).

FACTOR	EXPRESSION DURING EMBRYO-GENESIS	FUNCTION	VASCULAR KO PHENOTYPE	REFERENCES
SCL/tal-1	HPC, hemangioblasts, brain	bHLH transcription factor, required f.hematopoietic lineage differentiation, regulates VEGFR-2 expression	defective angiogenic remodeling in yolk sac	(Visvader *et al.*, 1998) (Robertson *et al.*, 2000) (Kappel *et al.*, 2000)
HESR1 (gridlock)	EC, presomitic mesoderm, brain and limbs	basic HLH TF, capillary formation in vitro	n.d.	(Henderson *et al.*, 2001)
dHAND	mesenchyme and derivatives	bHLH transcription factor	defects in SMC differentiation	(Yamagishi *et al.*, 2000)
Tfeb	labyrinthine trophoblasts	basic HLH TF	defects in placental vascularization	(Steingrimsson *et al.*, 1998)
bHLH-EC2	Paraxial mesoderm, HPC, EC, myoblasts	bHLH TF	n.d.	(Quertermous *et al.*, 1994)
HIF-1	Widespread (neuroepithelium , heart, primitive gut, thymus, kidney; hypoxia responsive)	bHLH-PAS TF, heterodimerizes with ARNT, hypoxia induced activation of VEGF, erythropoietin, glycolytic enzymes	disorganized yolk sac and cephalic vascularization	(Iyer *et al.*, 1998; Jain *et al.*, 1998; Ryan *et al.*, 1998)
HIF-2 (EPAS-1)	EC, urogenital ridge, kidney	bHLH-PAS, heterodimerizes with ARNT	defective remodeling of primary vascular plexus	(Jain *et al.*, 1998; Peng *et al.*, 2000; Tian *et al.*, 1998)
ARNT	neuroepithelium , heart, primitive gut, lung	bHLH-PAS, heterodimerizes with PAS proteins	defective angiogenesis in yolk sac and branchial arches, abnormal placentation	(Maltepe *et al.*, 1997) (Abbott and Buckalew, 2000; Jain *et al.*, 1998)
MEF2C	EC, SMC	MADS-box TF	defects in remodeling of the primary vascular plexus, no SMC differentiation	(Lin *et al.*, 1998)
SMAD5	mesenchyme, somites	MADS-box TF	defects in angiogenesis and SMC differentiation	(Chang *et al.*, 1999; Yang *et al.*, 1999)
Ets-1	mesoderm-derived tissues including EC and HPC,	Ets-protein, induces expression of MMPs and migration in EC, regulates expression of VEGFR-2, VEGFR-1,	n.d.	(Kola *et al.*, 1993) (Oda *et al.*, 1999) (Kappel *et al.*, 2000; Wakiya *et al.*, 1996)
Fli1	EC, HC, meso-dermal tissues	Ets-like TF, regulator of megakaryo-cytopoiesis	hemorrhaging, impaired hematopoiesis	(Spyropoulos *et al.*, 2000; Vlaeminck-Guillem *et al.*, 2000)
ELF-1	heart, liver, brain, T cells, EC	Ets-protein, transactivator of Tie1 and Tie2 genes	n.d.	(Dube *et al.*, 2001)
NERF2	EC-specific of NERF gene	Ets-protein, transactivator of Tie1 and Tie2 genes	n.d.	(Dube *et al.*, 1999)
TEL	HC, EC	Ets-protein	defects in yolk sac angiogenesis	(Wang *et al.*, 1997)
LKLF	EC, primitive vertebrae, lung buds,	Krueppel-like zinc finger TF	hemorrhage, defects in the recruitment of VSMC and pericytes	(Kuo *et al.*, 1997)
GATA-2	EC, HPC, CNS endocardium,	Zinc finger TF, regulates expression of VEGFR-2, PECAM and endothelin-1	hematopoietic defects	(Kawana *et al.*, 1995) (Gumina *et al.*, 1997) (Kappel *et al.*, 2000; Tsai *et al.*, 1994)
Hhex	angioblasts, HPC, endoderm, thyroid primordium	homeobox TF	n.d.	(Thomas *et al.*, 1998)

HOXB3	neuroectoderm, branchial arches and derivatives	homeobox TF, capillary formation in vitro	n.d.	(Myers *et al*., 2000)
Prox-1	lymphatic EC, CNS	homeobox TF,	arrest of lymphatic development	(Wigle and Oliver, 1999)
AML-1	EC, HPC	CBF subunit, required for definitive hematopoiesis	angiogenic defects, rescued by angiopoietin-1 administration	(Takakura *et al*., 2000)
Fra1	widespread	bZip	endothelial differentiation, VEGFR-2 regulation	(Schreiber *et al*., 2000)
COUP-TFII	mesenchyme	nuclear receptor TF, regulates angio-poietin-1 expression	defects in yolk sac angiogenesis,	(Pereira *et al*., 1999)
LMO2	HPC, EC	LIM-domain TF, bridging molecule for multimeric transcription complexes (including SCL, GATA-1)	defects in angiogenic remodeling	(Yamada *et al*., 1998) (Yamada *et al*., 2000)
Foxf1	splanchnopleuric mesoderm, yolk sac endothelium, sclerotome, mesenchyme of primitive gut	forkhead TF	no yolk sac vasculogenesis	(Mahlapuu *et al*., 2001)

Table 1. Transcription factors in vascular development

The goal of this thesis was to analyze the structure, expression and function of *Vezf1*. The focus of this analysis will be placed on the elucidation of the vascular component of *Vezf1* function. Towards this goal, I have generated loss- and gain-of-function mutations of *Vezf1* in ES cells and embryos and analyzed the effects of *Vezf1* inactivation and overexpression *in vitro* and *in vivo*. In addition, I have initiated studies to characterize the *Vezf1* promoter and the embryonic expression pattern of *Vezf1*.

2. EXPERIMENTAL PROCEDURES

2.1 General molecular biology techniques

All molecular biology procedures were performed according to standard protocols (Sambrook *et al.*, 1989) or the manufacturer's instructions, respectively. Composition of solutions and protocols used during the presented project are provided only if they differ from the provided manufacturer's instructions. Clones and PCR products were sequenced on a Perkin-Elmer ABI 310 automated sequencer in the Core Facility of the Scripps Research Institute.

2.2 Computer programs

The following computer programs were used in this study:

MacVector 5.2	Sequence analysis, Restriction mapping
MatInspector professional2.1	Identification of consensus transcription factor binding sites
BLAST	Sequence analysis, Database search
DNA Star	Sequence analysis, alignment
Prosite	Protein analysis
Scion Image	Image analysis
Openlab	Acquisition of digital images
Endnote 4	Bibliography
Canvas 7	Graphics
Photoshop 5.5	Image Processing
Microsoft Excel 2000	Data Processing
Microsoft Word 2000	Word Processing

2.3 Structural and expression analysis of *Vezf1*

2.3.1 RNA in situ hybridization

Procedures for embedding, sectioning and m RNA *in situ* hybridization are essentially as described previously (Leahy *et al.*, 2000). Briefly, staged mouse embryos fixed in 4%

paraformaldehyde were embedded in paraffin at 60°C overnight following a series of dehydrating washes, from 50% to 100% ethanol, and a final 30 minutes wash in xylene. Material sectioned at 6 μm was deparaffinized in xylene, rehydrated, digested with proteinase K for 7.5 minutes, treated with acetic anhydride in 0.01M triethanolamine and dehydrated prior to a 16 hour hybridization with ^{35}S-radiolabeled antisense mRNA probes (final probe concentration 35 cpm/ml) in 50% formamide hybridization buffer. [α-^{35}S]UTP methionine (1250 Ci/mmol) was obtained from NEN/Dupont; Cambridge, USA. Posthybridization washes of increasing stringency (50% formamide, 2xSSC, 0.1xSSC) and 1 hour RNaseA treatment at 37°C were included to reduce background. Slides were dehydrated through a series of ethano/NH_4OH washes and dried for 1 hour. Slides were dipped in Kodak NBT-2 emulsion, dried over night and exposed for five days to two weeks at 4°C. Material was counter-stained toludine blue, dehydrated and coverslipped. Photographs were taken using a Leica Leitz DMRB Microscope. The following probes were used: *Vezf1*, probe A (nt 3-776) and probe B (nt 1397-2331); cDNA clone 10-1 (nt 1397-2899 of the published *Vezf1* cDNA sequence); *Flk-1* (Yamaguchi *et al.*, 1993) and *Flt-1* (Fong *et al.*, 1995), both obtained from J. Rossant (Mount Sinai Hospital, Toronto); *Tie2* (Sato *et al.*, 1993), obtained from T. Sato (Southwestern Medical Center); *EphrinB2* and *Eph4* (Wang *et al.*, 1998), both obtained D. Anderson (Caltech, Pasadena).

2.3.2 Northern blot analysis

Total RNA from ES cells and EBs was isolated using the Qiagen RNeasy Mini Kit. Total RNA isolation from mouse embryos was performed using Trizol (Life Technologies). 10 μg of RNA was seperated on a 0.4M formaldehyd/1% agarose gel and transferred to nitrocellulose membranes (Optitran, Schleicher and Schuell). Filters were hybridized to 1x10^7 CPM of a raqndom hexamer-primed [α-^{32}P]-dCTP radiolabeled prob overnight in 50 % formamide, 5xSSC, 1xDenhardts, 0.1% SDS, 50 μg/ml denaturated salmon sperm DNA at 42°C. Blots were washed at increasing stringency, with the final two washes at 65°C in 0.2xSSC, 0.1% SDS for 30 minutes each and exposed to Kodak Biomax film at -80°C overnight. The following probes were used: *Vezf1*, probe A (nt 3-776), probe B (nt 1397-2331) and probe C (nt 774-1120); cDNA clones 10-1 and 10-2. To control for RNA loading, filters were stripped and hybridized with [α-^{32}P]dCTP-labeled mouse GAPDH cDNA plasmid.

2.3.2 Cloning of the 5' genomic region of the *Vezf1* gene

Using a 5' *Vezf1* cDNA fragment as probe (nucleotides 3-776 of the published mouse *Vezf1* cDNA sequence (Xiong *et al.*, 1999); GeneBank accession# AF104410) one phage clone was isolated from a mouse 129/Sv lambda genomic library (kindly provided by F. Ramirez, Mount Sinai School of Medicine, New York) in an initial screen of $1x10^6$ plaques. Library screening and phage purification was essentially performed as described (Sambrook et al. 1989). Restriction mapping analysis of the genomic insert, pV20, showed that it contained the first and second exon seperated by 4kb of intronic sequence, as well as 15kb of genomic sequence upstream of exon 1.

2.3.4 Analysis of the *Vezf1* gene structure

The following oligonucleotides were used for the PCR amplification of the *Vezf1* exon-intron boundaries:

Intron 2:	5'-GTCTCATGAAGGAGGCATCACCA-3'
	5'-ACATGTTTTACATGACAGCTTAGGT-3'
Intron 3:	5'-ACCTAAGCTGTCATGTAAAACATGT-3'
	5'-CTTTGGCTCTGCCCAGTTGTCTT-3'
Intron 4:	5'-AAGACACATGGGCAGAGCCAAAG-3'
	5'-CTGCTTCCCTGGCCAGCTTGTCA-3'
Intron 5:	5'-TGAGACTGTGGGAAGAAGCTGTC-3'
	5'-GTGTCGTAGCAGCCGTGGAGGTT-3'

The amplified fragments were cloned into pCR4-Topo (Invitrogen) and sequenced in the DNA Core facility of The Scripps Research Institute. The intron-sizes were estimated by size separating the amplified fragments via gel-electrophoresis and comparing them to known DNA size standards.

2.3.5 cDNA library screening

A random-primed E11.5 mouse embryonic cDNA library (Clontech) was screened using the 5'*Vezf1* cDNA fragment (nucleotides 3-776) as a probe. After screening 500000 plaques, 5 positive phage clones were isolated. Library screening and phage purification were essentially performed as described (Sambrook et al. 1989). The inserts of the phage clones were amplified by PCR using λgt11 primers (Clontech) and subcloned into pCR4-Topo (Invitrogen). One phage clone was identified by sequence analysis that contained an

insert with additional 81 nucleotides upstream of the previously described cDNA sequence.

2.3.6 RLM-RACE

To determine the transcriptional start site of the *Vezf1* gene by RNA Ligase Mediated Rapid Amplification of cDNA ends (RLM-RACE), mouse E10-12 RACE-Ready cDNA (Ambion) was used as a template. The sequences of the nested gene-specific primers are:

RA1: 5'-GCTGCCTGCTGTTGGTGATGGGAT-3'

RA2: 5'-AGGCGGAGGAGGCGACAACAAA -3'

A 110 bp fragment was amplified, subcloned into pCR4-Topo (Invitrogen) and sequenced. A random-primed E11.5 mouse embryonic cDNA library (Clontech) was screened using the 5'*Vezf1* cDNA fragment (nucleotides 3-776) as a probe. After screening 500000 plaques, 5 positive phage clones were isolated. Library screening and phage purification were essentially performed as described (Sambrook et al. 1989). The inserts of the phage clones were amplified by PCR using λgt11 primers (Clontech) and subcloned into pCR4-Topo (Invitrogen). One phage clone was identified by sequence analysis that contained an insert with additional 81 nucleotides upstream of the previously described cDNA sequence.

2.3.7 Construction of Vezf1 promoter analysis constructs

The reporter plasmid pβgal-Basic (Clontech) was used for generating the *Vezf1* promoter reporter constructs. For p700V, a 700 bp BamHI/HindIII fragment of upstream genomic sequence was inserted into the BglII/HindIII site of the MCS of pβgal-Basic. p5V was generated by inserting a 4.5 kb BglII/AscI 5' genomic fragment into BglII/AscI restricted p700V.

The constructs p700I and p5I contain in addition to the 5' genomic sequences the 4.5 kb first intron. The intronic fragment was excised from pV20 (J.W. Xiong, unpublished) with BamHI and ligated into the BamHI site of pβgal-Basic downstream of the SV40 poly(A) site.

2.3.8 Transient transfection assays

Bovine aortic endothelial cells (BAEC), SV40 transformed endothelial cells (SVEC4-10), and NIH3T3 cells were transiently transfected using Lipofectamine 2000 reagent (Life Technologies). TK-Renilla (Promega) was co-transfected with β-galactosidase reporter constructs to normalize for transfection efficiency. Each construct was transfected at least

9 times in three independent experiments. In each experiment, 5 µg pµgal-Basic reporter construct, 1µg TK-Renilla and, if applicable, 5 µg of pEts1 (kindly provided by W.Aird, Beth Israel Deaconess Medical Center, Boston) or Egr-1 (A. Er-Long, TSRI, LaJolla) expression plasmid were transfected. Cell lysates were prepared 48 hours after transfection and β-galactosidase as well as luciferase assays were performed using a chemiluminescent β-gal reporter assay (Roche) and a dual-luciferase reporter assay system (Promega), respectively, according to the manufacturer's instructions.

2.4 Analysis of *Vezf1* function by gene inactivation

2.4.1 Generation of the Vezf1 locus targeting constructs

To generate the targeting vector (pVezf1koneo was constructed by J. W. Xiong), a 8 kb EcoR V/Xho I genomic fragment containing the first exon, 6 kb of 5' and 2 kb of 3' flanking intronic sequence was subcloned into pBluescriptIISK (Stratagene), of which the Eag I site had been deleted. From this intermediate, pV15-1, a 200 bp Eag I fragment was released containing the first 45 nt of the coding region including the ATG translation initiation codon. After blunting and ligation of Not I linkers a 5.1 kb IRES-*lacZ*gt1.2*neo* cassette was inserted, which had been isolated from pw196a (T. Lufkin, Mount Sinai School of Medicine, New York) via Xho I restriction digest, blunting, ligation of Not I linkers and Not I restriction digest. The resulting construct was designated pVezf1koneo. It was linearized for electroporation using a unique Xho I site in the polylinker of pBluescriptIISK.

A 1.5 bB puromycin resistence cassette was isolated from pKOSelectPuro (Stratagene) by Asc I restriction digest, blunted and ligated to Not I linkers. This fragment was inserted into the Not I site of pV15-1 to generate pVezf1kopuro. It was linearized for electroporation by Xho I restriction digest.

2.4.2 ES cell growth, transfection, infection and selection

R1 ES cells (Nagy *et al.*, 1990) were maintained on gelatin-coated dishes in DMEM (high glucose) containing 15% heat-inactivated fetal calf serum, 0.1 mM β-mercaptoethanol, 20mM HEPES, pH7.3, 0.1 mM non-essential amino acids, and 1000 U/ml LIF on γ-irradiated primary embryonic fibroblasts as feeder layer. For electroporation, $2x10^7$ ES cells were mixed with 10 µg of linearized DNA in 0.9 ml of HEPES buffered saline (HBS), pH 7.05 in a 0.4 cm cuvette and electroporated at 400V, 125 µF with a Biorad

gene pulser. After 24 hours, cells were plated in selection medium with either 200 μg/ml G418. Antibiotic resistant ES cell clones were picked after 10 days and expanded for Southern blot analysis. Hyperselection was performed at concentrations ranging from 400 to 1000 μg/ml G418 for 10 days. For retroviral infection of ES cells, undiluted virus supernatant was added to $1x10^6$ cells per 6 cm dish in the presence of polybrene at 4 μg/ml. Antibiotic resistant ES cell clones were selcted in medium containing 2 μg/ml puromycin for 10 days.

2.4.3 Genotyping of embryos and ES cells

Tail tips, yolk sacs or ES cells were digested overnight at 55°C in 0.2M NaCl, 50mM Tris-HCl (pH7.4), 5mM EDTA, 1% SDS buffer containing 100mg/ml proteinase K. After digestion, the mixture was extracted in successive steps with equal volume of phenol:chloroform (1:1), chloroform and then precipitated with 2 volumes of absolute ethanol. The resulting pellet was washed with 70 % ethanol, air dried and resuspended in 100 μl of TE (10mM Tris-HCl, pH7.5, 1mM EDTA).

10μg of genomic DNA was digested with the appropriate restriction enzyme, separated on 0.8% agarose gels and transferred to nitrocellulose membranes (Optitran, Schleicher and Schuell). Filters were hybridized to $1x10^7$ CPM of a [α-^{32}P]-dCTP radiolabeled probe overnight in 5xSSC, 2xDenhardt's, 0.05% SDS, 100 μg/ml denaturated salmon sperm DNA. Blots were washed at increasing stringency, with the final two washes at 65°C in 0.2xSSC, 0.1% SDS for 30 minutes each and exposed to Kodak Biomax film at -80°C overnight. The following probes were used to screen *Vezf1* knockout ES clones and mice: a 500bp BamH I/ Pst I fragment from pm1-135' (J. Xiong) corresponding to exon 2 as 3' probe and a 1.8 kb EcoRV intronic fragment as 5' probe.

Yolk sac DNA from embryos of various developmental stages was used for PCR genotyping. 100ng of template DNA was used per amplification reaction. PCR conditions: 30s at 95°C denaturing, 30s at 62°C annealing, 1min 72°C elongation, repeat 35 times. Primer sequences for the wild type locus:

G2: 5'-GCGTCCCGGAGGTTACCGAAGTGG-3'

G4: 5'-GGAACAGGAACGCGGTCCAGTTGG-3',

the recombinant locus:

INR1: 5'-TTTCTCTGGGCCGCGGGGTGGT-3'

NE3: 5'-GCGGGGATCTCATGCTGGAGTT-3'.

PCR products were analyzed on a 1% agarose gel.

2.4.4 Generation of mutant mice

ES cells from three independently derived *Vezf1*$^{+/-}$ clones were microinjected into C57Bl/6 donor blastocysts, which were subsequently implanted into CD1 pseudopregnant females. The resulting male chimeras were mated with C56Bl/6 females and agouti offspring were genotyped by Southern blot analysis. The mutant allele was then bred into the outbred CD-1 strain. Intercrosses from heterozygous F1 (129/SvxC57Bl/6xCD-1) mice were analyzed for viability at various developmental stages.

For further analysis, the mutant *Vezf1* allele was bred into the 129/Sv and C57Bl/6 inbred strains to create congenic mouse lines.

2.4.5 Whole mount β-galactosidase staining of embryos

EBs and embryos of various developmental stages were collected in PBS on ice and fixed in 4% paraformaldehyde (PFA) at 4°C for 2 hours. Embryos were rinsed in PBS 3 times and stained in 5mM KferroCN, 5mM KferriCN, 2mM $MgCl_2$, 500μg/ml X-GAL, 1xPBS at 37°C over night.

2.4.6 Whole mount embryo PECAM-1 staining

Embryos were dissected out and fixed in 4% paraformaldehyde in PBS overnight at 4°C. They were then dehydrated through a methanol series and stored at in 100% methanol at -20°C. The embryos were bleached in 6% hydrogen peroxide/methanol for 1 hour at room temperature and rehydrated through a methanol series to PBS/0.1% Tween 20 (PBST). They were blocked in 3% instant skim milk/PBST (PBSMT) twice for 1 hour. The embryos were incubated with rat anti-mouse CD31 (PECAM-1) monoclonal antibody (Pharmingen) diluted 1:50 in PBMST at 4°C overnight. Embryos were washed with PBSMT five times, 1 hour at 4°C, and then incubated with peroxidase-conjugated donkey anti-rat secondary antibody (Jackson Immunoresearch) in PBST overnight at 4°C. Peroxidase reaction was visualized with DAB/hydrogen peroxide.

2.4.7 Histological Analysis

Embryos between embryonic day (E) 8.5-16.5 were isolated and fixed in 4% paraformaldehyde (PFA) overnight at 4°C, dehydrated and embedded in paraffin. Serial sections (5 m) were stained with hematoxylin and eosin (H&E). Standard H&E staining was performed in the following order: 2 minutes each in: 100%, 95% ethanol and water; 6 minutes in hematoxylin; 30 seconds in water; 10 seconds in acid alcohol (70% ethanol/ 0.01% HCL); 30 seconds in water; 30 seconds in 0.005% NH_4OH; 30 seconds in water; 4 minutes in 1% Eosin; dehydration to xylene; coverslip.

2.4.8 Immunohistochemistry

Paraffin sections were deparaffinized and rehydrated. Antigen retrieval was accomplished by incubation at 95°C in Target Retrieval Solution (DAKO Corp.) for 30 minutes. Endogenous peroxidase activity was quenched by incubation with 5% hydrogen peroxide in methanol for 5 minutes. Specimen were incubated with anti-smooth muscle actin antibody (EPOSanti-SM A/HRP; DAKO Corp.) for 1 hour at room temperature. After washing with PBS, peroxidase reaction was visualized with diaminobenzidine (DAB)/hydrogen peroxide. For CD31 staining, sections were pretreated with Proteinase K (36 g/ml) for 30 min at 37°C to retrieve antigen and then incubated with rat anti-mouse CD31 antibody (Pharmingen) overnight at 4°C. After washing, samples were incubated with biotinylated anti-rat secondary antibody and peroxidase reaction was visualized using the tyramide amplification system (NEN). VEGFR-3 staining was accomplished by incubation with monoclonal rat-anti-mouse VEGFR-3 antibody (Kubo *et al.*, 2000) and overnight at 4°C. After washing, samples were incubated with biotinylated anti-rat secondary antibody and peroxidase reaction was visualized using the tyramide amplification system (NEN). For LYVE-1 staining, embryo sections were pretreated with 0.25mg/ml trypsin in 0.05M Tris, pH 7.8. Sections were incubated overnight at 4°C with polyclonal rabbit-anti-mouse LYVE-1 antibody (Prevo *et al.*, 2001). After washing, samples were incubated with biotinylated anti-rabbit secondary antibody and peroxidase reaction was visualized using the tyramide amplification system (NEN). Antibody stained sections for all antibodies were counterstained with hematoxylin.

2.4.9 Cultivation of megakaryocytes from embryonic livers

E11.5 embryos were collected in PBS. Embryonic livers were isolated and placed into DMEM-low glucose/10%/FCS/10ng/ml mTPO. Livers were disrupted by drawing them first through a 20g, then a 25g needle. Cells from one liver were seeded into one well of a 6-well dish and incubated at 37°C and 5% CO_2. After 6 days of culture cells were analyzed by Wright-Giemsa staining

2.4.10 Vessel Morphometry

PECAM-1 stained sections of E13.5 wild type and heterozygous mutant embryos were counterstained with hematoxylin. Sections were imaged with a digital camera (Pixera, Los Gatos, CA). Images were processed by using Scion Image (Frederick, MD) software. PECAM-1 positive structures were automatically counted and their area was measured. Differences in vascularity (number of and area occupied by CD31-positive structures per embryo microscopic field) were determined for each section. Endothelial linear density was determined by quantitating the number of endothelial cells (nuclei of PECAM-1 positive cells), per wessel wall unit. A total of 3 heterozygous mutant embryos was analyzed. The analysis was performed in collaboration with Dr. Humphrey Gardener, Biogen, Cambridge.

2.4.11 RT-PCR analysis

Total RNA was isolated from E10.5 embryos using Trizol (Life Technologies) and treated with DNaseI (Life Technologies) according to the manufacturer's instructions. Total RNA (2 □g) was reverse transcribed using random hexamers with the Superscript First Strand Synthesis System (Life Technologies) according to the manufacturer's instructions. PCR was performed on 1□l of the RT reaction in a volume of 50 □l using Hotstar Taq polymerase (Qiagen). The PCR conditions were as follows: initial denaturation at 95°C for 10 minutes followed by up to 35 cycles of denaturation at 95°C (1 minute), annealing at 58°C (1 minute), and extension at 72°C (1 min). 5 □l aliquots were taken after 25, 30 and 35 cycles and amplified PCR products were analyzed by electrophoresis on a 2% agarose gel. PCR primer pairs were as follows:

Flk-1: 5'-TCTGTGGTTCTGCGTGGAGA-3',
5'-GTATCATTTCCAACCACCCT-3';

Flt-1: 5'-TGTGGAGAAACTTGGTGACCT-3',
5'-TGGAGAACAGCAGGACTCCTT-3';

Flt-4:	5’-CACCGAAGCAGACGCTGATGAT-3’
	5’-AGCTGCTGTCTGCGAAGAAG-3’;
VEGF:	5’-GTAACGATGAAGCCCTGGAGTG-3’
	5’-TGAGAGGTCTGGTTCCCGAAAC-3’;
Tie1:	5’-TCTTTGCTGCTCCCCACTCT-3’
	5-’ACACACCATTCGCCATCAT-3’;
Tie2:	5’-CCTTCCTACCTGCTACTTTA-3’
	5’-CCACTACACCTTTCTTTACA-3’;
Ang1:	5’-AAGGGAGGAAAAAGAGAAGAAGAG-3’,
	5’-GTTAGCATGAGAGCGCAT TTG-3’;
Ang2:	5’-TGCCTACACTACCAGAAGAAC-3’,
	5’-TATTTACTGCTGAACTCCCAC-3’;
Notch1:	5’-TGCCTGAATGGAGGTAGGTGCGAA-3’,
	5’-GCACAGCGATAGGAGCC GATCTCA-3’;
Notch4:	5’-CCAAGAGATTCCCTTAAACTCGG-3’,
	5’-CCAGAGTTTAGGGATTCTC G-3’;
Dll4:	5’-GACTGAGCTACTCTTACCGGGTCA-3’,
	5’-CTTACAGCTGCCACCATTTC GACA-3’;
EphrinB2:	5’-CTGTGCCAGACCAGACCAAGA-3’,
	5’-CAGCAGAACTTGCATCTTG TC-3’;
EphB4:	5’-CAGGTGGTCAGCGCTCTGGAC-3’,
	5’-ATCTGCCACGGTGGTGAGTC- 3’;
Tbx1:	5’-GTTGCAGCCTTCGCAGCCAGCA-3’,
	5’-TAGTGTACTCGGCCAGGTGTA GCA-3’;
LKLF:	5’-CCACACATACTTGCAGCTACAC-3’,
	5’-CCATCGTCTCCCTTATAGAAAT A-3’;
EDG-1:	5’-TAGCAGCTATGGTGTCCACTAG-3’,
	5’-GATCCTGCAGTAGAGGATGG C-3’;
Endoglin:	5’-TACTCATGTCCCTGATCCAGCC-3’,
	5’-GTCGATGCACTGTACCTTTTT CC-3’;
VE-cadherin:	5’-GGATGCAGAGGCTCACAGAG-3’,
	5’-CTGGCGGTTCACGTTGGACT-3’;
ET-1:	5’-TGTCTTGGGAGCCGAACTCA-3’,

5'-GCTCGGTTGTGCGTCAACT TCTGG-3';

Vezf1: 5'-GTCTCATGAAGGAGGCATCACCA-3',

5'-ACATGTTTTACATGACAGCT TAGGT-3';

β-actin : 5'- GTGGGCCGCTCTAGGCACCAA -3',

5'- CTCTTTGATGTCACGCACGATTTC -3'.

Gene expression analysis for the *in vitro* differentiation of ES cells was carried out using the RT-PCR method described by Brady et al. (Brady and Iscove, 1993). Reverse transcription, poly(A) tailing and PCR procedures were performed as described, with the exception that the X(dT) oligonucleotide was shortened to 5'-GTTAACTCCGAG AATTC$(T)_{24}$-3'. The amplified products from the PCR reaction were separated on agarose gels and transferred to a Zeta-probe GT membrane (Biorad). The resulting blots were hybridized with ^{32}P randomly primed cDNA fragments (Ready-to-Go Labeling, Pharmacia) corresponding to the 3' region of the genes (Kennedy *et al.*, 1997).

2.4.12 Hematopoietic precursor colony assay

For the generation of EBs, ES cells were trypsinized into a single-cell suspension and plated at 1000 cells/ml into differentiation medium containing IMDM supplemented with 15% FCS, 2 mM L-glutamine (Life Technologies), 0.5 mM ascorbic acid (Sigma), and $4.5x10^{-4}$ M MTG in 60 mm Petri grade dishes. After 6 days in suspension culture, EB cells were plated in 1% methylcellulose containing 10% plasma-derived serum (PDS; Antech), 5% protein-free hybridoma medium (PFHM-II; Life Technologies) plus the following cytokines: c-kit ligand (KL; 1% conditioned medium), IL-11 (25ng/ml), IL-3 (1% conditioned medium), GM-CSF (3ng/ml), G-CSF (30ng/ml), M-CSF (5ng/ml) and IL-6 (5ng/ml). Primitive erythroid colonies were scored at day 5-6 of culture, whereas definitive erythroid (BFU-E), macrophage, mast cell, granulocyte/macrophage and mixed colonies were counted at day 7-10 of culture.

2.5 Overexpression of *Vezf1* during embryonic development

2.5.1 Generation of the *Vezf1* expression construct

The plasmid containing the full length *Vezf1* cDNA sequence, pVezf1, was generated in a 3 part ligation with the 1.3 kb Xba I/Pvu II fragment from p34 (J. Xiong, nt 1-1350), the 1

kb Pvu II/Xho I fragment from p64 (J. Xiong, nt 1351-2350) and the Xho I/Xba I restricted pBluescriptIIKS. A 4 kb IRESlacZpA cassette was isolated from pw61 (T. Lufkin) by Xho I restriction digest, blunted with T4 DNA polmerase and cloned into the EcoR V site of pVezf1. The resulting Vezf1IRESlacZpA fragment was excised using Not I and Xho I and blunted with T4 DNA polymerase. After ligation of Not I linkers it was cloned into the Not I site of pSPTg.T2FXK (T. Sato, Southwestern Medical Center, Dallas) to generate Tie2VIL.

2.5.2 Generation of Tie2VIL transgenic mice

Transgenic mice were generated by pronuclear injection into F1 (C57Bl/6xBALB/c) oocytes, which were subsequently implanted into CD1 pseudopregnant females. Blastocyst and pronuclear injections were performed by Dr. Kevin Kelly in the Transgenic Core Facility, Mount Sinai School of Medicine, New York or in the Transgenic Facility at the Scripps Research Institute, La Jolla.

2.5.3 Genotyping of transgenic mice

Transgenic mice and embryos were genotyped by slot blot analysis using a 3 kb HindIII/NdeI lacZ fragment from p□gal-Control (Clontech) as probe. For genotyping by PCR, primer sequences are as follows:

LacZA: 5'-GCATCGAGCTGGGTAATAAGCGTTGGCAAT-3'

LacZB: 5'-GACACCAGACCAACTGGTAATGGTAGCGAC-3'

PCR products were analyzed on a 1% agarose gel.

3. RESULTS

3.1 Structural and expression analysis of *Vezf1*

3.1.1 Reevaluation of the *Vezf1* cDNA structure

The goal of this thesis was to analyze the function of *Vezf1* during mouse embryonic development and to elucidate the mechanisms that regulate *Vezf1* expression. The original premise of these studies was that *Vezf1* is a zinc finger transcription factor whose expression during embryogenesis is restricted to endothelial cells and their precursors, as reported in (Xiong *et al.*, 1999). However, while the analysis of *Vezf1* function and regulation of its expression was already at an advanced state, I discovered mounting evidence that challenged this premise. This evidence, in large part, was accumulated through the analysis of the NCBI (National Center for Biotechnology Information) sequence databases that were generated as a result of the recent sequencing efforts of the human and mouse genome. In particular, the following observations led to a reevaluation of the identity of *Vezf1*:

1. Database searches using the published *Vezf1* sequence identified a novel murine cDNA, *Zneu1* (AF184973), encoding a putative Notch4-like protein, in the 3' UTR of the published *Vezf1* sequence (nt 2475-3681). Except for the first 225 bp of *Zneu1* 5' UTR sequence, which do not align, mouse *Zneu1* shares 98% sequence identity with the *Vezf1* 3' UTR (Fig 3).

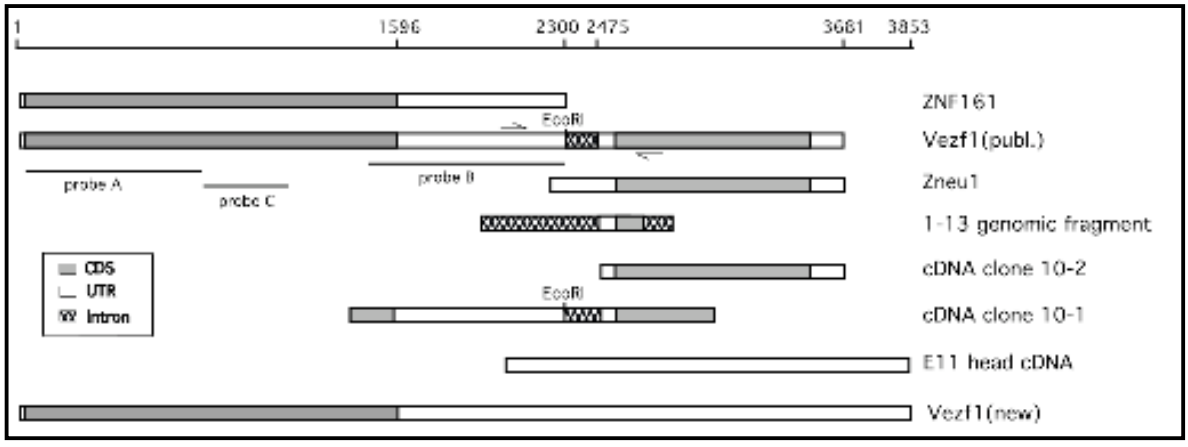

Figure 3. Analysis of the *Vezf1* cDNA structure. Nucleotide positions of the *Vezf1* cDNA are indicated in the top bar.

2. Alignment of the published *Vezf1* cDNA sequence with the human and mouse non-redundant (NR) and expressed sequence tag (EST) databases identified a gap of 175 bp between nucleotide position 2330 and 2475 of the *Vezf1* sequence (Fig 4). The *Vezf1* cDNA sequence immediately upstream of this gap is characterized by a poly(A)-like stretch (a succession of 27 adenosine residues interrupted by a single cytosine) followed by an EcoRI restriction site, while nucleotide position 2475 corresponds to the 5' end of the putative *Zneu1* cDNA in the published *Vezf1* 3' UTR sequence. Attempts to amplify RNA transcripts spanning this EST-gap by RT-PCR were unsuccessful. However, database searches identified a mouse E11 embryo head cDNA clone (AK018086) that overlaps with 3' UTR sequences of *Vezf1* (nt 2118-2330) and extends an additional 1523 bp in the 3' direction without overlapping with any *Vezf1* 3' UTR sequences downstream of nucleotide position 2330 (Fig 3).

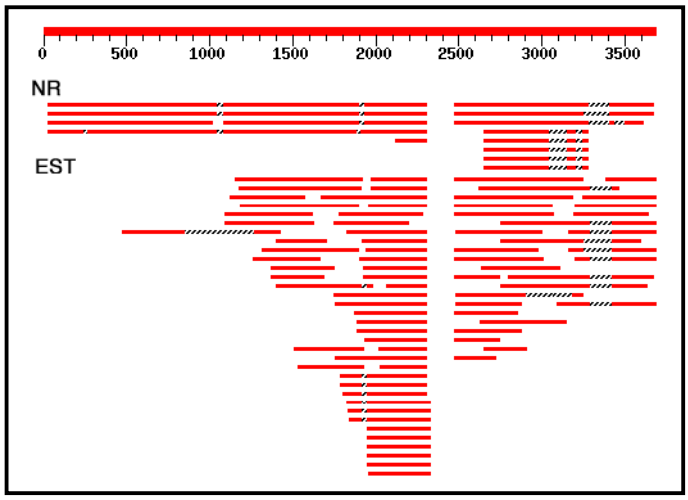

Figure 4. Alignment of the published *Vezf1* cDNA sequence (AF104410) (top bar, nucleotide positions are indicated) with sequences in the non-redundant (NR) and expressed sequence tag (EST) data bases.

3. Analysis of the high throughput genomic sequences databases identified a 224 kb mouse genomic contig, RP23-199A2 ((AL593853), which contains *Vezf1* sequences from nucleotide position 1 to 2330 and the complete sequence of the E11 embryo head cDNA clone (AK018086), but shows no overlap with the 3' *Zneu1* containing region of the published *Vezf1* cDNA.

4. The human ortholog of *Zneu1*, ZNEU1, has been mapped to human chromosome 9q34.3. This region is syntenic to the proximal end of mouse chromosome 2, the segment to which *Vezf1* was localized. The *Vezf1* locus was mapped by using a primer pair in the 3' flanking genomic DNA of the 1-13 insertion (see introduction). In contrast, the mouse genomic contig RP23-199A2 ((AL593853), which contains the complete *Vezf1* gene, is derived from mouse chromosome 11.

Taken together, these findings suggest that the published *Vezf1* sequence represents a chimeric cDNA clone that contains two open reading frames (ORF) corresponding to two unrelated genes, *Vezf1* and *Zneu1* (Fig. 3). In light of these findings, I revisited the cloning and expression analysis of *Vezf1* as described in (Xiong *et al.*, 1999).

3.1.2 Reexamination of the Cloning of *Vezf1*

A 0.9 kb fragment of 3' flanking host genomic DNA from retroviral insertion 1-13 was used for screening an E7.5 mouse embryonic cDNA library (provided by J. Gerhart, Columbia University). This fragment contains 124 bp of exonic sequence that overlap with nucleotides 226 to 352 of the *Zneu1* cDNA (Fig. 3), encompassing 36 bp of 5' UTR and 88 bp of putative coding sequence (corresponding to nucleotides 2475-2599 of the published *Vezf1* sequence). Sequences up- and downstream of the exonic region do not contain any homology to the published *Zneu1* sequence and are presumably intronic. Two cDNA clones, 10-1 and 10-2, were isolated in the cDNA library screen. They overlap in the region encompassing 5' UTR and 5' putative coding sequences of *Zneu1*. 10-2 spans the complete ORF of *Zneu1* and contains, in addition, 3' untranslated sequences including the polyadenylation signal and the poly(A) stretch. 10-1, in contrast, extends in the 5' direction and overlaps with 900 bp of the 3' end of human ZNF161. 10-1 contains the poly(A)-like stretch followed by an EcoRI site at position 2331 of the published *Vezf1* sequence. As EcoRI was used for the construction of the mouse E7.5 cDNA library in λZapII, it appears likely that 10-1 represents a chimeric cDNA clone. The 1-13 genomic flanking DNA aligns exclusively with sequences downstream of the EcoRI site in the published *Vezf1* sequence. This suggests that the retroviral insertion in clone 1-13 had occurred into the *Zneu1* rather than the *Vezf1* gene, implicating that the endothelial-cell restricted expression pattern of the AP reporter gene observed in embryos derived from clone 1-13 (Xiong *et al.*, 1999) reflects the expression of the endogenous *Zneu1* rather than the *Vezf1* gene.

3.1.3 Expression analysis of *Vezf1*

Previous expression analysis of *Vezf1* during mouse embryogenesis by RNA *in situ* hybridization utilized the cDNA clones 10-1 and 10-2 to prepare the antisense probes. Both probes gave identical results and produced the reported endothelial cell-specific

expression pattern. To reexamine the expression of *Vezf1* (from hereon, *Vezf1* refers to the gene that is encoded by nt 1-2330 of the published *Vezf1* sequence), two new *in situ* hybridization probes were designed. Probe A corresponds to the 5' region of the *Vezf1* coding region (nucleotides 3-776), while probe B consists of the 3' region of the gene (nt 1397-2331) containing 3' UTR sequences as well as 160 nucleotides of 3' coding region (Fig. 3). In sagittal sections of E12.5 and E13.5 embryos rather widespread *Vezf1* expression was observed with either antisense probe. Expression appeared to be strongest in the forebrain, branchial arches, the lung and the vertebral column (Fig 5A, D). No signal was detected for the sense control probes (Fig. 5B, E). Moreover, expression was undetectable in *Vezf1* KO embryos (Fig. 5C, F, see Results section, Chapter for generation of *Vezf1* KO embryos), confirming the specificity of the probe (and the successful inactivation of the *Vezf1* gene). In contrast, probe 10-1 produced an endothelial specific expression pattern in wildype as well as in *Vezf1* KO embryos (Fig. 5G, I).
In E9.5 wild type embryos, *Vezf1* was found to be expressed in a widespread manner (Fig. 6A). Similar to E12.5, strongest expression was detected in the brain and the neural tube. In addition, *Vezf1* was expressed at low levels in the extraembryonic yolk sac (Fig. 6C), where it appears to be concentrated around yolk sac blood islands (Fig. 6B, C).

To confirm the results obtained by RNA *in situ* hybridization, Northern blot analysis was performed (Fig. 7). Using probes A, B and C (corresponding to nt 774-1120, Fig. 3), a major 4.2 kb *Vezf1* transcript was detected in E10.5 wild type embryos, as previously reported (Xiong *et al.*, 1999). In heterozygous embryos, reduced *Vezf1* expression was observed, whereas *Vezf1* mRNA was undetectable in *Vezf1* KO embryos (Fig. 7). In contrast, probe 10-2 hybridizes to a 1.8 kb transcript, presumably *Zneu1*, in wild type, heterozygous and homozygous *Vezf1* KO embryos, but does not detect the 4.2 kb *Vezf1* transcript. Consistently, probe 10-1, which overlaps with *Vezf1* and *Zneu1* cDNA sequences, detects both, the 4.2 kb *Vezf1* and the 1.8 kb *Zneu1* message (Fig. 7).

In summary, these data demonstrate that the published *Vezf1* sequence represents a chimeric cDNA clone containing *Vezf1* (corresponding to nucleotides 1 to 2330 of the published sequence) and the putative *Zneu1* gene (nucleotides 2475 to 3681). The retroviral insertion 1-13 that showed an endothelial-restricted embryonic expression pattern reflects the endogenous expression of *Zneu1* rather than *Vezf1*. *Vezf1*, in contrast,

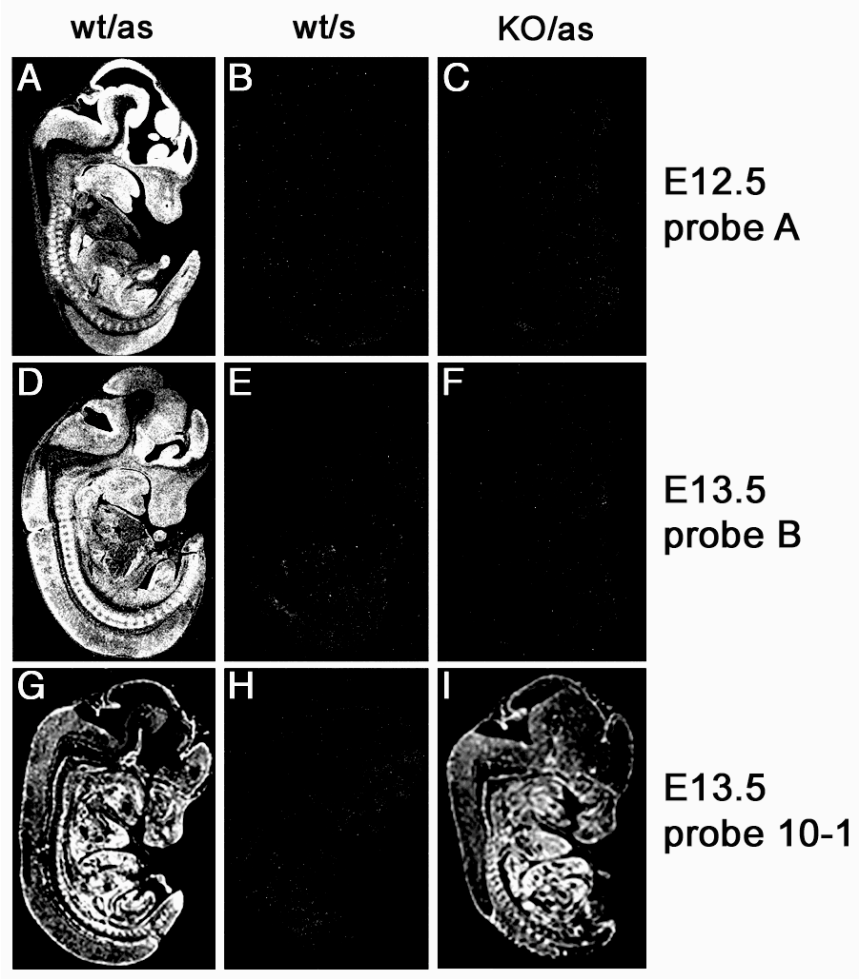

Figure 5. Expression analysis of *Vezf1* in mouse embryos by RNA *in situ* hybridization. Dark field images of sagittal sections through E12.5 and E13.5 embryos. Antisense probes corresponding to the 5' (nt 3-776, probe A) and the 3' untranslated (nt 1397-2331, probe B) region of *Vezf1* detect widespread expression of the *Vezf1* mRNA in wildtype E12.5 (A) and E13.5 (D) embryos. No signal is detected in *Vezf1* KO embryos (C, F) or with sense control probes (B, E). The 10-1 antisense probe, in contrast, detects an endothelial-restricted transcript in wildtype and KO embryos (G, I). No signal is detected with the sense probe (H).

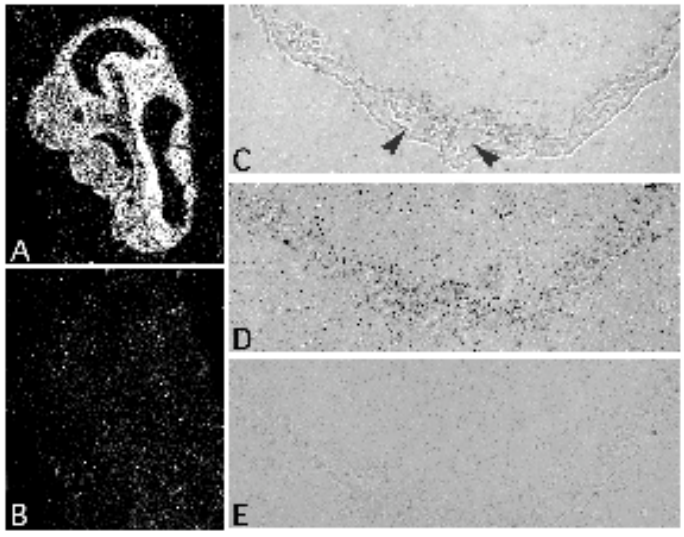

Figure 6. RNA *in situ* hybridization analysis of *Vezf1* expression in E9.5 embryos. (A) Dark field image of a sagittal section through an E9.5 embryo hybridized to the *Vezf1*-specific probe C (see Fig. 3). *Vezf1* is expressed in a widespread fashion. Highest expression is found in the brain and the neural tube. (C) Phase contrast image of a transverse section through an E9.5 yolk sac. Arrowheads indicate yolk sac blood islands. (D) Bright field image of the section shown in C. Low levels of *Vezf1* expression are detected, which appear to be concentrated around the yolk sac blood islands. No signal was detected with sense control probes (B, E).

displays widespread expression in embryos, as assessed by RNA *in situ* hybridization. In the following sections of the results part the functional and structural analysis of *Vezf1* will be presented.

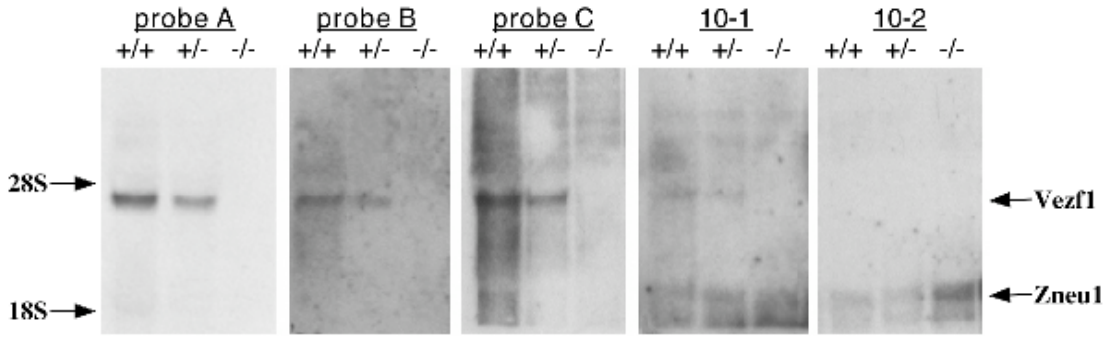

Figure 7. Northern blot analysis of *Vezf1* expression. The *Vezf1*-specific probes A, B and C (compare Fig. 3) detect the 4.2 kb *Vezf1* transcript in wildtype and heterozygous, but not in KO E10.5 embryos. Probe 10-2 hybridizes to a major 1.8 kb Zneu1 transcript. The chimeric probe 10-1 detects both, the 4.2 *Vezf1* and the 1.8 kb Zneu1 message.

3.1.4 Cloning of the 5' genomic region of the *Vezf1* gene

In order to generate a targeting construct for the *Vezf1* locus and to isolate the promoter/enhancer region of the *Vezf1* gene, genomic DNA from a mouse129/Sv genomic lambda library (kindly provided by F. Ramirez, Mount Sinai School of Medicine, New York) was isolated. Using an [□-^{32}P]-labeled cDNA fragment that spans nucleotides 3-776 of the published mouse *Vezf1* cDNA sequence ((Xiong *et al.*, 1999); GeneBank accession# AF104410) as probe, one positive phage clone containing a 20 kb genomic insert was identified after screening a total of approximately 1x10^6 plaques. Restriction mapping, subcloning of restriction fragments and partial sequence analysis of the genomic insert revealed that it contained the first and second coding exons of *Vezf1* of 153 and 695bp length, respectively, separated by 4.5 kb of intronic sequence, as well as 15kb of genomic sequence upstream of exon 1 (Fig. 8A). A 2 kb EcoRI fragment, containing 614 bp of 5' genomic sequence, the first exon and 1320 bp of intron 1, was subcloned and completely sequenced for further analysis.

3.1.5 Analysis of the *Vezf1* gene structure

As detailed above, the *Vezf1* cDNA corresponds to nucleotides 1 to 2330 of the published cDNA sequence. Moreover, a mouse E11 embryo head cDNA clone (AK018086) was found through database search (see above) that overlaps with 3' UTR sequences of *Vezf1* (nt 2118-2330) and extends an additional 1523 bp in the 3' direction. Thus the total length

of the *Vezf1* cDNA appears to be 3853 bp (Fig. 3). Alignment of the extended *Vezf1* cDNA with the human high throughput genomic sequences database identified a homologous 3' UTR region for the human *Vezf1* ortholog, ZNF161(XM_010997) (Koyano-Nakagawa *et al*., 1994), expanding the published ZNF161 cDNA sequence by 1546 bp to a total length of 3876 bp. The extended *Vezf1* and ZNF161 cDNAs show an overall sequence identity of 90% and are 86.5% identical in the 3' UTR region.

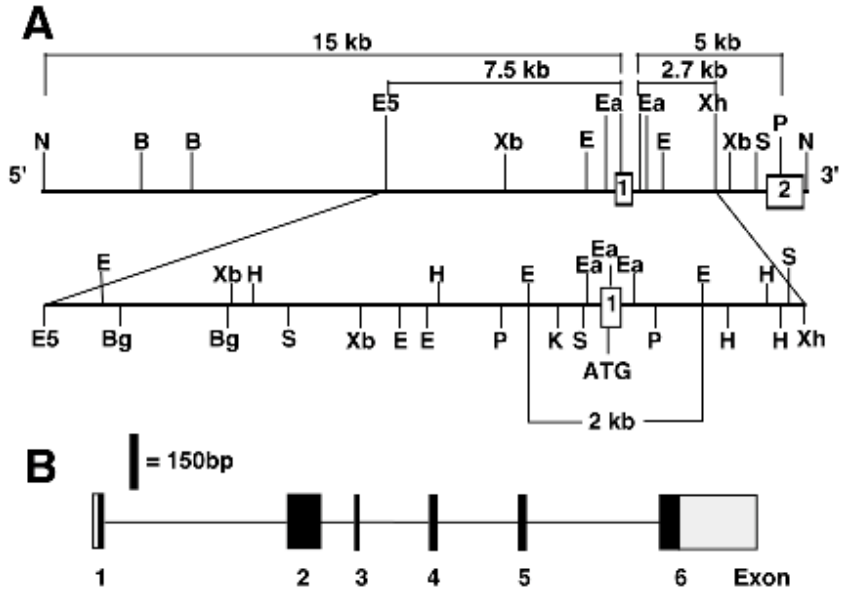

Figure 8. (A) Restriction map of the 20 kb genomic *Vezf1* clone. The first and the second exons are represented as boxes and are separated by the 4.5 kb first intron. Recognition sites of restriction endonucleases: B, BamHI; Bg, BgllI; E, EcoRI; Ea, EagI; E5, EcoRV; H, HindIII; K, KpnI; P, PstI; S, SacI; Xb, XbaI; Xh, XhoI.
(B) Structure of the *Vezf1* gene. Filled and open boxes represent coding and non-coding exons, respectively. Exon numbers are indicated.

To analyze the structure of the *Vezf1* gene, the cDNA sequences of mouse *Vezf1* and its human ortholog ZNF161 were used to search the electronic sites provided by the International Genome Consortium for the public work draft of the human and mouse genome (Science 2000, 289:1471). Initially, a working draft contig from human chromosome 17 (NT_010651.5) was identified that contained sequences corresponding to the complete ZNF161 cDNA sequence. More recently, a 224 kb mouse genomic contig, RP23-199A2 (AL593853), was isolated that contained the entire *Vezf1* gene. Putative exon-intron boundaries of the *Vezf1* gene were determined by the divergence of the genomic sequence from the sequence of the *Vezf1* cDNA. The putative exon-intron boundaries were subsequently PCR amplified from genomic DNA using primer pairs that span the introns and verified by DNA sequencing. As shown in Fig. 8B, the *Vezf1* gene consists of 6 exons and 5 introns and has a total length of 15.6 kb. Each of the splice donor

and acceptor sequences displayed consensus GT and AG dinucleotides, respectively (Table 2). The first exon contains the 5' UTR and 33 bp of coding sequence. The region that encodes the six zinc finger motifs extends from exon 2 to exon 4. The glutamine stretch is encoded by exon 5, and exon 6 contains the 3' end of the coding region, including the proline-rich region activation domain, and the complete 3' UTR. The analysis of the gene structure of the human *Vezf1* ortholog, ZNF161, revealed that it was identical to that of *Vezf1* with respect to the number, the position and the size of the exons, as well as the nucleotide sequences at the exon-intron boundaries; however differences in the sizes of the introns were observed (human intron sizes are shown in brackets in Table 2).

Exon number	Exon size in bp	5' splice donor	3' splice acceptor	Intron position	Intron size in bp
1	153	AGgtac		153	4556 (4713)
2	695	AGgtac	acagGC	848	893 (757)
3	64	AAgtaa	acagGC	912	1462 (1093)
4	184	AAgtag	gcagAC	1096	2020 (1289)
5	153	AGgtca	atagCG	1249	2840 (4265)
6	2604		ttagAA		

Table 2. Exon-Intron organization of the *Vezf1* gene. Intron sizes in parentheses represent intron sizes of the human ortholog.

3.1.6 Identification of the *Vezf1* transcriptional start site

The *Vezf1* cDNA is 3853 bp in length. It contains 1558 bp of coding sequence and is flanked at the 5' end by 39 bp of untranslated region and at the 3' end by 2256 bp of 3' UTR sequences. However, on Northern blots using RNA from embryos and endothelial cell lines, a major *Vezf1* transcript of approximately 4.2 kb length is detected. Taking into account that the average length of a poly(A) stretch is around 300 nucleotides in length and considering the relatively small size of the *Vezf1* 5' UTR, we concluded that it was likely that the 3853 bp cDNA did not represent a full length mRNA and lacked additional 5' untranslated sequences.

In an effort to identify additional 5' UTR sequences, a random-primed E11.5 mouse embryonic cDNA library (Clontech) was screened using the 5'*Vezf1* cDNA fragment (probe A, nt 3-776) as a probe. After screening $5x10^5$ plaques, one phage clone was isolated that contained an insert that extended 83 nucleotides 5' of the published cDNA

sequence. To determine if the 5'end of this clone corresponds to the transcriptional start site of the *Vezf1* mRNA, RNA Ligase Mediated Rapid Amplification of cDNA ends (RLM-RACE) was employed (Schaefer, 1995). RLM-RACE represents a major improvement to the classic RACE technique and is designed to amplify cDNA only from full-length capped mRNA. A random-primed mouse E10-E12 RACE-Ready cDNA (Ambion) was used as a template for two successive rounds of PCR amplification with nested, gene-specific primers. A single 110 bp fragment was amplified. Sequence analysis of the 110 bp fragment and alignment with 5' genomic sequences located the transcriptional start site 122 bp upstream of the ATG translation initiation codon in an initiator-like pyrimidine-rich sequence (Fig. 9B), consistent with the 5' end of the cDNA clone previously obtained by library screening (described above).

3.1.7 Characterization of the 5' flanking and first intron region of the *Vezf1* gene

A particularly striking feature of the *Vezf1* gene is the high G/C content of its 5' region. The 2 kb EcoRI fragment, containing 614 bp of 5' genomic sequence, the first exon and 1320 bp of intron 1 sequence, has an average G/C content of 65%, while the 620 bp region upstream of the ATG initiation is 72% G/C rich. By contrast, bulk genomic DNA has a G/C content of only 40% (Cross and Bird, 1995). A total of 31 recognition sites for the restriction enzyme HpaII (CCGG) were found in the 2 kb EcoRI genomic fragment. An abundance of HpaII sites is referred to as CpG island, a characteristic feature of housekeeping genes, often located in the upstream region of genes (Cross and Bird, 1995). The presence of this putative CpG island in the 5' region of the *Vezf1* gene strongly suggests that this region contains the *Vezf1* promoter sequences. However, no apparent TATA box or CAAT box was found in the 5' upstream region. The absence of a TATA sequence is thought to be a characteristic of promoters of genes with housekeeping functions (Bird, 1986; Lavia *et al.*, 1987), but has also been reported for cell type-specific and developmentally regulated promoters present, for example, in the *Flk-1* and □2-*integrin* genes (Javahery *et al.*, 1994; Rönicke *et al.*, 1996; Zutter *et al.*, 1994).

The 614 bp fragment of 5' genomic *Vezf1* sequence is 91% identical to the corresponding upstream region of the human ZNF161 gene. Thus, it appears likely that conserved regulatory transcription factor binding sites are located in this region. The MatInspector professional program (Matrix Family Library Version 2.2) (Quandt *et al.*, 1995) was used

to search for transcription factor consensus binding sites in the putative *Vezf1* promoter region. Sequence inspection revealed five potential AP-2-, four potential SP1- and three potential NF-κB-binding sites (Imagawa *et al.*, 1987) (Jones and Tjian, 1985) (Lenardo and Baltimore, 1989) (Fig. 9). In addition, the 5' upstream region contains a single putative binding site for c-Ets1 and four sites for Egr-1. Both proteins have previously been shown to be functionally important for several endothelial promoters, including Flk-1 and Tie2 (Dube *et al.*, 1999; Kappel *et al.*, 2000; Silverman and Collins, 1999). Furthermore, four potential binding sites for MZF1, a zinc finger transcription factor involved in erythromyelogenic differentiation (Perrotti *et al.*, 1995), are present in the proximal promoter region.

The regulatory elements of the endothelial-specific murine genes *Tie2* and *Flk-1* have been well characterized *in vitro* and *in vivo* (Dube *et al.*, 1999; Kappel *et al.*, 1999; Kappel *et al.*, 2000; Ronicke *et al.*, 1996; Rönicke *et al.*, 1996; Schlaeger *et al.*, 1997; Schlaeger *et al.*, 1995). A common feature of both genes is the requirement of regulatory transcription factor binding sites within the 5'-promoter region as well as the first intron to achieve endothelial-specific expression. Thus, to identify additional possible regulatory elements, the 1320bp first intron sequence was analyzed using the MatInspector professional program. The intronic fragment contains putative binding sites for LMO2 (Yamada *et al.*, 2000), a LIM domain transcription factor, ARNT (Abbott and Buckalew, 2000; Maltepe *et al.*, 1997; Yamada *et al.*, 2000), a transcriptional regulator that heterodimerizes with PAS proteins including HIF1α, SCL/tal-1 (Visvader *et al.*, 1998), a bHLH protein that is co-expressed with Flk-1 in hemangioblasts, and COUP, a steroid/thyroid nuclear receptor transcription factor (Pereira *et al.*, 1999; Zhou *et al.*, 2000) (Fig. 9A), all of which have been implicated in angiogenic remodeling of the early embryonic vasculature by gene inactivation studies. The subsequent identification of the mouse genomic contig RP23-199A2 ((AL593853), which contains the complete *Vezf1* gene, enabled the inclusion of the complete first intron sequence in the analysis. Thus, in addition, several potential binding sites for GATA-1 and c-Ets1 were detected in sequences 3' of the EcoRI site in the first intron. Both of these transcription factors have been shown to regulate the promoter activity of several endothelial genes (Gumina *et al.*, 1997; Iljin *et al.*, 1999; Kappel *et al.*, 2000; Kawana *et al.*, 1995; Lelievre *et al.*, 2001).

Figure 9. (A) Analysis of *Vezf1* promoter and first intron sequences in the 2 kb genomic EcoRI fragment. Symbols indicate putative binding sites for known transcription factors. The position of the transcriptional start site (TSS), as determined by RLM-5' RACE, is indicated by the arrow.
(B) Nucleotide sequence of the 5' region of the *Vezf1* gene. The nucleotide sequence of a 779 bp fragment, containing the 614 bp of 5' genomic region, the first exon and part of the first intron, is shown. The position of the transcriptional start site is indicated by the arrow. indicates the 5' end of the published *Vezf1* cDNA (AF104410). The asterisk marks the beginning of the first intron. Potential binding sites for transcription factors are underlined.

3.1.8 Functional analysis of *Vezf1* promoter and intronic sequences

To investigate whether the *Vezf1* promoter was located in the characterized 5' flanking region and to assess the contribution of the first intron to the promoter activity, transient transfection assays using -galactosidase reporter gene constructs were performed. Genomic fragments containing 5 kb (p5V) or 700 bp (p700V) of upstream sequences,

respectively, were subcloned into the multi-cloning site (MCS) of the βgal-Basic reporter plasmid (Clontech). To test for the presence of regulatory elements within the first intron, 4.5 kb of intronic sequence were inserted downstream of the poly(A) site into p5V and p700V to generate p5I and p700I, respectively. These reporter constructs were transiently transfected into SVEC4-10 cells, a SV40-transformed murine endothelial cell line (O'Connell and Edidin, 1990). NIH3T3 fibroblasts were used as control to determine whether the promoter and/or enhancer activity was endothelial-specific. Transfection efficiencies were standardized by cotransfecting a constitutive luciferase reporter plasmid (TK-Renilla, Promega), and promoter activities were normalized to the activity of the empty βgal-Basic reporter construct. As a control for an endothelial cell-specific promoter, Tie2lacZ was included in the assay. The *lacZ* gene in Tie2lacZ is expressed under the control of the Tie2 promoter and minimal enhancer fragment. This combination of Tie2 promoter and enhancer elements had been shown previously to confer uniform vascular endothelial cell-specific reporter gene expression in both embryonic and adult transgenic mice (Schlaeger *et al.*, 1997; Schlaeger *et al.*, 1995).

Figure 10A shows a comparison of the promoter activities in SVECs and NIH3T3 cells. The reference construct Tie2lacZ has the highest promoter activity in the endothelial cell line (4.3-fold increase over base-line levels), but shows only moderate expression in NIH3T3 cells, confirming the endothelial cell-specificity of the Tie2 regulatory elements. Among the *Vezf1* reporter constructs analyzed, strongest promoter activity in both cell lines is observed for p700V. p700V shows a 5.5-fold increase of β-galactosidase activity in NIH3T3 cells, and a 3.7-fold increase in SVECs. p5V displays an overall lower promoter activity (3.6-fold in NIH3T3, 2.6-fold in SVECs), whereas p700I and p5I do not show any appreciable β-galactosidase expression (between 1.5- and 2-fold over baseline). Taken together, these findings indicate that the 5' proximal 700 bp fragment confers promoter activity in this reporter gene assay. However, the *Vezf1* promoter constructs tested here do not contain any autonomous endothelial-specific regulatory elements. p700V, as well as p5V, although active in SVECs (93% and 65% of Tie2lacZ activity), show higher expression levels in NIH3T3 than in SVEC cells (144% and 130% of the activity in SVECs, respectively). Furthermore, negative regulatory elements seem to be present in the first intron and the 5' upstream genomic region between position –700 and –5000 bp that function in the endothelial and the fibroblast cell line.

Sequence analysis of the 5' proximal region and intron 1 regions revealed a single putative c-Ets1 binding site at position –28 to –19 and 3 c-Ets1 sites within the first intron (see above; Fig. 9). In addition, four Egr-1 sites are located in the *Vezf1* 5' proximal region (Fig. 9). Both of these proteins were shown to regulate the promoter activity of several endothelial genes (see above). To investigate whether these transcription factors can activate the *Vezf1* promoter in *vitro*, c-Ets1 or Egr-1 expression plasmids were co-transfected together with the *Vezf1* reporter constructs into SVEC4-10 and NIH3T3 cells, and reporter gene expression was analyzed as described above. As shown in Figure 10B, overexpression of either c-Ets1 or Egr-1 in NIH3T3 cells does not affect the promoter activity of any of the reporter constructs tested, including Tie2lacZ. In addition, co-transfection of c-Ets1 or Egr-1 expression plasmids into SVECs does not affect the promoter activity of p700V (Fig. 10C). However, p700I, p5V and p5I show moderate increases of β-galactosidase activity in the presence of overexpressed c-Ets1 (200%, 135% and 145% of activity without co-transfected c-Ets1, respectively) and Egr-1 (162%, 102% and 136%, respectively), suggesting that c-Ets1 and Egr-1 can abrogate or ameliorate the negative regulatory effects mediated by first intron and 5' upstream (position –700 to –5000) regions.

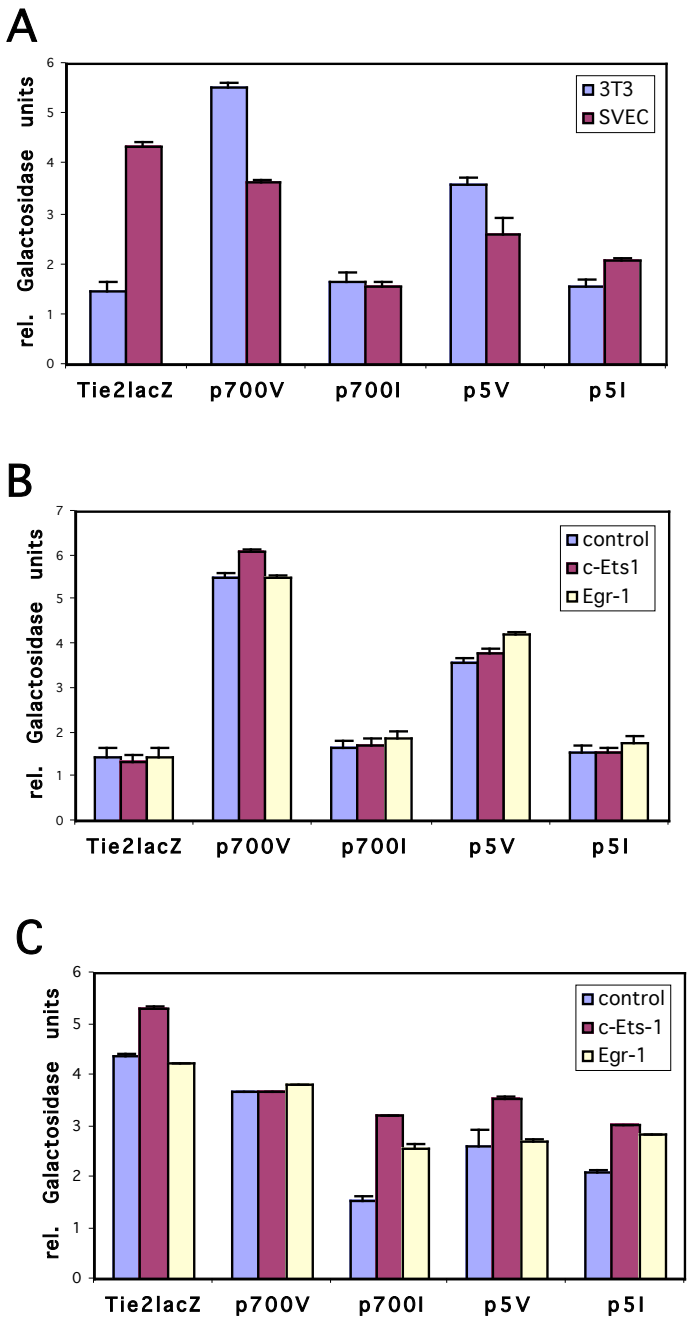

Figure 10. Functional analysis of the *Vezf1* promoter and intronic sequences *in vitro*. (A) Promoter activities of *Vezf1* reporter constructs relative to the activity of empty gal-Basic vector. *Vezf1* reporter constructs were generated as described in "Experimental Procedures" and transfected into SVECs and NIH3T3 cells. Transfection efficiencies were normalized by cotransfection of TK-Renilla. Values represent the averages of at least three independent experiments.
(B) Promoter activities of *Vezf1* reporter constructs in NIH3T3 cells cotransfected with c-Ets1 or Egr-1 expression plasmids.
(C) Promoter activities of *Vezf1* reporter constructs in SVECs cotransfected with c-Ets1 or Egr-1 expression plasmids.

3.2 Analysis of *Vezf1* function by gene inactivation

3.2.1 Targeted disruption of the *Vezf1* gene in mouse ES cells by homologous recombination

To disrupt *Vezf1* in mouse ES cells, a targeting vector was constructed that replaces the translated portion of the first coding exon and the proximal part of the first intron with a promoterless IRES-*LacZ* gene and a *neo* expression cassette (Fig. 11A). This targeting strategy was designed to create a *Vezf1* null allele and to enable analysis of *Vezf1* expression in mice by generating a *Vezf1-lacZ* hybrid transcript driven by the endogenous *Vezf1* promoter elements. The targeting construct contains 6 kb of homologous sequence at its 5' end and 2 kb at its 3' end, respectively. Construction of the targeting vector, electroporation into the 129/Sv-derived ES cells line R1 (Nagy *et al.*, 1990) and selection of ES cells were performed by Dr. Jing-Wei Xiong, a postdoctoral fellow in Dr. Heidi Stuhlmann's laboratory. 96 G418 resistant clones were isolated and genotyped by Southern blot DNA analysis using 5' and 3' external fragments as probes. Three out of 96 clones (V2, V86, and V74) displayed the expected homologous recombination-specific banding pattern when analyzed with both the 5' and the 3' external probes. Figure 11B illustrates the results from Southern blot analysis of BamHI-digested DNA using a 5' 0.8 kb genomic EcoRV fragment that lies outside the region of homology as probe. In addition to the 16 kb wild type fragment (see lane 1 for parental R1 ES cells), a 9kb band, diagnostic for the targeted allele, is detected in DNA from clones V2, V74 and V86. All three clones were used to generate chimeric mice by microinjection into C57BL/6 blastocysts. Microinjections were performed by Dr. Kelvin Kelly in the transgenic core facility at the Mount Sinai School of Medicine, New York. Chimeric males derived from all three ES cell clones transmitted the targeted allele successfully through the germ line.

To produce ES cell clones that carry the introduced mutation in both alleles, a G418 hyperselection protocol was employed (Mortensen *et al.*, 1992). These *Vezf1*$^{-/-}$ cells will be instrumental in analyzing the effects of the inactivation of *Vezf1 in vitro*, The presence of the weak, synthetic gt1.2 promoter (Wang and Lufkin, 2000) to drive *neo* expression in the targeting construct permits to select for homozygous mutants at elevated G418 concentrations. In this experiment, heterozygous ES cells were selected at concentrations between 400 and 1000 □g/ml G418 for 10 days. After screening 400 clones by Southern

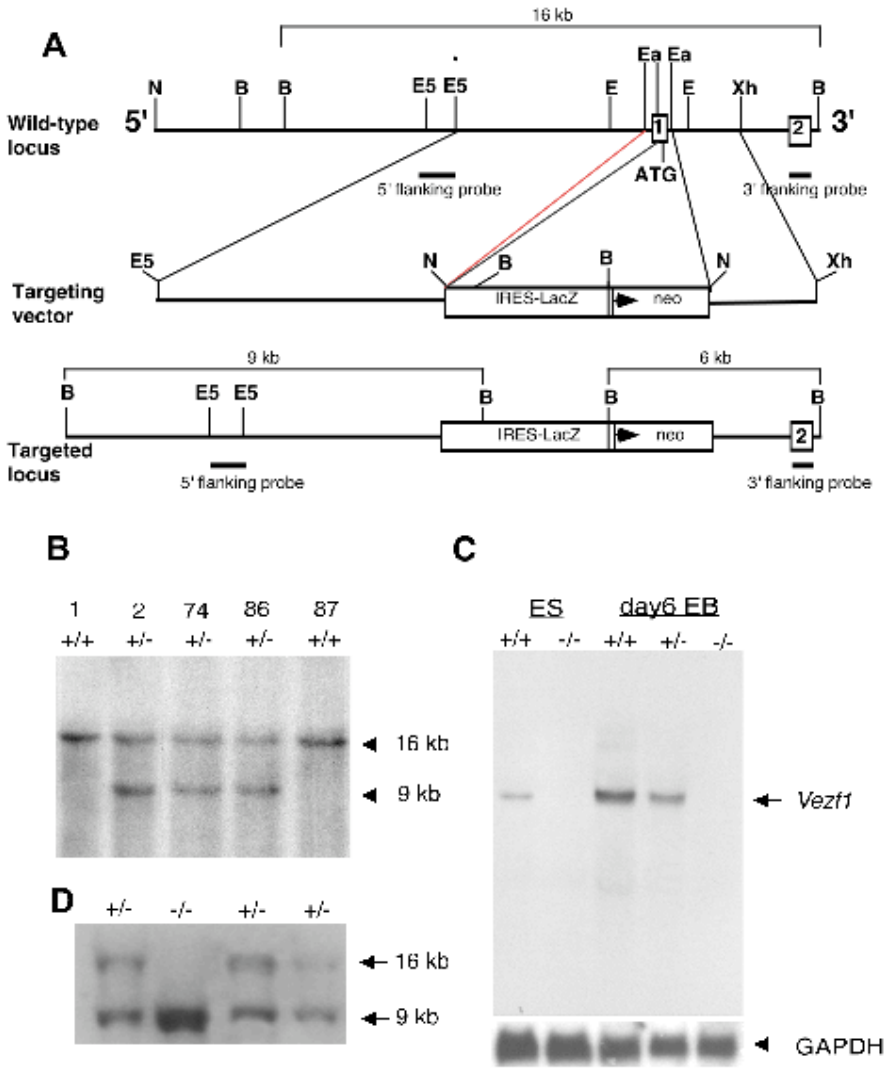

Figure 11. Targeted inactivation of the *Vezf1* gene.
(A) Targeting strategy. Part of the first exon containing the translation initiation codon ATG was to be deleted and replaced with a promoterless IRES-*LacZ*/neo expression cassette. The red line indicates the actual targeting event, in which the IRES-Neo/neo expression cassette was inserted upstream of the transcriptional start site.
(B) Genomic DNA from transfected ES cells was digested with BamHI, blotted, and hybridized with the 5' flanking probe. Sizes of hybridizing fragments are indicated. Genotypes of ES cells are indicated at the top of the lane.
(C) Northern blot analysis using total RNA from ES cells and day 6 embryoid bodies (EBs) with a probe corresponding to exon 2 of the *Vezf1* gene. Genotypes are indicated at the top of the lane. Filters were rehybridized with GAPDH probe to control for RNA loading.
(D) Southern blot analysis of DNA isolated from ES cell clones subjected to a G418 hyperselection protocol. Conditions used are as described in (B).

blot analysis, one positive clone was identified (Fig. 11D). Due to the inefficiency of this approach, a second strategy to obtain homozygous mutant ES cells was devised. A new targeting vector was constructed with the *neomycin* resistance gene expression unit replaced with a *puromycin* module, thus allowing for the targeting of the wild type allele in heterozygous ES cell clones. Given the frequency of 3% for the initial targeting event in

wild type R1 ES cells, the expected targeting frequency for the second *Vezf1* allele is 1.5 % (as both, the wild type and the mutant alleles can be subject to the homologous recombination event). However, the analysis of 400 puromycin resistant clones did not yield any additional homozygous mutant clones.

To confirm that *Vezf1* was disrupted by the targeting scenario, Northern blot analysis of total RNA isolated from ES cells and day 6 embryoid bodies (EBs) was performed. Using a [□-^{32}P] dCTP-labeled probe corresponding to the first two exons (probe A in Figure 4; nucleotides 3-776), which account for about half of the *Vezf1* coding sequence, low levels of a *Vezf1*-specific transcript of 4.2 kb length were detected in wild type R1 ES cells (as shown previously (Xiong *et al.*, 1999), whereas no *Vezf1* message was detectable in the undifferentiated *Vezf1*$^{-/-}$ ES cell clone (Fig. 11C) Similarly, *Vezf1* was found to be expressed at elevated levels in wild type day 6 embryoid bodies (EBs), but showed reduced expression in *Vezf1*$^{+/-}$ EBs and was undetectable in *Vezf1*$^{-/-}$ EBs (Fig. 11C). Subsequent Northern blot analysis of total RNA from E10.5 embryos using probes corresponding to exons1-2, exons 3-5 and the 3' UTR of *Vezf1* (probes A, C and B) confirmed the absence of *Vezf1* transcripts in homozygous mutant embryos (Fig. 7). In addition, *Vezf1* mRNA could not be amplified from RNA of *Vezf1*$^{-/-}$ embryos using the more sensitive quantitative real time RT-PCR approach (data not shown). Taken together, these results demonstrate that targeting of the *Vezf1* locus resulted in the disruption of the *Vezf1* transcripts and generated a null allele.

Attempts to visualize *Vezf1* expression employing the inserted IRES-*LacZ* reporter gene in heterozygous and homozygous mutant days 6 EBs by histochemical □ galactosidase staining did not produce any signal. This finding prompted the reexamination of the construction of the targeting vector. Sequence analysis of the 5' genomic region revealed the presence of a previously overlooked EagI restriction site 91 bp upstream of the transcriptional start site. Thus, as EagI was used for the insertion of the IRES-*LacZ* cassette in the construction of the targeting vector, the entire first exon had been deleted in the targeting construct (Fig 11A). Accordingly, the IRES-*LacZ* reporter gene was inserted into the untranscribed 5' genomic region, rendering it nonfunctional as monitoring device for endogenous *Vezf1* expression.

3.2.2 Analysis in a mixed genetic background

Chimeric males were mated with C57BL/6 females to generate F1 (129/SvxC57BL/6) offspring. Agouti F1 animals were genotyped by Southern blot analysis of tail DNA using the 5' external fragment as probe. Male animals that were heterozygous for the targeted allele were bred with outbred CD-1 females to generate a large number of heterozygous F2 offspring for the initial characterization of the phenotype. Offspring from intercrosses of heterozygous F2 ((129/SvxC57BL/6)xCD-1) mice were analyzed for viability between embryonic day 10.5 (E10.5) and 3 weeks of age. As shown in Table 3, no viable *Vezf1*$^{-/-}$ offspring were recovered among 46 pups analyzed at 3 weeks of age. However, stillborn *Vezf1*$^{-/-}$ pups were found that displayed signs of severe hemorrhaging in the head and trunk region. These appeared at about 60% of the expected Mendelian frequency, suggesting that the *Vezf1* mutation is perinatal lethal. To account for the remaining 40% of homozygotes, embryos at various stages of gestation were isolated and their yolk sacs were genotyped by Southern blot or PCR analysis. E10.5 and E11.5 embryos showed Mendelian segregation of the *Vezf1*$^{-/-}$ genotype, and up to E11.5, embryos appeared phenotypically normal.

DEVEL. STAGE	# OF EMBRYOS/PUPS	+/+	+/-	-/-
E10.5	14	3	7	4
E11.5	14	3	6	5
E12.5	44 2 resorbed	16 0	26 0	2 2
E13.5	10	3	7	0
E14.5	35 1 resorbed	10 0	20 0	5 1
E15.5	12 2 resorbed	2 0	9 0	1 2
E16.5	2	1	1	0
P0	53	15	30	8 (stillborn)
P21	46	16	30	0

Table 3. Genotypes of progeny from heterozygous intercrosses in a mixed genetic background.

Beginning at E12.5 and continuing until birth, hemorrhaging embryos that were in the process of being resorbed were observed (Table 3). Histological analysis revealed that homozygous mutant embryos showed different degrees of internal bleeding and vascular malformations (data not shown, see below) in the head and the trunk region. Interestingly,

vascular abnormalities were also observed in heterozygous mutant embryos, albeit at a low frequency (~10%).

In summary, in a mixed and outbred genetic background, a variable mutant phenotype is observed. Death, presumably due to hemorrhaging and vascular malformations, occurs between E12.5 and birth, classifying the mutation as embryonic lethal with incomplete penetrance.

3.2.3 Analysis in the C57BL/6 background

The practical effect of analyzing a mutation in a variable genetic background is that any variation in the mutant phenotype between individual animals might be attributable to unknown, segregating modifier genes rather than the mutation itself (Ihle, 2000). Thus, to test if the observed variability of phenotype was a consequence of the mixed genetic background, the mutated allele was backcrossed into the C57BL/6 inbred strain in order to create (genetically uniform) congenic mouse lines. For this, *Vezf1*$^{+/-}$ males were mated with C57BL/6 females and offspring were genotyped by PCR. Mice are considered congenic after ten generations of backcrossing. With an estimated generation time of 3 months the derivation of congenic strains would require at least two and a half years of breeding. Therefore, due to time constraints, the phenotypical analysis of the F5 backcross generation will be presented here. In the F5 backcross generation, the genetic background is greater than 90% congenic.

CROSS	# OFFSPRING/# LITTERS	+/+	+/-
Vezf1+/- x C57BL/6	296 /59	174 ~ 59%	122 ~ 41%

Table 4. Genotypes of adult offspring in the F4 C57BL/6 background.

While producing a large number of F4 mice for the subsequent intercrosses, an under-representation of heterozygous mice was noticed (Table 4). When genotyped at weaning age heterozygous mice appeared phenotypically normal and were fertile, but were recovered at a ratio of only 80% of the expected frequency. Thus, the viability of heterozygous mice appears to be reduced, as about 1/5 of *Vezf1*$^{+/-}$ animals appear to die before birth (as no reduction in the heterozygous offspring number was observed between

birth and weaning). This finding is consistent with the vascular defects detected in *Vezf1*$^{+/-}$ embryos in the outbred background (see above).

To examine the mutant phenotype in the F5 C57BL/6 generation, embryos from intercrosses of heterozygous F4 mice were isolated between E8.5 and birth (Table 5). Embryos were initially inspected visually under a dissection microscope, overtly abnormal embryos were photographed and yolk sacs were collected for genotyping. Manifestations of the *Vezf1* KO phenotype became apparent at E9.5. Viable *Vezf1*$^{-/-}$ embryos were recovered at a frequency of 14% (instead of the expected Mendelian distribution of 25%). Five out of nine (56%) of the E9.5 *Vezf1*$^{-/-}$ embryos displayed varying degrees of internal hemorrhaging in the pericardial cavity and within the head and abdomen (Fig. 12A). At later stages of embryonic development, *Vezf1*$^{-/-}$ embryos, some of them overtly hemorrhaging, were found at sub-Mendelian frequencies up to E16.5, but no stillborn homozygous mutants were detected (Table 5). An example of an E12.5 *Vezf1*$^{-/-}$ embryo with extensive hemorrhaging in the head and neck region is shown in Figure 14A.

DEVEL. STAGE	# OF EMBRYOS	+/+	+/-	-/-
E 8.5	9	2	6	1
E 9.5	60	18	33	9 (5)
E10.5	33	8	21	4 (2)
E11.5	30	6	21	3 (1)
E12.5	56	14	36 (7)	6 (2)
E13.5	14	1	12 (3)	1
E14.5	13	5	7	1
E16.5	11	2	8	1 (1)
P0	21	9	13	0

Table 5. Genotypes of embryos for the F5 C57BL/6 backcross generation. Values in parentheses indicate hemorrhaging embryos.

Starting at E12.5, approximately 20% of heterozygous embryos showed localized edema and hemorrhaging in the back and neck region (Table 5, Fig. 16A, B). At E13.5, these embryos appeared bloated, displaying massive edema, hemorrhaging, and signs of tissue necrosis in back and neck (Fig. 16D, E). *Vezf1*$^{+/-}$ embryos with this mutant phenotype could not be detected at later embryonic stages, and presumably did not survive beyond E14.5.

In summary, in the F5 C57BL/6 backcross generation we observed a variable mutant phenotype that is more severe than that in the mixed genetic background. We detected an earlier onset of the mutant phenotype in *Vezf1*$^{-/-}$embryos, with internal bleeding and death

becoming apparent at E9.5, as well as a higher occurrence of vascular defects and lethality in heterozygous embryos. This incompletely penetrant, haploinsufficient (autosomal) phenotype implicates that *Vezf1* acts in a tightly regulated, dose-dependent manner during vascular development. It is important to note that this haploinsufficient phenotype is not caused by imprinting of the *Vezf1* wild type allele, as both male and female *Vezf1*$^{+/-}$ mice were used for backcrossing and both sexes generated viable heterozygous offspring.

3.2.3.1 Vascular remodeling defects and hemorrhaging in E9.5 *Vezf1*$^{-/-}$ embryos

As the first vascular abnormalities were observed at E9.5, the morphology of the developing vasculature of E9.5 *Vezf1*$^{-/-}$ embryos and yolk sacs were characterized in detail. For this, whole-mount immunohistochemical staining using monoclonal antibodies against platelet endothelial cell adhesion molecule-1 (PECAM-1), a specific marker for endothelial cells (Baldwin *et al.*, 1994), was employed. PECAM-1-stained wild type (Fig. 12D) and heterozygous embryos exhibited a complex, hierarchically organized vessel architecture. In the trunk region, the dorsal aorta, the first three aortic arch arteries, the anterior cardinal vein and the intersomitic vessels were easily recognizable. On their dorsal side, the intersomitic vessels branched into a highly arborized capillary network that extended anteriorly into the neck region of the embryo. The head showed a delicately structured vascular system with large caliber vessels extending from the anterior cardinal vein and the internal carotid artery branching into a finer vascular lattice. *Vezf1*$^{-/-}$ embryos, in contrast, displayed an overall less developed and disorganized vascular network (Fig. 12B). Homozygous mutant embryos had normally formed dorsal aortae and cardinal veins, indicating that vasculogenesis had occurred properly, but displayed abnormalities in the aortic arch artery system. In all embryos examined, a functional second aortic arch artery was missing, and half of these embryos displayed a rudimentary first branchial arch artery that had failed to develop a lumen (Fig. 12B and E). In addition, the vasculature in the neck region and the dorsal region of the intersomitic vessels showed poor organization and was less branched than in their wild-type counterparts (Fig. 12B, D). Finally, the vasculature in the head of *Vezf1*$^{-/-}$ mutant embryos appeared disorganized and under-developed, although large and small caliber vessels were visible (Fig. 12B).

Histological analysis of parasagittal sections through PECAM-1 stained E9.5 *Vezf1*$^{-/-}$ embryos confirmed the defects in the aortic arch artery system. Figure 12E shows a representative embryo, in which the first aortic arch artery is abnormally shaped, while the

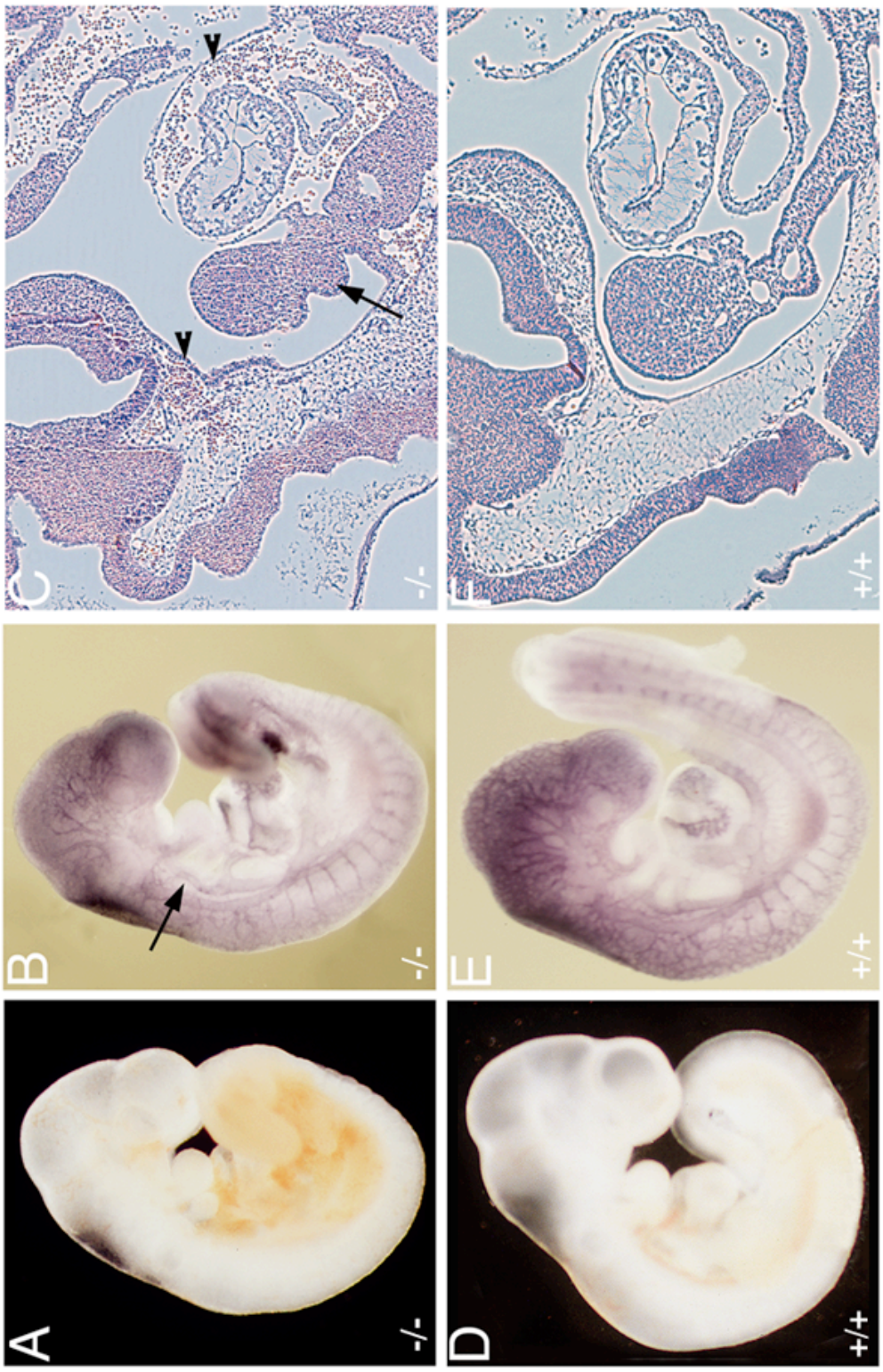

Figure 12. Vascular defects in E9.5 *Vezf1*$^{-/-}$ embryos Photomicrographs of E9 *Vezf1*$^{-/-}$ (A) and wild type (D) embryos. *Vezf1*$^{-/-}$ embryos displayed hemorrhaging in the head, the trunk and the pericardial cavity. (B and E) Whole mount immunohistochemistry for PECAM-1. The vasculature in head, neck and dorsal part of intersomitic vessels of *Vezf1*$^{-/-}$ embryos (B) appeared disorganized and less developed than in wild type controls (E). The arrow indicates the absence of the second aortic arch artery in *Vezf1*$^{-/-}$ embryos. (C and F) Histological sections of E9.5 embryos. *Vezf1*$^{-/-}$ embryo (C) displayed hemorrhaging in the head and the pericardial cavity (arrowheads). Note also the absence of the second aortic arch artery (arrow). (F) Wild type control.

second one is missing altogether. Furthermore, histological analysis revealed distinct sites of internal bleeding, typically in the head and trunk. In the embryo shown in Figure 12E, the pericardial cavity was enlarged and filled with blood. In addition, an unusual number of dilated, hemorrhaging vessels was observed in the head.

The analysis of the E9.5 *Vezf1*$^{-/-}$ yolk sacs vasculature by PECAM-1 staining did not reveal any vascular abnormalities. Consistent with normal vascular remodeling, E9.5 *Vezf1*$^{-/-}$ yolk sacs displayed a regular hierarchical vascular pattern that was indistinguishable from that of wild-type controls at the whole-mount level (Fig. 13A, B).

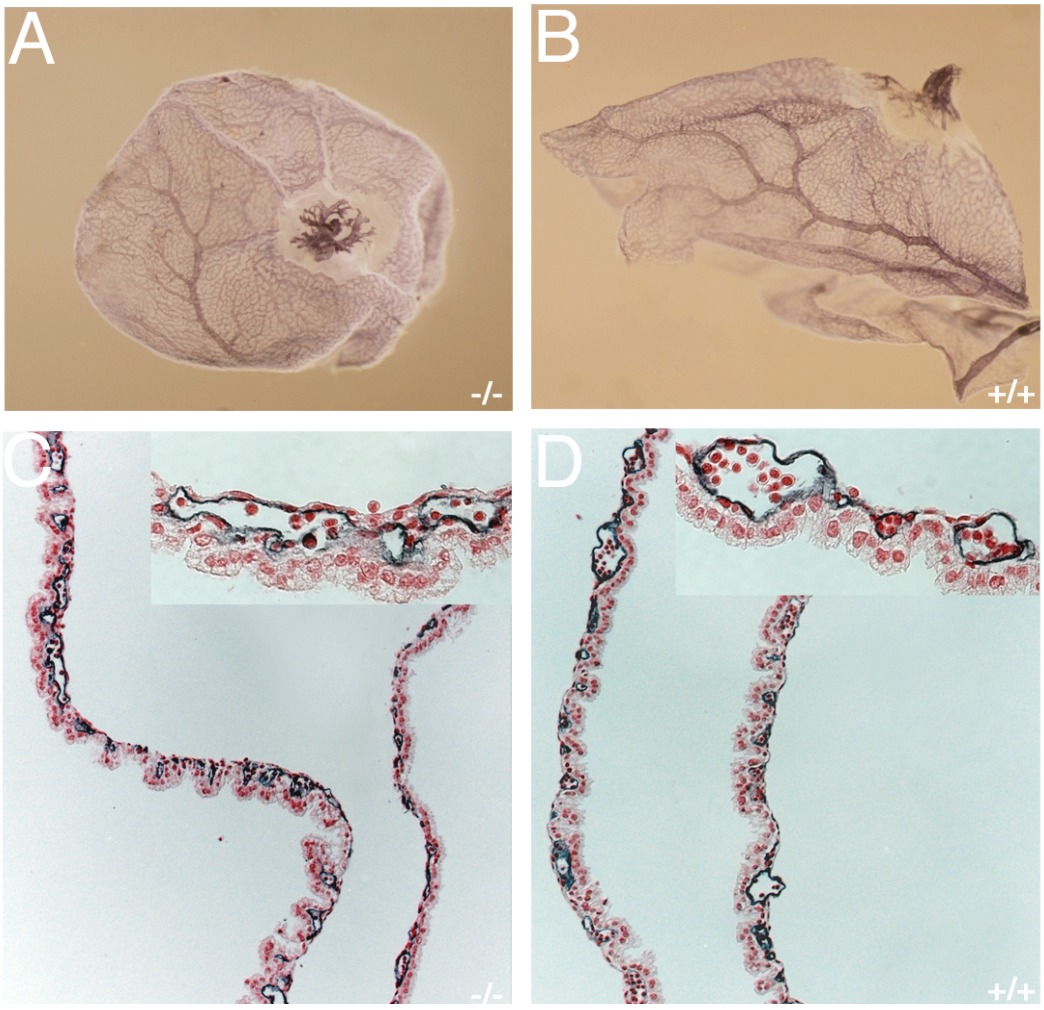

Figure 13. Normal vascular development in *Vezf1*$^{-/-}$ yolk sacs.
Whole-mount PECAM-1 staining of E9.5 *Vezf1*$^{-/-}$ yolk sacs (A) revealed a regular hierarchical vascular pattern that is indistinguishable from that of wild type controls (B).
Histological sections of PECAM-1 stained *Vezf1*$^{-/-}$ yolk sacs (C) did not show any signs of vascular disorganization or lesion. (D) Wild type control.

Furthermore, histological sections of *Vezf1*$^{-/-}$ mutant yolk sacs displayed normal looking blood islands and vascular patterns, and did not show any signs of vascular lesions and

hemorrhaging (Fig. 13C, D). Taken together, these data demonstrate that expression of *Vezf1* is neither essential for the formation of the primary vascular plexus (vasculogenesis) nor for early embryonic hematopoiesis (as embryonic vessels are filled with blood). However, a significant proportion of E9.5 embryos require *Vezf1* for proper vascular development. In particular, E9.5 *Vezf1*$^{-/-}$ embryos show defects in angiogenic remodeling of the vasculature in the aortic arch system, the head, the neck and the dorsal part of the intersomitic vessels. In addition, frequent sites of internal bleeding are detected in E9.5 *Vezf1*$^{-/-}$ embryos, indicating that *Vezf1* function is required for the maintenance of the integrity of the embryonic vasculature.

3.2.3.2 Analysis of E12.5 *Vezf1*$^{-/-}$ embryos

A fraction of homozygous mutant embryos survive up to E16.5, and their gross examination showed localized hemorrhaging (Table 5, Fig. 14A). To analyze the development of the vascular system in *Vezf1*$^{-/-}$ embryos at late midgestation, sagittal sections of E12.5 embryos were stained with anti-PECAM-1 antibody. The PECAM-1 staining revealed that the E12.5 *Vezf1*$^{-/-}$ embryos displayed apparently normal vascular patterning that is indistinguishable from that observed in age-matched wild type littermates (Fig. 14E, F), demonstrating normal angiogenic remodeling in these embryos.
The development of all organ systems including the heart and the placenta appeared normal in histological sections of H+E stained *Vezf1* $^{-/-}$embryos (Fig. 14C and D). However, localized hemorrhaging was observed, typically in the head and in the neck region, indicating that the integrity of the vasculature is compromised in E12.5 *Vezf1* KO embryos. The representative E12.5 *Vezf1*$^{-/-}$ embryo shown in Figure 14C displays hemorrhaging in the subcapsular mesenchyme of the head and in the jugular region.

3.2.3.3 Normal smooth muscle cell maturation and recruitment in *Vezf1*$^{-/-}$ embryos

After the initial formation of the vascular plexus, blood vessels mature by stabilizing the endothelial network through recruitment of vascular smooth muscle cells (VSMCs) and pericytes that ultimately results in the investment of vessel walls with mural cells. VSMCs first appear on the ventral side of the aorta in E10.5 embryos, followed by migration to the

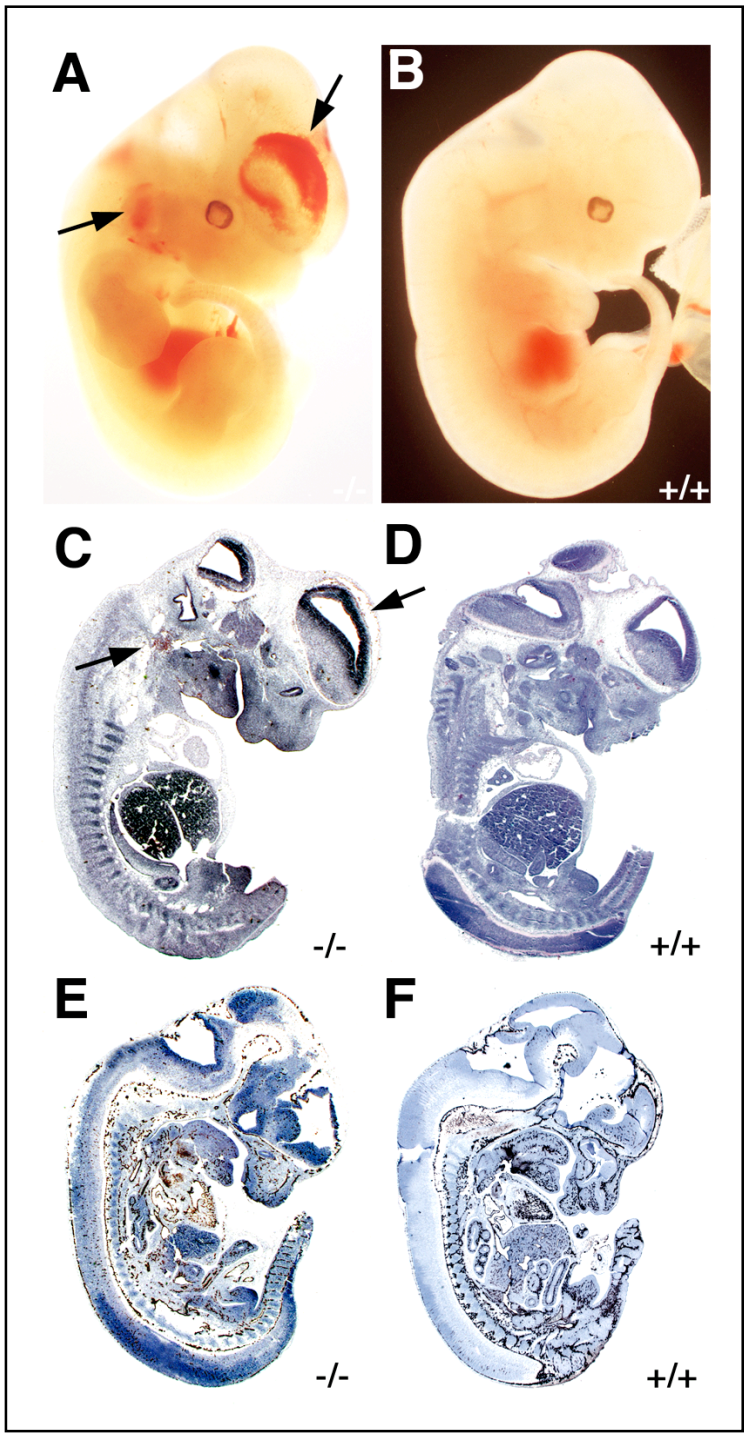

dorsum. By E11.5, the aorta is completely enveloped by VSMCs. Defects in the differentiation and/or recruitment of VSMCs or pericytes lead to the formation of destabilized, leaky blood vessels and consequently lethal hemorrhage, as has been shown previously in mice lacking Edg-1, LKLF and PDGF-B (Liu *et al.*, 2000) (Kuo *et al.*, 1997) (Lindahl *et al.*, 1997)

Figure 14. Hemorrhaging in E12.5 *Vezf1*$^{-/-}$ embryos. Whole-mount images of E12.5 *Vezf1* KO (A) and wild type (B) embryos. The E12.5 KO embryo displayed hemorrhaging in the in the jugular region and the subcapsular head mesenchyme (arrows).
Histological analysis of E12.5 KO (C) and wildtype (D) embryos. Arrows indicate bleeding in the jugular region and the subcapsular head mesenchyme.
Immunohistochemical PECAM-1 staining revealed normal vascular patterning in KO (E) and wild type embryos (E).

To address this aspect of vessel development in E12.5 *Vezf1* KO embryos, VSMCs were identified by immunohistochemical staining with anti-SM□-actin antibodies (anti-SM□A). In parasagittal sections of anti-SM□-actin stained E12.5 wild type and *Vezf1*$^{-/-}$ embryos, the dorsal aorta was found to be completely surrounded by VSMCs (Fig. 15A, B). Likewise, cross sections through the dorsal aorta and umbilical artery demonstrated that both vessels were enclosed by several layers of VSMCs in mutant as well as in wild-type embryos (Fig. 15C, D). These results demonstrate that differentiation and recruitment of

VSMCs are normal in E12.5 *Vezf1*$^{-/-}$ embryos and exclude mural cell defects as a cause for the observed vascular defects.

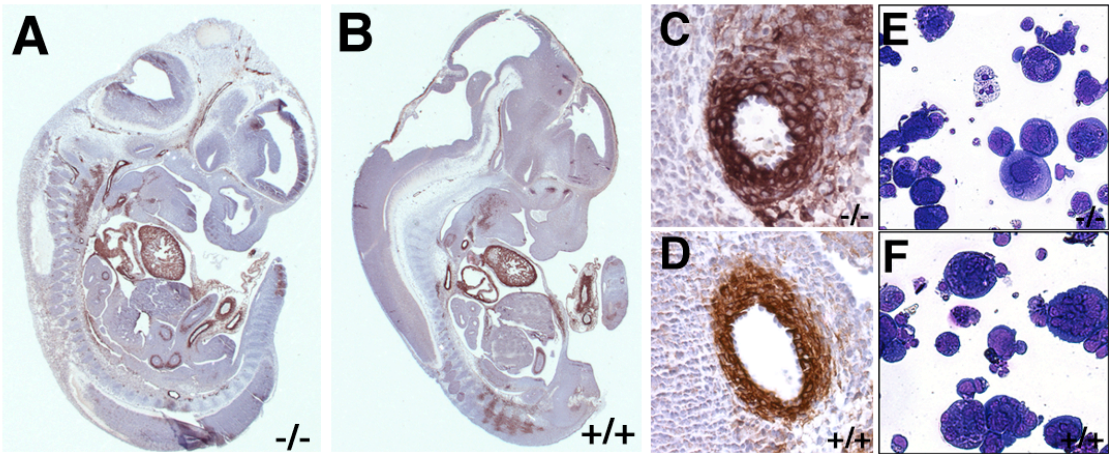

Figure 15. Normal vascular smooth muscle cell and megakaryocyte development in E12.5 *Vezf1*$^{-/-}$ embryos. SM□-actin staining of sagittal sections demonstrates normal vascular smooth muscle cell (VSMC) differentiation and recruitment in *Vezf1* KO (A) and wild type (B) embryos.
In transverse sections, the dorsal aorta is found to be surrounded by several layers of VSMCs in *Vezf1* KO (C) and wild type (D) embryos.
Wright-Giemsa staining of in vitro cultured E12.5 embryonic liver cells reveals normal megakaryocytopoiesis in *Vezf1*$^{-/-}$ embryos (E). (F) Wild type control.

3.2.3.4 Normal megakaryocyte development in *Vezf1* $^{-/-}$ embryos

Defects in the differentiation of megakaryocytes have been shown to lead to defective platelet formation and control of coagulation, resulting ultimately in lethal hemorrhaging (Spyropoulos *et al.*, 2000). Thus, it was investigated if loss of *Vezf1* function could lead to aberrant megakaryocytopoiesis. To address this question, fetal liver cells from E12.5 from wild type and *Vezf1*$^{-/-}$ embryos were cultivated *in vitro* and analyzed for their potential to give rise to megakaryocytes (Era *et al.*, 1997). After 5 days of culture, megakaryocytes and proplatelet differentiation became apparent in both, wild type and mutant cultures. The analysis of cytospin preparations of these cultures by Wright-Giemsa-staining confirmed normal megakaryocyte differentiation in homozygous mutant embryos (compare Fig. 15E and F). This finding demonstrates that *Vezf1* is not required for the differentiation of megakaryocytes and supports the notion that the intra-embryonic bleeding in *Vezf1*$^{-/-}$ embryos is a direct result of vascular deficiencies.

3.2.3.5 Vascular malformations in E13.5 *Vezf1*$^{+/-}$ mutant embryos

Starting at E12.5 localized hemorrhaging and edema became apparent in about 20% of the *Vezf1*$^{+/-}$ embryos (Fig. 16A, B and C). By E13.5, these embryos appeared bloated and displayed massive edema and bleeding in the back and neck region (Fig. 16D, E and F).

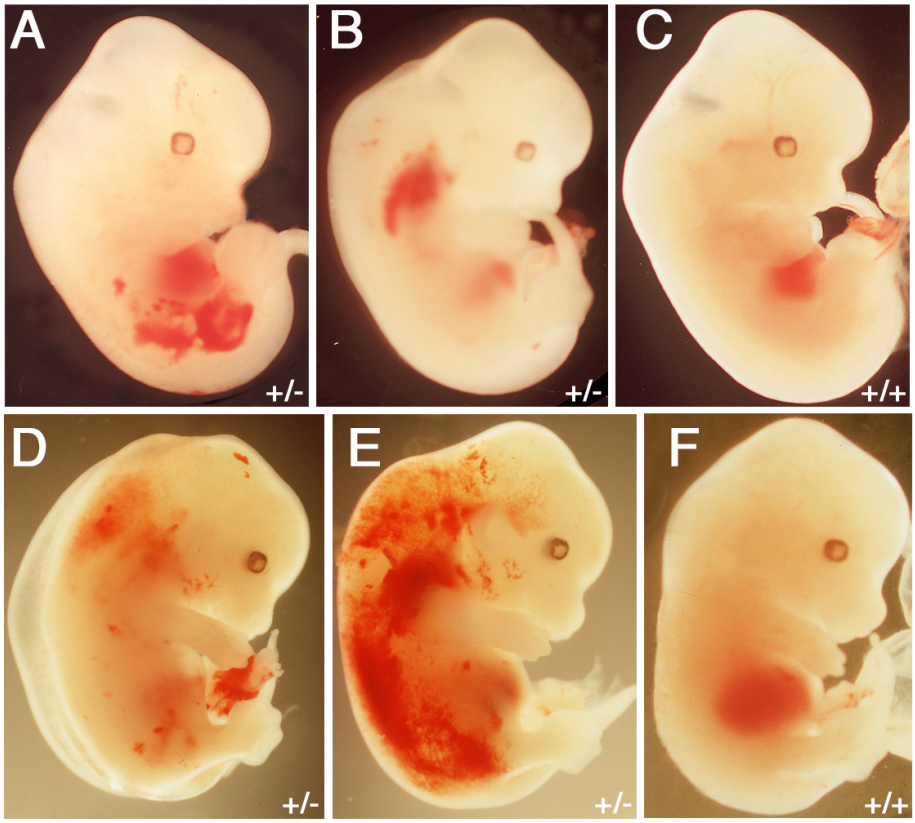

Figure 16. Hemorrhaging and edema in *Vezf1*$^{+/-}$ embryos.
Photomicrographs of E12.5 (A-C) and E13.5 (D-F) embryos. Hemorrhaging became apparent in the jugular and perimesonephric region of E12.5 *Vezf1*$^{+/-}$ embryos (A and B). E13.5 *Vezf1*$^{+/-}$ embryos (D and E) displayed severe hemorrhaging and edema in back and neck. (C, F) Wild type controls.

Histological analysis revealed severe edema, with tissue swelling and masses of loose connective tissue and mesenchymal cells separated by interstitial fluid, as well as subcutaneous bleeding in the back and neck region of heterozygous E13.5 embryos (Fig. 17A, 18G, H). Furthermore, in H+E stained parasagittal sections, a dramatic increase in the number of vessels was detected in the dorsal part of the heterozygous embryos in close association with the jugular sac (Fig. 17A, C, E, F). These vessels appeared enlarged, irregular shaped, anastomosing and often hemorrhaging. PECAM-1-staining was used to outline the vascular endothelium in parasagittal sections of these embryos. The staining revealed that the *Vezf1*$^{+/-}$ embryos displayed an overall normal looking vascular pattern and that hypervascularization was confined to the jugular region (Fig. 18A, C). High-power photomicrographs of PECAM-1 stained sections in the region of

hypervascularization identified occasional sites of vascular lesions, with erythrocytes leaking out into the surrounding mesenchymal tissue (Fig. 18E, F), indicating the loss of vessel integrity. Quantitative morphometric analysis (performed in collaboration with Dr. Humphrey Gardener, Biogen, Cambridge) of the PECAM-1 stained sections confirmed that the overall vessel number and the total vessel area were increased in the mid back region of the heterozygous embryos (Fig. 19). Morphometric analysis further showed that the endothelial cell density (i.e. the number of endothelial cells per vessel wall unit) was higher in the *Vezf1*$^{+/-}$ embryos than in the wild type controls. Taken together, these results suggest that localized endothelial hyperproliferation leads to the formation of aberrant, dysfunctional vessels in the back and neck of *Vezf1*$^{+/-}$ embryos.

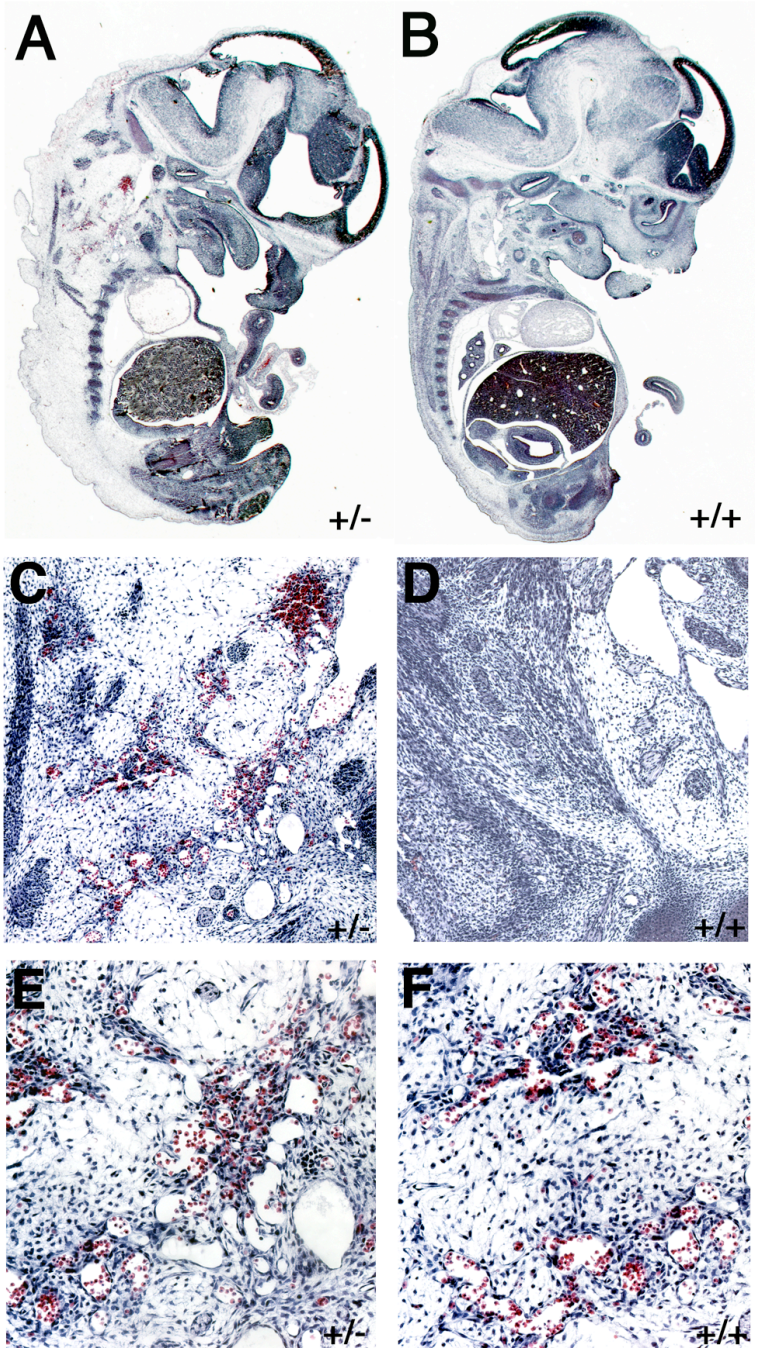

Figure 17. Histological analysis of heterozygous E13.5 embryos.
H+E staining of parasagital sections of E13.5 *Vezf1*$^{+/-}$ (A) and wild type embryos (B) demonstrate severe edema in the back region as well as hypervascularization and hemorrhaging in the jugular area of the heterozygous embryos. (C-F) Higher magnification images of the jugular region of heterozygous (C, E, F) and wild type (D) embryos.

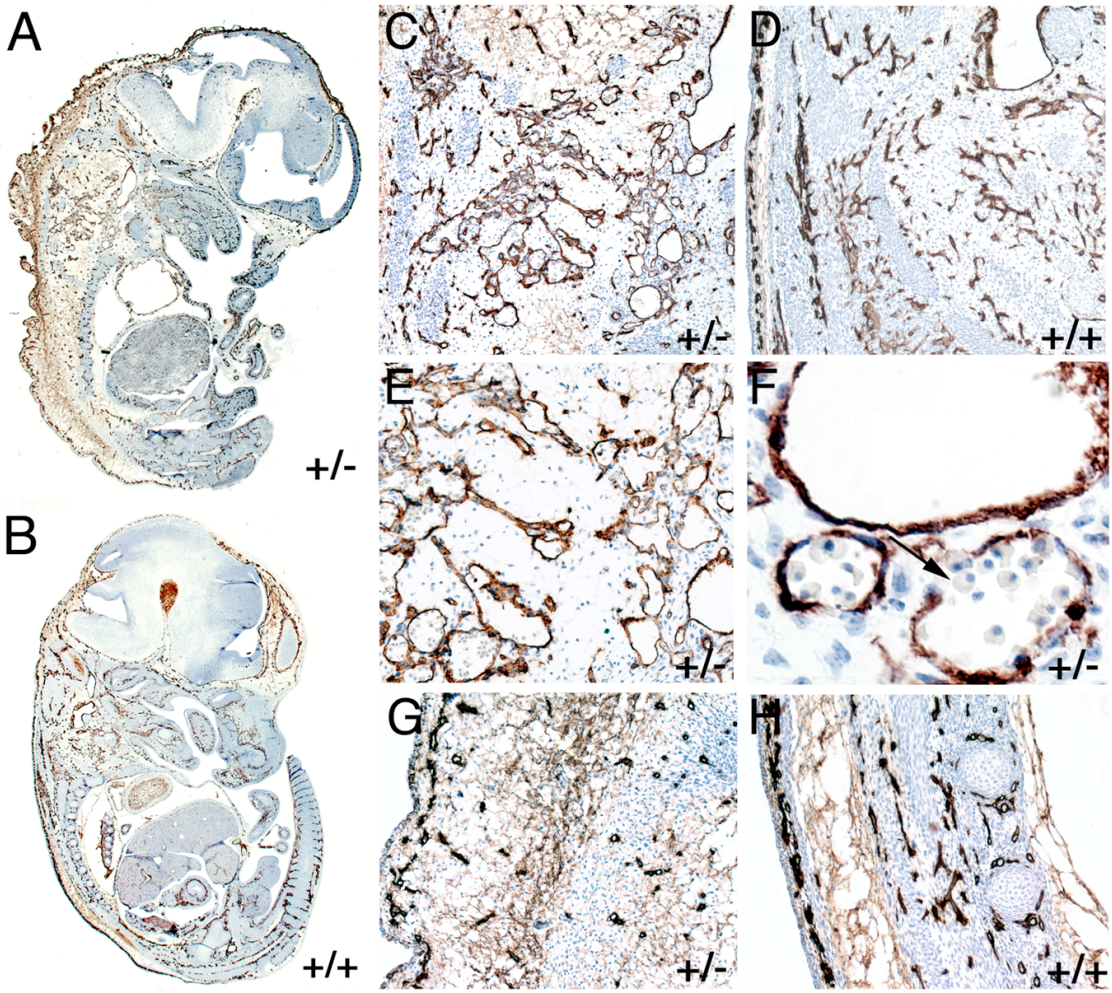

Figure 18. PECAM-1 staining of heterozygous E13.5 embryos. PECAM-1 staining to outline the embryonic vasculature confirmed that hypervascularization was confined to the neck region of heterozygous embryos (A). (C-F) High magnification photomicrographs of the jugular region. In heterozygous embryos sites of vascular lesions associated with erythrocytes leaking into the surrounding connective tissue (arrow) were detected in the neck region (F). Heterozygous mutant embryo (G) displayed tissue swelling and masses of loose connective tissue characteristic of severe edema in the back and neck region. (B, D, H) Wild type controls.

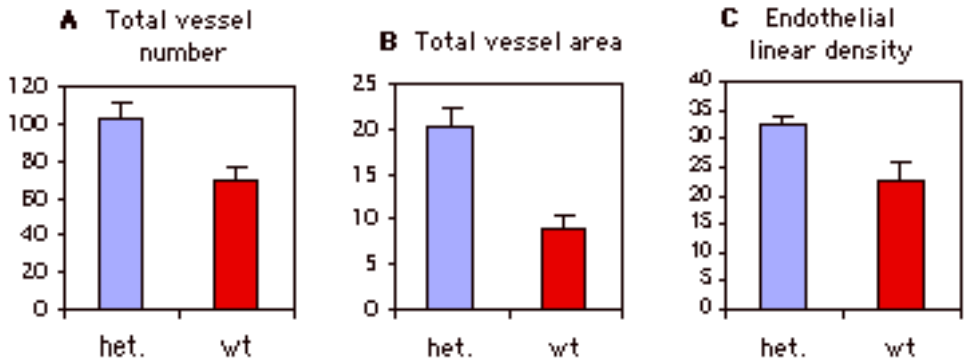

Figure 19. Quantitative morphometric analysis of the vasculature in the jugular region of heterozygous and wildtype E13.5 embryos. (A) Total vessel number, (B) Total vessel area, (C) Endothelial linear density (n=3).

3.2.3.6 Lymphatic hypervascularization in E13.5 *Vezf1*$^{+/-}$ mutant embryos

Vascular defects in the heterozygous embryos appeared to be confined to the jugular region. This is the major site of sprouting of the developing lymphatic vessels from the venous system (Sabin, 1909), a process that becomes apparent between E12.5 and E13.5 in the mouse embryo (Kaipainen *et al.*, 1995; Kukk *et al.*, 1996). To determine whether this process was affected in E13.5 *Vezf1*$^{+/-}$ embryos, parasagittal sections were analyzed for the expression of the lymphatic markers VEGFR-3 (Flt-4) (Kubo *et al.*, 2000) and LYVE-1 (Banerji *et al.*, 1999; Prevo *et al.*, 2001). VEGFR-3 is expressed in venous endothelium during early embryonic development but becomes restricted to the lymphatic vessels after their formation (Kaipainen *et al.*, 1995). Thus by E13.5, VEGFR-3 is most prominently expressed at the site of lymphatic vessel development in the jugular region (Dumont *et al.*, 1998; Kukk *et al.*, 1996). LYVE-1 is a receptor for the glycosaminoglycan hyaluronan and is specifically expressed in the lymphatic endothelium (Banerji *et al.*, 1999; Prevo *et al.*, 2001). During embryogenesis, LYVE-1 is first detected around E12.5, marking the nascent lymphatic vessels (D. Jackson, MRC Oxford, personal communication).

VEGFR-3 (Fig. 20 B, H) and LYVE-1 (Fig. 20 A, J) expression in wild type embryos was detected in the endothelium lining the jugular sac and in small capillaries of the neck mesenchyme. In *Vezf1*$^{+/-}$ embryos, in addition to these structures, also the hyperplastic vessels in the jugular region stained positive for the two lymphatic markers (Fig. 20 A, C, G, I). In contrast, they did not express SM□-actin, a marker for artery-associated VSMCs (20 E, F). These findings suggest that the hyperplastic vessels in the neck region of the heterozygous embryos are of lymphatic nature. This is an unexpected finding, as some of these vessels clearly do contain red blood cells, a defining characteristic of blood vascular structures, arteries and veins. Lymphatic vessels are thought to sprout from the existing venous system (Sabin, 1909). The apparently contradictory finding that the hyperplastic vessels in the jugular region of the E13.5 *Vezf1*$^{+/-}$ mutant embryos express markers specific for lymphatic endothelium and at the same time contain blood suggests that the process of lymphatic sprouting from the venous system is defective in the E13.5 *Vezf1*$^{+/-}$ mutant embryos

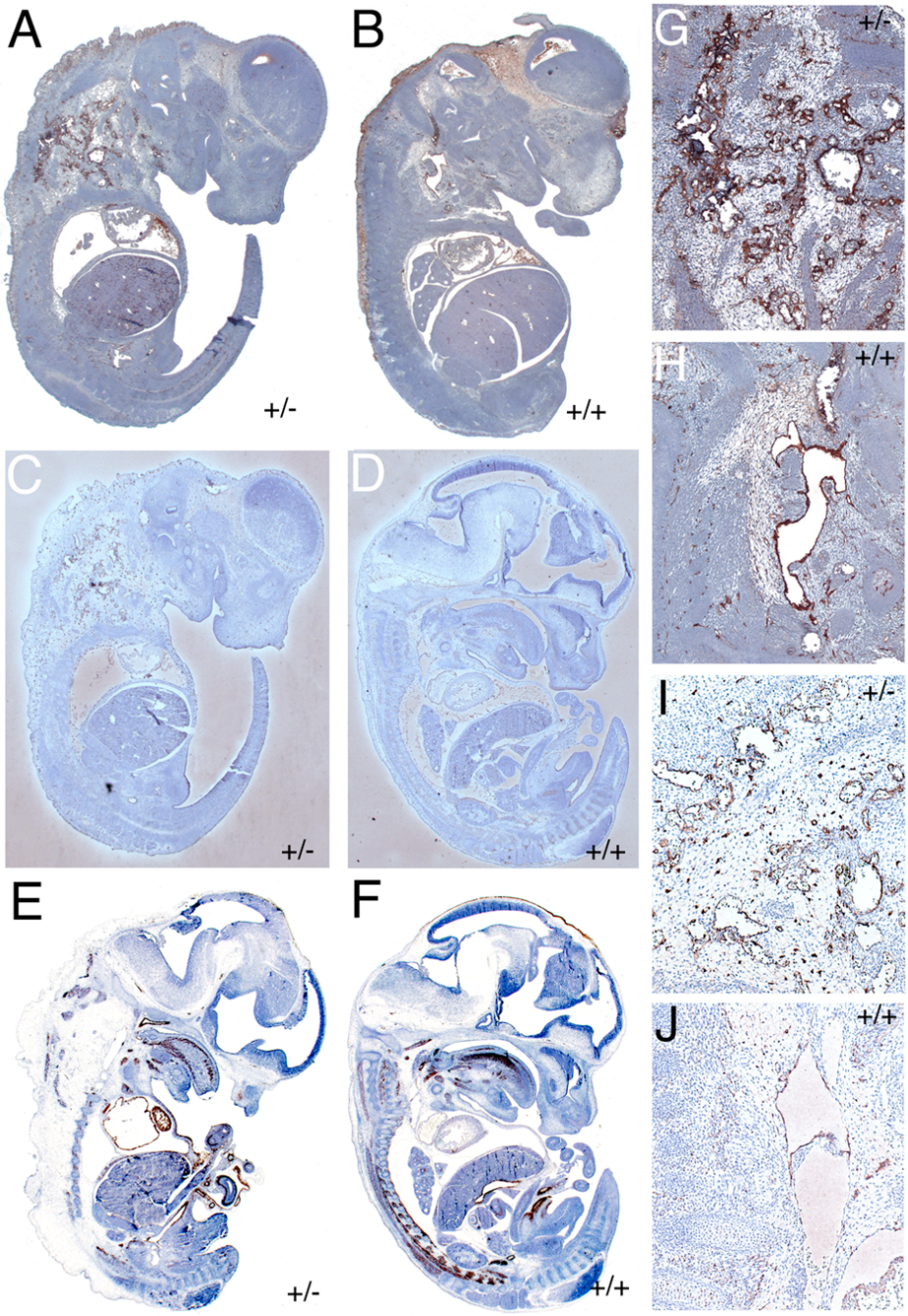

Figure 20. Lymphatic hypervascularization in heterozygous E13.5 embryos. The hyperplastic vessels in the jugular region of heterozygous E13.5 embryos stain positive for the lymphatic markers VEGFR-3 (A, G) and LYVE-1 (C, I), but are negative for the blood vessel marker SM□-actin (E). (B, D, F, H, I) Wild type controls.

3.2.3.7 Analysis of E12.5 *Vezf1*$^{+/-}$ mutant embryos

To study the etiology of the observed hypervascularization phenotype in heterozygotes, E12.5 *Vezf1*$^{+/-}$ embryos were analyzed. H/E stained sections revealed sites of hemorrhaging and in the subcutaneous space, the head and to a lesser degree also in the neck region of E12.5 *Vezf1*$^{+/-}$ embryos (Fig. 21). PECAM-1, VEGF-3 and LYVE-1

staining was used to outline the vasculature of these embryos (Fig. 21). Although the jugular sacs frequently appeared enlarged, hypervascularization in the jugular region was not apparent in these embryos. This finding suggests massive lymphatic expansion between E12.5 and E13.5 in *Vezf1*$^{+/-}$ embryos.

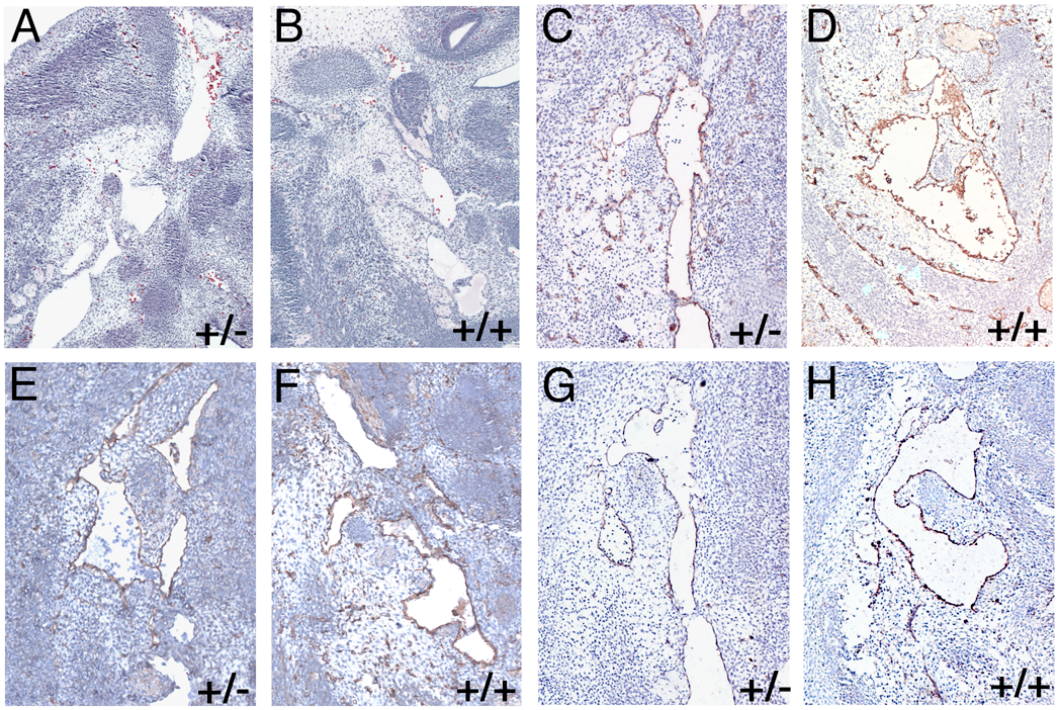

Figure 21. Immunohistochemical analysis of E12.5 *Vezf1*$^{+/-}$ and wild type embryos. H+E (A, B), PECAM-1 (C, D), VEGFR-3 (E, F) and LYVE-1(G, H) staining of the jugular region.

3.2.3.8 Gene expression analysis

Results presented thus far show that loss of *Vezf1* function leads to defects in three different aspects of vascular development: endothelial cell proliferation, angiogenic remodeling and maintenance of vascular integrity. A number of factors have been implicated in these processes and shown to display similar or partially overlapping mutant phenotypes in gene inactivation studies (Carmeliet, 2000). To assess whether loss of *Vezf1* function could be correlated with changes in expression levels for any of these factors, semi-quantitative RT-PCR analysis was performed on total RNA isolated from E10.5 *Vezf1* $^{-/-}$ embryos and wild type littermates. Because of the incompletely penetrant phenotype, E10.5 *Vezf1* KO embryos were selected for this analysis that displayed clear signs of hemorrhaging and vascular malformations. In particular, expression of the following groups of genes was examined:

1) *VEGF* and its tyrosine kinase receptors *Flt-1, Flk-1* and *Flt-4* (VEGFR-1, -2 and –3), which have been shown to be required for both vasculogenesis and angiogenesis

(Carmeliet *et al.*, 1996a; Ferrara *et al.*, 1996; Fong *et al.*, 1995; Fong *et al.*, 1999; Shalaby *et al.*, 1997; Shalaby *et al.*, 1995).In addition, in the case of *Flt-1* and *Flk-1*, specific binding of VEZF1 to a CCCCGC core element in their respective promoters was demonstrated by Xia Sun in Dr. Stuhlmann's laboratory (Sun *et al.*, 2001).

2) *Angiopoietin1* and *2,* their cognate tyrosine kinase receptor *Tie2*, and the closely related orphan receptor *Tie1*. These genes have been reported to play important roles in the angiogenic remodeling of the embryonic vasculature (Maisonpierre *et al.*, 1997; Sato *et al.*, 1995; Suri *et al.*, 1996).

3) *Notch1*, *Notch4* and their ligand *Dll 4*, which have been implicated in vascular morphogenesis (Krebs *et al.*, 2000).

4) *EphrinB2* and its receptor *EphB4*, which demarcate embryonic arterial versus venous endothelium and are involved in vascular remodeling (Adams *et al.*, 1999; Krebs *et al.*, 2000; Wang *et al.*, 1998).

5) *LKLF*, a Krüppel-like zinc finger transcription factor, *Edg-1*, the G-protein-coupled receptor for shingosine-1-phosphate, and *Endoglin*, an accessory TGF-receptor, all of which show hemorrhaging KO phenotypes (Kuo *et al.*, 1997; Li *et al.*, 1999; Liu *et al.*, 2000).

6) *Tbx-1*, a T-box transcription factor, which is required for development of the aortic arch artery system in a gene-dosage dependent manner (Lindsay *et al.*, 2001).

7) *VE-cadherin*, an endothelial cell adhesion molecule that regulates endothelial cell survival (Carmeliet *et al.*, 1999).

8) *Endothelin-1,* a vasoconstrictive signaling peptide, whose inactivation leads to malformations in the aortic arch system (Kurihara *et al.*, 1994) and whose human promoter has been recently shown to be transactivated by VEZF1 *in vitro* (Aitsebaomo *et al.*, 2001).

Primer pairs for *Vezf1* and *-actin* were included in the analysis as negative control and to normalize for RNA amounts, respectively. Results from this analysis are shown in Fig. 22. Whereas *Vezf1* transcripts were absent in *Vezf1*$^{-/-}$ embryos, each gene examined was expressed in *Vezf1* $^{-/-}$ embryos at levels comparable to those of wild type control embryos. Therefore, VEZF1 does not appear to regulate the expression of any of these genes. However, it cannot be excluded that quantitative differences in the expression levels of these genes are subtle and beyond the resolution of this RT-PCR analysis.

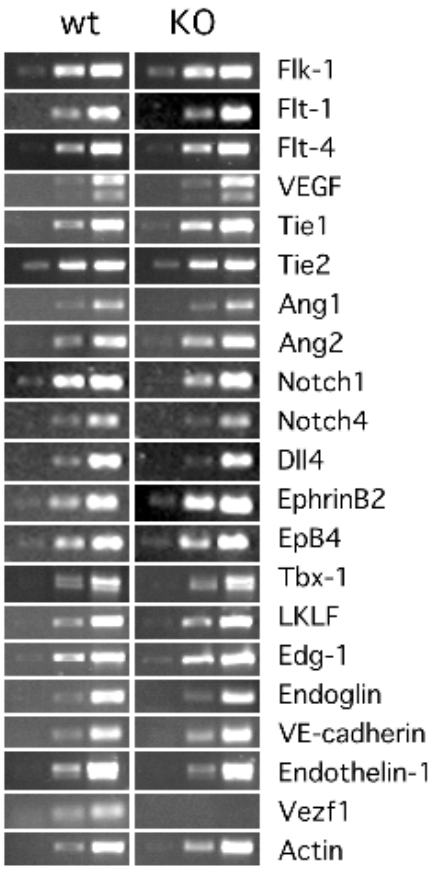

Figure 22. Gene expression analysis of *Vezf1*$^{-/-}$ embryos. Semi-quantitative RT-PCR was performed on total RNA isolated from E10.5 *Vezf1* KO and wildtype embryos.

Figure 23. RNA in situ hybridization gene expression analysis in KO and wild type E11.5 embryos.

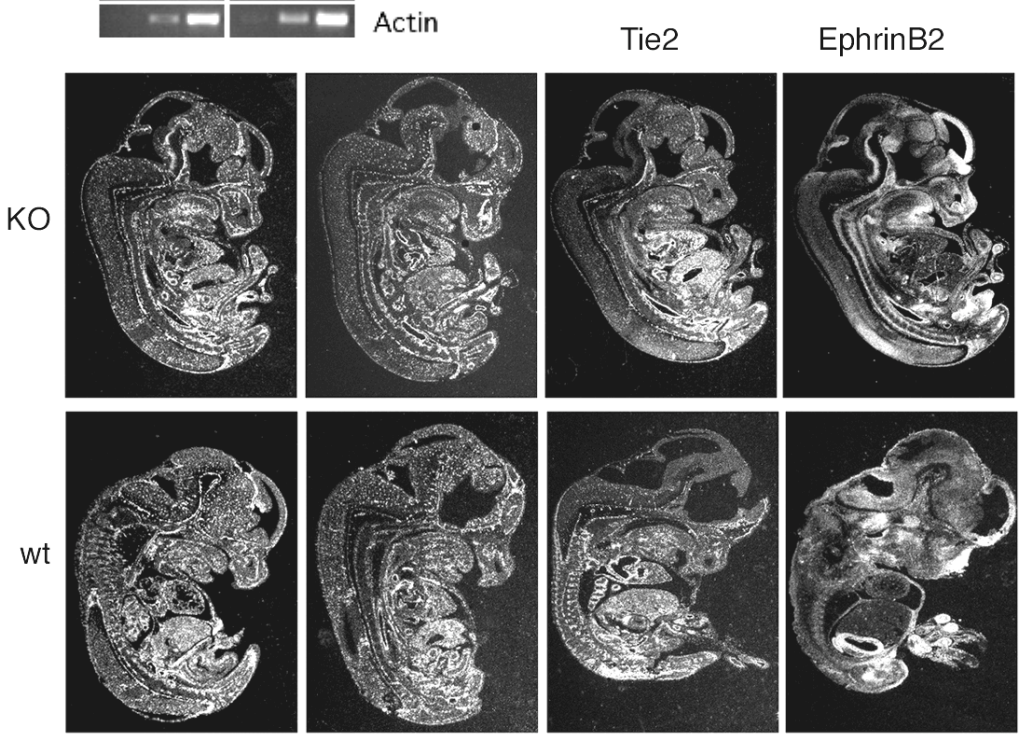

In addition, the spatial distribution of the transcripts for *Flk-1, Flt-1, EphrinB2* and *Tie2* in E11.5 embryos was analyzed by RNA *in situ* hybridization. No differences in the amount and the distribution of these transcripts between KO (23A, B, C, D) and wild type

embryos (23E, F, G, H) were detected, demonstrating that these genes are not directly regulated by VEZF1.

3.2.4 Analysis of the *Vezf1* KO phenotype in the 129/Sv background

As described above, the phenotype of the *Vezf1* KO appears to be influenced by the genetic background of the mice that are used for the analysis. Therefore, we sought to analyze the mutant phenotype, in addition to the C57/BL6 strain, in the 129/Sv inbred background. As the R1 ES cell line used for the gene targeting is 129/Sv derived, germline chimeras were mated to 129/Sv females to generate mice in the 129/Sv inbred background. However, these matings did not yield any heterozygous offspring. Therefore, the mutant *Vezf1* allele was backcrossed into the 129/Sv strain by mating heterozygous F1 (129/SvxC57BL/6) males with 129/Sv females. Because backcrosses with 129/Sv females resulted in few pregnancies with small litter-sizes, the mutant allele has so far only been passed onto the F3 generation. Table 6 shows the genotypes of embryos obtained from intercrosses between F2 *Vezf1*$^{+/-}$ 129/Sv mice.

DEVEL. STAGE	# OF EMBRYOS	+/+	+/-	-/-
E 9.5	7	1	4	2 (2)
E10.5	11 4 resorbed	2 -	7 1	2 (1) 3
E12.5	6 4 resorbed	1 -	5 4	- -

Table 5 Genotypes of embryos for the F3 129/Sv backcross generation. Values in parentheses indicate hemorrhaging embryos.

To this point, only a limited number of embryos has been analyzed. However, several E9.5 and E10.5 *Vezf1* $^{-/-}$ embryos were isolated, whose development appeared to be arrested at the late primitive stage (E7.5) (Fig. 24). In addition, resorbed heterozygous embryos were detected at E10.5 and E12.5. These findings suggest an earlier, more pronounced mutant phenotype in the 129/Sv than the C57/BL6 background.

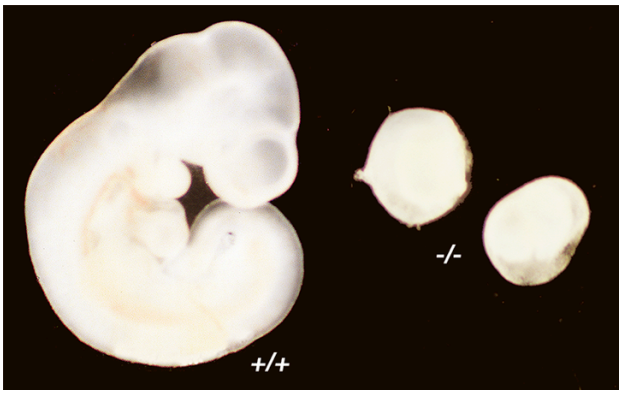

Figure 24. Phenotype of E9.5 *Vezf1* KO embryos in the 129/Sv genetic background.

3.2.4.1 Expression analysis of endothelial and hematopoietic markers in embryoid bodies

The analysis of the mutant phenotype in the 129/Sv background was hampered by the low breeding efficiency of the 129/Sv mice. However, preliminary data suggested an early lethal phenotype in *Vezf1* KO embryos (see above), possibly at the stage of endothelial and hematopoietic lineage development. To further address this question, *Vezf1* mutant ES cells were analyzed for their developmental potential in the embryoid body (EB) *in vitro* differentiation system. Several studies have shown that the developmental programs found in the normal embryo are recapitulated during the formation of EBs (Choi, 1998; Keller, 1995). Thus, the differentiation of ES cells provides a preferred model system to examine early lineage differentiation processes *in vitro*, especially as mouse embryos at the corresponding early stages of development are difficult to access and the amount of tissue available for study is limited.

To assess whether endothelial and hematopoietic lineage specification were affected in *Vezf1* $^{-/-}$ EBs, the expression of a panel of markers genes that had been used previously to define the early stages of endothelial and hematopoietic lineage development in EBs (Choi *et al.*, 1998; Kennedy *et al.*, 1997) was analyzed by semi-quantitative RT-PCR. These experiments were performed in collaboration with Dr. Gordon Keller, Mount Sinai School of Medicine, New York. Specifically, we examined the expression of the following genes: *Flk-1* (VEGF-R2), encoding vascular endothelial growth factor receptor tyrosine kinase 2, expressed in the earliest stages of endothelial and hematopoietic development (Kabrun *et al.*, 1997; Millauer *et al.*, 1993; Yamaguchi *et al.*, 1993); *Tie2*, encoding the angiopoietin receptor tyrosine kinase, expressed in endothelial cells (Dumont *et al.*, 1992; Sato *et al.*, 1993); *SCL/tal-1* encoding a helix-loop-helix transcription factor, expressed in the developing endothelial and hematopoietic lineages (Kallianpur *et al.*, 1994); and *Rex-1*, encoding a zinc-finger transcription factor, expressed in pluripotent ES cells and downregulated upon their differentiation (Rogers *et al.*, 1991). As shown in Figure 25A, the expression patterns for these genes changed in a dramatic fashion upon differentiation into EBs and in case of the wild type control correlated well with previous analysis (Keller *et al.*, 1993; Kennedy *et al.*, 1997). In the wild type control (R1), *Rex-1* was found to be expressed in ES cells and to be downregulated in day 6 EBs. In contrast, expression of *Flk-1, Tie2* and *SCL/tal-1* was undetectable (*Flk-1, SCL/tal-1*) or marginally detectable

(*Tie2)* in undifferentiated ES cells, but showed a robust upregulation in day 6 EBs, consistent with the formation of the endothelial and hematopoietic lineages. Marker gene expression in heterozygous ES cells and EBs was indistinguishable from that in wild type controls, indicating that loss of a single *Vezf1* allele does not interfere with hematopoietic and endothelial lineage differentiation. For the homozygous mutant clone (-/-), however, a different marker gene expression profile was observed. *Rex-1* was expressed in the same fashion as in the control, indicating that *Vezf1* $^{-/-}$ ES cells differentiate efficiently *in vitro*. Expression of *Flk-1* and *SCL/tal-1* was not detected and that of *Tie2* was not found to be upregulated in day 6 EBs (Fig. 25A). These findings indicate that endothelial and hematopoietic lineage differentiation are compromised in the absence of functional *Vezf1*. Furthermore, the fact that the development of both lineages is affected in *Vezf1* $^{-/-}$ EBs, might suggest a defect at the level of hemangioblast differentiation or earlier.

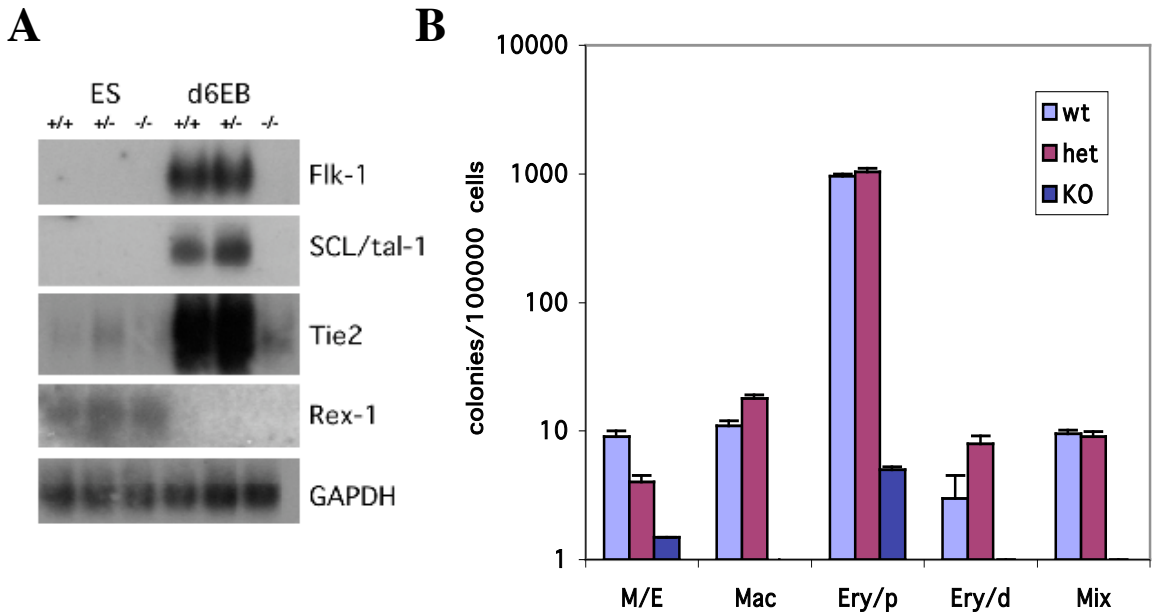

Figure 25. (A) Expression analysis of various differentiation marker genes in ES cells and day 6 EBs. Total RNA was analyzed by semi-quantitative RT-PCR. Genotypes are indicated at the top of the lane.
(B) Hematopoietic progenitor assay. Day 6 EBs were analyzed for the potential to give rise to hematopoietic precursor colonies. Error bars indicate standard deviations from 3 independent triplicate experiments. Ery/p, primitive erythroid; Ery/d, definitive erythroid; Mac, macrophage; M/E, bipotential E^{d}/Mac; Mix, mixed colonies.

3.2.4.2 Hematopoietic progenitor assays

The formation of the hematopoietic system represents a succession of developmental programs that begin with primitive erythropoiesis in the yolk sac and progressing to the definitive, multilineage hematopoiesis in the intra-embryonic aorta-gonad-mesonephros region (AGM) and fetal liver (Keller *et al.*, 1999). This sequence of events is recapitulated

in the *in vitro* differentiation system of ES cells, which thus provides a good assay for defining the role of a specific gene at distinct stages of hematopoietic development.

Therefore, to characterize the stage at which hematopoietic development is blocked in *Vezf1* $^{-/-}$ EBs, mutant ES cells were examined for their potential to generate hematopoietic progenitor colonies (Keller, 1995). In this assay, day 6 EBs were dissociated and single cells were plated in semisolid medium containing a cocktail of hematopoietic growth factors and cytokines that support the development of all hematopoietic lineages (Keller, 1995). Colonies that develop from the hematopoietic precursors are scored visually between 5-10 days following the initiation of culture. The types of precursors present in the cultures depends on the age of the EBs with plated day 6 EBs giving rise to primitive erythroid (E^p), definitive erythroid (E^d), macrophage (Mac), bipotential E^d/Mac, and multipotential precursor colonies.

As shown in Figure 25B, day 6 EBs from wild type and heterozygous mutant ES cells gave rise to all five types of hematopoietic colonies and contained similar numbers of precursors for each type. In contrast, *Vezf1*$^{-/-}$ ES cells displayed only residual hematopoietic differentiation potential. Thus, greatly reduced numbers of primitive erythroid and bipotential E^d/Mac, and no definitive erythroid, macrophage and multipotential progenitor precursor colonies were detected. These findings indicate that *Vezf1* may play a pivotal role in the development of the primitive erythroid and definitive hematopoietic lineages. Furthermore, the formation of low numbers of primitive erythroid and bipotential E^d/Mac in cultures derived from *Vezf1* $^{-/-}$ ES cells suggests for a permissive rather than an instructive function of *Vezf1* in the development of these lineages.

3.3 Vascular overexpression of *Vezf1*

The inactivation of *Vezf1* leads to vascular remodeling defects and hemorrhaging in KO embryos. Furthermore, even loss a single *Vezf1* allele results in lymphatic hypervascularization and embryonic lethality, indicating that *Vezf1* functions in a tightly regulated, dose-dependent manner during the development of the vascular system. Thus, to examine, whether excess levels of *Vezf1* might interfere with vascular development, a strategy to overexpress *Vezf1* specifically in the developing vasculature was devised. This gain-of-function approach to study *Vezf1* function is ongoing and preliminary data will be presented here.

Regulatory sequences of the endothelial-specific receptor tyrosine kinase *Tie2* gene were used to overexpress *Vezf1* in the vascular system during mouse embryonic development (Dumont *et al.*, 1992) (Sato *et al.*, 1995). Previously, a combination of promoter and first intron sequences of the *Tie2* gene had been shown to confer uniform and endothelial-specific expression in virtually all blood vessels in developing embryos (*Tie2* starts to be expressed around E9.5) and adult animals (Schlaeger *et al.*, 1995) (Schlaeger *et al.*, 1997). Therefore, an expression construct, Tie2VIL was designed in which the *Vezf1* cDNA (nt 1-2330) was placed under the control of the murine *Tie2* promoter and enhancer elements (Fig. 26A). In addition, an IRES-*LacZ* expression cassette was inserted downstream of the *Vezf1* cDNA to allow visualization of transgene expression by histochemical β-galactosidase staining.

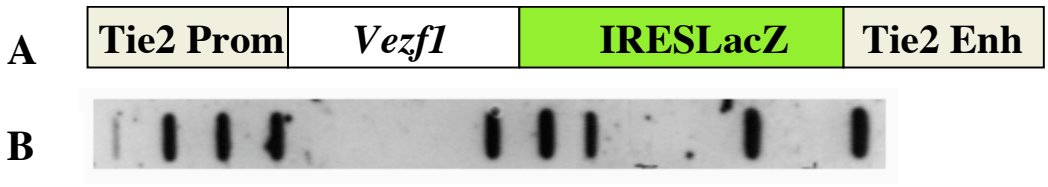

Figure 26. (A) Schematic representation of the Tie2VIL expression construct. (B) Slot blot analysis to identify transgenic founders.

Nine male transgenic founders were generated by microinjection of Tie2VIL into F1 (C57BL/6xC3H) oocytes (performed in the transgenic core facility at the Scripps Research Institute), as analyzed by slot blot hybridization using a *LacZ*-fragment as probe (Fig. 26B) and by PCR. The transgenic founders were bred with C57BL/6 females to generate F1 transgenic mice and to isolate E12.5 transgenic embryos for the analysis of transgene expression by histochemical β-galactosidase staining. Transgenic embryos from three

founders (#1, 14 and 17) were identified that showed weak albeit vascular expression patterns of the *LacZ* reporter gene (data not shown). Transgenic embryos and adult F1 mice from the transgene expressing lines 1, 14 and 17 did not show any signs of vascular dismorphogenesis or leakiness and appeared generally healthy and normal. However, intercrosses of F1 mice derived from transgenic lines 1, 14 and 17 produced offspring that was easily distinguishable from wild type controls.

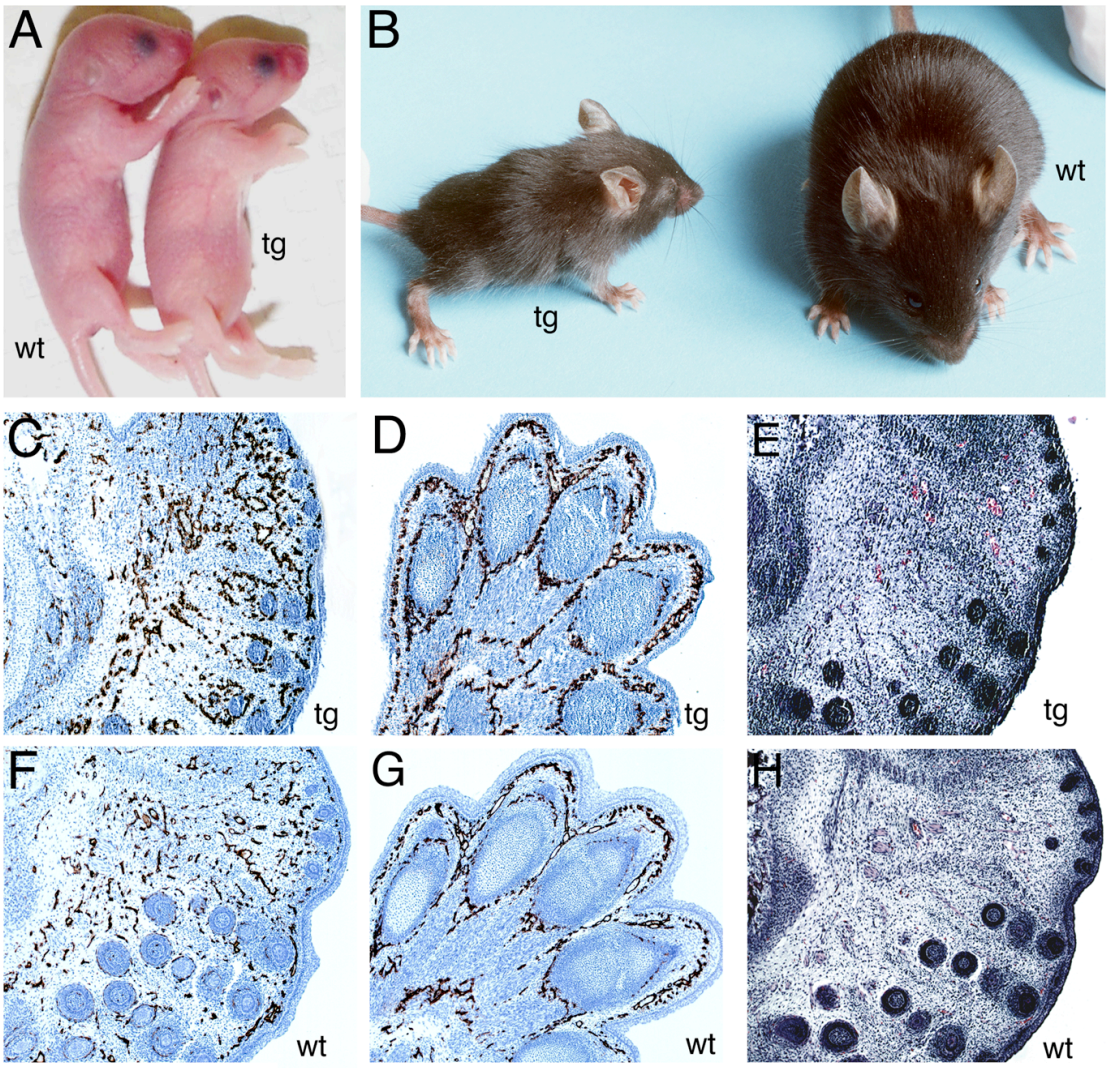

Figure 27. Phenotype of *Vezf1* transgenic mice. (A) Transgenic newborns had snouts and ears that were markedly redder than those of their wild type littermates. (B) At 3 weeks of age, transgenic mice were much smaller than wild type littermates and appeared generally unhealthy, displaying shaking and seizures. PECAM-1 staining revealed more numerous and enlarged vessels in snouts (C) and hindlimbs (D) of E16.5 transgenic embryos as compared to wild type littermates (F, G). (E, H) Histological sections of the snouts of E16.5 transgenic and wild type embryos.

Approximately 30% (presumably homozygous transgenic) of the newborn transgenic animals from these intercrosses had snouts and ears that were markedly redder than those of their wild type littermates (Fig. 27A). In addition, these transgenic newborns displayed

an increased number of large blood vessels in their skin as compared to wild type controls (Fig. 27A). At 3 weeks of age, these transgenic mice were much smaller than the wild type animals and appeared generally unhealthy, displaying shaking and seizures (Fig. 27B). These mice usually died between 3 and 5 weeks of age. Inspection of the internal organs of these mice revealed severe internal bleeding in the chest and abdominal cavity (data not shown).

Parasagittal sections of E16.5 transgenic embryos from F1 intercrosses of transgenic lines 1, 14 and 17 were analyzed by immunohistochemical PECAM-1 staining. This analysis identified transgenic embryos (presumably homozygous transgenics) that had more numerous and enlarged vessels in snouts and hindlimbs in comparison to wild type littermates (Fig. 27C, D, F, G). In histological section, these vessels appeared to be intact and did not show any signs of leakiness and hemorrhaging (Fig. 27E, H).

4. DISCUSSION

4.1 *Vezf1* is a widely expressed transcription factor

The major goal of this thesis was to elucidate the function of *Vezf1* during the development of the murine vascular system. The original premise of this study was that *Vezf1* is a zinc finger transcription factor whose expression during embryogenesis is restricted to endothelial cells and their precursors, as reported in (Xiong *et al.*, 1999). However, it is demonstrated here that the published *Vezf1* cDNA represents a chimeric cDNA clone, which contains two open reading frames corresponding to two independent genes, *Vezf1* and *Zneu1*. Furthermore, it is shown that *Zneu1* is expressed in an endothelial cell-restricted fashion, whereas *Vezf1* shows widespread expression during mouse embryonic development.

Chimeric cDNA clones, which harbor intermolecularly ligated cDNA inserts, represent a highly undesirable artifact in the construction of cDNA libraries, and their relative abundance critically determines the quality of a given cDNA library (Ohara *et al.*, 1997; Sambrook *et al.*, 1989). The frequency of chimeric clones in the mouse E7.5 cDNA library used to clone the endogenous gene corresponding to the 1-13 retroviral insertion is not known (J. Gerhart, Columbia University, personal communication). Accordingly, statements about the quality of this library cannot be made.

Apart from being a chimera, the published *Vezf1* cDNA displays two additional artifactual features that were introduced during library construction. The first one is the presence of a 175 bp stretch of intronic sequence (nt 2300-2475 of the published *Vezf1* sequence), indicating that an incompletely spliced transcript was used as template for the reverse transcription reaction of the *Zneu1* portion of cDNA clone 10-1. Secondly, database searches identified a mouse E11 embryo head cDNA clone (AK018086) that overlaps with 3' UTR sequences of *Vezf1* (nt 2118-2330) and extends the *Vezf1* cDNA sequence by an additional 1523 bp to a total length of 3853 bp. This finding indicates that the poly(A)-like stretch between nucleotide position 2303 and 2330 of the *Vezf1* cDNA sequence functioned as internal priming site in the poly(dT) primed first strand cDNA synthesis reaction of the 5' *Vezf1* portion of cDNA clone 10-1.

The total length of the reconstructed *Vezf1* cDNA is 3853 bp with the 3' UTR being 2256 bp in length. A homologous 3' UTR region was identified by database search for the human *Vezf1* ortholog ZNF161. This extended ZNF161 cDNA sequence presumably represents the L (long 3' UTR) clone mentioned in (Koyano-Nakagawa *et al.*, 1994), which contains an additional 1.3 kb of 3'UTR sequence compared to the published ZNF161 sequence. Only the sequence of the S (short 3' UTR), internally primed version of ZNF161 had been submitted to GeneBank. The mouse *Vezf1* and human ZNF161 cDNAs share an overall sequence identity of 90% and are still 86.5% identical in the 3' UTR region. This high degree of sequence homology extends into the proximal promoter region, which is 91% identical, and is suggestive of a high extent of functional conservation in the 3' UTR and promoter sequences between the mouse and the human genes. The high degree of homology between *Vezf1* and ZNF161 is also reflected in the genomic organization, which is identical with respect to the number, the position and the size of the exons, as well as the nucleotide sequences at the exon-intron boundaries for these two genes.

It was demonstrated in this study, that the retroviral insertion 1-13, which displayed the reported endothelial restricted expression pattern and led to the isolation of the *Vezf1* cDNA, corresponds to the *Zneu1* gene. Therefore, the expression pattern of *Vezf1* during mouse embryonic development was examined. Previously reported Northern blot analysis had shown that *Vezf1* and also its human ortholog ZNF161 were expressed ubiquitously and detected in every tissue examined (Koyano-Nakagawa *et al.*, 1994; Xiong *et al.*, 1999). Employing RNA *in situ* hybridzation, *Vezf1* was found, consistent with above mentioned Northern blot analysis, to be expressed in virtually every organ in mouse embryos. Expression levels varied between organs and appeared to be strongest in the brain, the neural tube, the liver, the branchial arches and the vertebral column. Furthermore, low levels of *Vezf1* expression were found in the extraembryonic yolk sac, where it appeared to be concentrated around the yolk sac blood islands.
Due to its strong, rather widespread expression, it was difficult to assess whether *Vezf1* was expressed in blood vessels and whether expression was restricted to the endothelial cell layer. However, *Vezf1* signal could be detected in transverse sections through embryonic vessels, suggesting that *Vezf1* is expressed at least in a subset of the embryonic vasculature.

Studies in the zebrafish system support the notion of widespread expression of *Vezf1*. The zebrafish ortholog of *Vezf1* has been cloned in M. Fishman's laboratory. Consistent with the data presented in this study, *zfVezf1* showed overall widespread embryonic expression. Expression was high in the brain and appeared robust in the embryonic vasculature (J.-W. Xiong and M. Fishman, Mass. Gen. Hospital, personal communication).

A polyclonal anti-VEZF1 antibody was recently generated by L. Campagnolo in Dr. Stuhlmann's laboratory. Preliminary analysis using this antibody found the VEZF1 protein to be expressed in a widespread yet less uniform manner than the *Vezf1* mRNA during embryogenesis, being detected predominantly in neuronal and mesenchymal tissues. Moreover, robust staining of vascular structures in the embryo proper and the extraembryonic yolk sac was detected. The discrepancy between protein and RNA expression could be explained by post-transcriptional regulatory mechanisms, which are often mediated by sequences in the 5' and 3' UTRs. In this respect, it is tempting to speculate that the high degree of homology between the untranscribed regions of mouse *Vezf1* and human ZNF161 may reflect a function in translational regulation of expression.

To study the mechanism of *Vezf1* expression, the *Vezf1* promoter was cloned and characterized in this study. It is shown here that the *Vezf1* promoter is G/C-rich and lacks a typical CAAT and TATA box, features characteristic of promoters of genes that are thought to have housekeeping functions with respect to cell proliferation and usually display broad tissue distribution in their expression (Bird, 1986; Lavia *et al.*, 1987). Thus, the architecture of the *Vezf1* promoter correlates well with the observed widespread expression pattern of *Vezf1 in vivo*.

RNA Ligase Mediated Rapid Amplification of cDNA ends (RLM-RACE) identified a single transcriptional start site 122 bp upstream of the ATG translation initiation codon, which is consistent with the 5' end of a cDNA clone previously obtained by library screening. The transcriptional start site lies in a pyrimidine-rich sequence, CCATGTT, which is homologous to the pyrimidine (Py)-rich core sequence, PyPyANPyPy, of an initiator element (Javahery *et al.*, 1994). An initiator element is capable of directing accurate transcription initiation in promoters that lack a TATA box (Smale, 1997). Interestingly, there are four potential Sp1-binding sites (Jones and Tjian, 1985) upstream

of the transcriptional start site of the *Vezf1* gene. It has been reported that Sp1 can interact with initiator sequences and enhance the level of basic transcription (Smale, 1997). It remains to be determined whether the putative Sp1 binding sites in the 5' proximal promoter region are involved in the control of *Vezf1* transcription.

The functional analysis of the promoter and first intron sequences identified a 700 bp proximal promoter fragment that conferred robust expression in both the fibroblast and endothelial cell line. This finding correlates well with the widespread expression pattern of *Vezf1 in vivo*. The inclusion of distal promoter and first intron sequences in the reporter constructs lead to a decrease in promoter activity in both cell lines, suggestive of negative regulatory elements within these sequences. Interestingly, the cotransfection of c-Ets1 and, to a lesser extent, also Egr-1 reverse the negative regulatory effects mediated by these sequences exclusively in the endothelial cell line. A single consensus binding site for c-Ets1 and four sites for Egr-1/Krox24 were detected in the proximal promoter region. Moreover, putative c-Ets binding sites were identified in the first intron sequence. Putative Ets binding sites are involved in the endothelium-specific expression of the *Tie1* and *Tie2* genes (Iljin *et al.*, 1999; Schlaeger *et al.*, 1997). Moreover, c-Ets1-binding has been shown to be required for endothelial-specific expression and activation of the *Flk-1* promoter *in vivo* (Kappel *et al.*, 1999; Kappel *et al.*, 2000). Thus, it is tempting to speculate that c-Ets is involved in regulating the endothelial expression of *Vezf1*. Electrophoretic mobility shift assays should elucidate whether c-Ets1 or Ets family members (Lelievre *et al.*, 2001) can functionally interact with the consensus binding sites. Moreover, mutational analysis of the c-Ets1 site *in vitro* and *in vivo* should reveal whether the binding sites are functionally significant in the regulation of *Vezf1* expression.

Egr-1 (early growth response factor-1), a zinc-finger transcription factor is inducibly expressed (e.g. in response to vascular injury) in endothelial cells and acts as a transcriptional activator of the expression of several endothelial genes including PDGF (Silverman and Collins, 1999). In a model proposed by Khachigian and Collins, activation of PDGF expression by Egr-1 is mediated by displacing Sp1, which is required for basal levels of transcription, from the G/C-rich region of the core promoter (Khachigian and Collins, 1997). The Egr-1 binding sites at positions –65 and –95 of the *Vezf1* promoter partially overlap with Sp1 sites. D. Lemons in Dr. Stuhlmann's laboratory has been able to

demonstrate specific binding of Egr-1 to these two putative binding sites via electrophoretic mobility shift assays (EMSA), suggesting a similar mechanism of Egr-1 mediated *Vezf1* activation as for PDGF. Mutational analysis of these binding sites *in vivo* should elucidate whether Egr-1 binding mediates constitutive endothelial expression or, alternatively, specific upregulation of *Vezf1* during vascular injury and phases of endothelial proliferation.

The analysis for the presence of consensus transcription factor binding sites within the first intron revealed putative sites for GATA factors (Orkin, 1992), Ets proteins (Lelievre *et al.*, 2001), LMO2 (Yamada *et al.*, 2000), ARNT (Abbott and Buckalew, 2000), SCL/tal-1 (Visvader *et al.*, 1998) and COUP (Zhou *et al.*, 2000). Interestingly, embryos lacking the latter four show angiogenic remodeling defects of the early embryonic vasculature reminiscent of those observed in *Vezf1* KO embryos, making them potential candidates as upstream regulators of VEZF1. In addition, binding sites for SCL/tal-1, GATA and Ets transcription factors have been identified as critical elements for the endothelium specific expression of several genes in transgenic embryos, including *Tie2* and *Flk-1* (Kappel *et al.*, 2000; Schlaeger *et al.*, 1997). In order to elucidate, if any of the identified consensus binding sites are functionally important for endothelial *Vezf1* expression, a deletion analysis of the first intron is currently ongoing in Dr. Stuhlmann's laboratory. Furthermore, the generation of transient transgenic embryos will reveal whether the identified promoter and first intron elements are sufficient to direct transgene expression in the developing embryo *in vivo*.

4.2 Zneu1

It was demonstrated in this study that *Zneu1* is an endothelial-cell restricted gene. Thus, *Zneu1* is a marker for vascular endothelial cells and their precursors. The only publicly available information regarding *Zneu1* is its cDNA sequence, which was directly submitted to GenBank (AF184973)). The human ortholog, ZNEU1, has been submitted under accession # AF186111. *Zneu1* is also referred to as Notch4-like protein. This name reflects the chromsomal localization of *Zneu1* within the NOTCH4-containig HLA class III region, as well as well as a shared protein motif, the EGF-like domain. Zneu1 and NOTCH4 do not share any homology apart from the EGF-like domain. No additional

structural motifs were identified in the Zneu1 protein sequence. Future functional studies on *Zneu1* will provide insights into its role during the development of the vascular system.

4.3 *Vezf1* is a critical regulator of vascular development

To determine the biological function of VEZF1, the *Vezf1* gene was disrupted by homologous recombination in ES cells. As *Vezf1* does not appear to be a member of a large family of related genes, functional redundancy was not expected for the inactivation of *Vezf1*. The absence of functional *Vezf1* transcripts in *Vezf1*$^{-/-}$ ES cells and embryos was demonstrated by Northern blot and RT-PCR analysis using different probes covering almost the entire *Vezf1* coding sequence, indicating that targeting of the *Vezf1* locus resulted in a null allele. The analysis of the effects of the inactivation of *Vezf1* in mouse embryos revealed that Vezf1 acts in a tightly regulated dose-dependent as well as in a strain dependent fashion during vascular development. Thus, in a mixed and outbred genetic background an incompletely penetrant, haplo-insufficient (autosomal), embryonic lethal phenotype with death associated with hemorrhaging and vascular malformations occurring between E12.5 and birth is observed. In the C57BL/6 background, an earlier onset of the mutant vascular phenotype was found. Preliminary data for the 129/Sv strain point to an even earlier defect, possibly at the level of hemangioblast differentiation. Strain (genetic background) specific phenotypes have been demonstrated in several gene inactivation studies. Targeted inactivation of the epidermal growth factor receptor (EGFR), for instance, resulted in peri-implantation death due to degeneration of the inner cell mass on a CF-1 background. On a 129/Sv background, homozygous mutants died at mid-gestation due to placental defects; on a CD-1 background, the mutants lived for up to 3 weeks and showed abnormalities in several organs (Threadgill *et al.*, 1995). Similarly, targeted deletion of the bHLH-repressor protein I-mfa in a C57Bl/6 background resulted in embryonic lethality around E10.5 due to placental defects. I-mfa-null embryos on a 129/Sv background had no placental defect, generally survived to adulthood, and exhibited delayed caudal neural tube closure and skeletal patterning defects (Kraut *et al.*, 1998).

4.3.1 *Vezf1*, a function in hemangioblast differentiation ?

The analysis of the *Vezf1* KO phenotype in the 129/Sv background is hampered by the poor breeding efficiency of this strain. So far only a limited number of *Vezf1* mutant embryos generated by intercrossing F2 heterozygous animals has been analyzed. However

it is noteworthy, that E9.5 *Vezf1*$^{-/-}$ embryos were isolated, whose development appeared to be arrested at the late primitive stage (E7.5). This early phenotype is consistent with the early differentiation defects observed in the *in vitro* analysis. Moreover, the fact that resorbed heterozygous embryos were detected at E10.5 and E12.5 supports the notion of an earlier phenotype in the 129/Sv than the C57BL/6 background. Further analysis of 129/Sv KO embryos should elucidate whether strain dependency is operative for the targeted mutation of the *Vezf1* gene. To expedite this analysis, chimeric mice have recently been rederived by blastocyst injection of heterozygous ES cells and male chimeras are currently mated to 129/Sv females to generate a 129/Sv *Vezf1 KO* congenic mouse line.

The analysis of the 129/Sv-derived mutant ES cells in the *in vitro* differentiation system suggests that VEZF1 is required for the development of both the endothelial and hematopoietic lineages and is consistent with a function of VEZF1 at the level of hemangioblast differentiation or even earlier. Semi-quantitative RT-PCR analysis revealed that the endothelial markers, *Flt-1* and *Tie2*, as well as the hematopoietic marker *SCL/tal-1* are downregulated in *Vezf1*$^{-/-}$ EBs. In contrast, no differences between wild type and homozygous mutant EBs are detected for the expression of *Rex-1*, a marker for undifferentiated ES cells, demonstrating that the inactivation of *Vezf1* does not lead to a general block of differentiation. Moreover, hematopoietic progenitor assays show that the hematopoietic differentiation potential of *Vezf1*$^{-/-}$ ES cell derived EBs is severely impaired. In future studies, to assess whether the inactivation of *Vezf1* affects the differentiation of other cell lineages, it will be useful to further define the defects in *Vezf1*$^{-/-}$ EBs by analyzing the expression of an extended panel of marker genes. This analysis could include the pan-mesodermal marker *Brachyury (T)* (Herrmann, 1991) and the following marker genes for mesodermally derived cell lineages: *Nkx-2.5* (cardiomyocytes) (Lints *et al.*, 1993), *myf5* (myocytes) (Montarras *et al.*, 1991), *βH1 globin* (primitive erythrocytes) (Palis *et al.*, 1999), *c-fms* (macrophages) (Palis *et al.*, 1999) and *c-myb* (definitive hematopoiesis) (Mucenski *et al.*, 1991), as well as markers for ectodermal (*Fgf-5*) (Haub and Goldfarb, 1991) and endodermal (*GATA 4*) (Heikinheimo *et al.*, 1994) differentiation.
It is worth noting that although two different approaches, G418 hyperselection and retargeting of the *Vezf1* locus, were used to generate *Vezf1*$^{-/-}$ ES cell clones, only one homozygous mutant ES cell clone was obtained after analyzing a total of 800 clones

(based on the initial targeting frequency for the *Vezf1* locus of 3%, 12 clones were expected). The one clone isolated was generally indistinguishable from wild type controls, displaying normal morphology and growth characteristics and differentiating efficiently *in vitro*, as judged by morphological appearance and down-regulation of *Rex-1* expression. However, for future studies, a rescue experiment, the reexpression of *Vezf1* during EB formation, should be designed to verify that the observed phenotype in *Vezf1*$^{-/-}$ EBs was indeed a consequence of the absence of *Vezf1* expression and not a clonal artifact.

4.3.2 *Vezf1* function in angiogenic remodeling and the maintenance of vascular integrity

The analysis of *Vezf1*$^{-/-}$ embryos in the F5 C57BL/6 background revealed that VEZF1 function is neither required for the early stages of vascular development, angioblast differentiation and vasculogenesis, nor for embryonic hematopoiesis. Instead, loss of *Vezf1* leads to an incompletely penetrant mutant vascular phenotype affecting angiogenesis, vascular hemostasis and lymphatic development. Vascular defects become apparent at day 9.5 of gestation in homozygous mutant embryos. E9.5 *Vezf1*$^{-/-}$ embryos display specific defects in the angiogenic remodeling process of the primary vascular plexus in the vasculature of the aortic arch system, the head, the neck and the dorsal part of the intersomitic vessels. In addition, several sites of hemorrhaging, typically in the head and trunk, are detected, indicating that the integrity of the vasculature is compromised in E9.5 KO embryos. Interestingly, no vascular abnormalities in E9.5 *Vezf1*$^{-/-}$ embryonic yolk sacs were detected, suggesting that *Vezf1* function is not required for yolk sac vascular development. This is a rather unexpected finding as *Vezf1* is expressed in the yolk sac mesoderm, and remodeling defects in the embryo proper are usually mirrored in the yolk sac vasculature (Adams *et al.*, 1999; Dumont *et al.*, 1994; Wang *et al.*, 1998).
At later stages of embryonic development, *Vezf1*$^{-/-}$ embryos that obviously survive this early crisis were detected. These embryos displayed normal morphology of the vascular system and all organ system examined, including heart and placenta, but showed distinct sites of internal bleeding, most prominently in the jugular region and the head.

Vezf1 shows widespread expression during embryonic development, which is especially high in the CNS. The gross morphological and histological analysis of *Vezf1* KO embryos, however, did not reveal any defects in organ systems other than the vasculature. Although subtle defects in other tissues cannot be excluded, this finding suggests that *Vezf1* is only

required for the formation and function of the vascular system. Alternatively, since the vascular system is the first organ system to evolve during development, the embryonic lethality associated with the vascular defects might therefore obscure additional later phenotypes in other organ systems. A conditional *Vezf1* KO approach, allowing the inactivation of *Vezf1* in particular tissues and/or in adult mice, should be able to elucidate possible additional *Vezf1* functions.

The observed hemorrhaging in E9.5 *Vezf1* KO embryos might be a consequence of the vascular remodeling defects, or, alternatively, it may constitute a primary defect. The analysis presented in this thesis does not allow distinguishing between these two possibilities. The occurrence of vascular leakage in later stage KO embryos without the association with vascular dismorphogenesis is consistent with a primary defect. Moreover, the fact that angiogenic remodeling defects similar to those found in E9.5 *Vezf1* KO embryos have been reported for the inactivation of several genes, including *angiopoietin1*, *Tie2*, *VEGFR-3*, *ephrinB2*, *EphB4*, *EphB2/B3* and *Notch1/Notch4*, which are not accompanied by hemorrhaging, further supports this notion (Adams *et al.*, 1999; Dumont *et al.*, 1998; Gerety *et al.*, 1999; Krebs *et al.*, 2000; Sato *et al.*, 1995; Suri *et al.*, 1996; Wang *et al.*, 1998). The mechanism underlying the compromised vascular integrity in *Vezf1* KO remains to be resolved. Two possible causes were addressed in this study, namely defects in VSMC differentiation and/or recruitment (Kuo *et al.*, 1997; Liu *et al.*, 2000) and defective megakaryocyte differentiation (Spyropoulos *et al.*, 2000). However, both processes were found to be normal in homozygous mutant embryos.

Another possible cause for the vascular fragility might be a defective coagulation system. Interestingly, emerging evidence implicates the clotting system in the process of angiogenesis during embryonic development. In a recent report, thrombin signaling through the protease-activated G protein-coupled receptor PAR1 has been demonstrated to directly regulate endothelial cell function during blood vessel formation (Griffin *et al.*, 2001). Moreover, tissue factor KO embryos show yolk sac vascular defects in addition to bleeding (Bugge *et al.*, 1996; Carmeliet *et al.*, 1996b). As vessel fragility and angiogenic remodling defects are observed in *Vezf1* KO embryos, this raises the intriguing possibility that *Vezf1* plays a role in coagulation function. The analysis of expression and activity of

the coagulation factors in *Vezf1* KO embryos should determine whether *Vezf1* is indeed involved in the regulation of the coagulation system.
Other possible mechanisms for the hemorrhaging in *Vezf1* KO mice are defects in the structural integrity of the endothelial cells themselves (Sato *et al.*, 1995), defective inter-endothelial cell contacts or defective interactions between endothelial cells and the underlying basal membrane (Vestweber, 2000). Ultrastructural analysis might be able to elucidate whether any of these processes are affected in *Vezf1* KO embryos.

Vezf1 is a zinc finger transcription factor, but its downstream target genes are not known. To identify genes that are regulated by *Vezf1*, the expression of a large canon of genes known to regulate endothelial cell proliferation, angiogenic remodeling and the maintenance of vascular integrity was examined. However, the loss of *Vezf1* function could not be correlated with changes in the expression levels of any of these genes. Thus, so far no downstream targets of *Vezf1* have been identified and the molecular mechanisms of VEZF1 function remain unclear. It is possible, of course, that *Vezf1* regulates the expression of yet unidentified genes. Expression profiling using cDNA micorarray chips should be instrumental in identifying the *Vezf1* target genes and thus provide an entry into the molecular mechanisms that underlie *Vezf1* function (Brown and Botstein, 1999).
In a recent study, ZNF161 binding and transactivation of the human *Endothelin-1* promoter *in vitro* was demonstrated (Aitsebaomo *et al.*, 2001). Interestingly, the analysis of mice deficient in Endothelin-1 (ET-1) revealed an incompletely penetrant phenotype that is complementary to that of *Vezf1*$^{-/-}$ embryos with respect to the aortic arch system, as the first and second aortic arch artery, which normally regress between E10.5 and E11.5, persist throughout embryonic development (Kurihara *et al.*, 1995; Kurihara *et al.*, 1994). ET-1 is expressed in the endocardium of the outflow tract the heart, the endothelium of the aortic arch arteries, the dorsal aorta and the epithelium of the pharyngeal arches in E10 embryos (Kurihara *et al.*, 1995). This finding makes *ET-1* a likely VEZF1 target gene. Furthermore, due to the reciprocal KO phenotypes one would postulate negative regulation of *ET-1* by VEZF1 and thus upregulation of *ET-1* in *Vezf1*$^{-/-}$ embryos. However, no differences in the levels of *ET-1* expression between E10.5 *Vezf1* KO and wild type embryos were detected by semi-quantitative RT-PCR. Future analysis of the spatial expression of *ET-1* by RNA *in situ* hybridization or immunohistochemical antibody staining should clarify whether *ET-1* expression is altered in *Vezf1* KO embryos.

4.3.3 *Vezf1*, a negative regulator of lymphatic development

Approximately 20% of the *Vezf1*$^{+/-}$ embryos displayed hypervascularization associated with edema and hemorrhaging in the jugular region indicating that *Vezf1* acts in a tightly regulated, dose-dependent manner during vascular development. This incompletely penetrant, haploinsufficient (autosomal) phenotype is caused neither by imprinting of the residual wildtype allele, nor by the generation of a dominant-negative VEZF1 mutant peptide. Only few incidents of haploinsufficiency with respect to vascular development have been reported. The only other transcription factor that acts in a gene dosage-dependent manner is the T-box factor Tbx-1, which is required for normal development of the pharyngeal arch arteries (Lindsay *et al.*, 2001). In addition, the growth factors, VEGF and TGF-β, display dose dependency in their vascular function (Carmeliet *et al.*, 1996a; Dickson *et al.*, 1995; Ferrara *et al.*, 1996).

Histological and quantitative morphometric analysis of E13.5 *Vezf1*$^{+/-}$ embryos suggests that endothelial hyperproliferation is the cause for the formation of aberrant and dysfunctional vessels specifically in the jugular region. The jugular region constitutes the first and major site of sprouting of the developing lymphatic vessels from venous system (Sabin, 1909), a process that is initiated around E12.5 in mouse embryos. Interestingly, the hyperplastic vessels in the jugular region stain positive for two lymphatic markers VEGFR-3 and LYVE-1, suggesting that they are of lymphatic nature (Banerji *et al.*, 1999; Dumont *et al.*, 1998; Kaipainen *et al.*, 1995; Prevo *et al.*, 2001). Furthermore, they do not express smooth muscle α-actin, a marker for the vascular smooth muscle cell layer, which is a hallmark of blood vascular structures. It has been reported that lymphatic capillaries may contain stagnant blood, which is removed into the venous circulation once the lymphatic system becomes functional (Clark, 1912; Lewis, 1905; Miller, 1913). This observation might explain the finding that the hyperplastic, lymphatic vessels, as they are dysfunctional, contain blood. Taken together, these data indicate that lack of a single *Vezf1* allele due to increased lymphatic endothelial cell proliferation results in deregulated lymphatic outgrowth from the venous system and/or lymphatic expansion. Accordingly, *Vezf1* would be a negative regulator of lymphatic development and/or lymphatic endothelial cell proliferation.

To gain a better understanding of the etiology of the lymphatic defect in heterozygous *Vezf1* embryos, it will be informative to examine the expression of the homeobox gene

Prox1. *Prox1* is a specific marker of a subpopulation of endothelial cells that gives rise to the lymphatic system (Oliver *et al.*, 1993; Wigle and Oliver, 1999). As early as E10.5, Prox1-positive cells are detected in the wall of the anterior cardinal vein. As development proceeds, these Prox1-positive cells bud from the anterior cardinal vein and migrate dorsoanteriorly to form the lymphatic jugular sacs. At later stages of development *Prox1* is expressed throughout the entire lymphatic system. In addition, podoplanin, a novel lymphatic mucoprotein (Breiteneder-Geleff *et al.*, 1999) and collagen IV, a basal membrane component that is exclusively associated with the blood vascular system (Ezaki *et al.*, 1990), should be useful markers to confirm the lymphatic nature of the hyperplastic vessels. Moreover, assays to measure cellular proliferation like BrdU-labeling of embryos (Wigle *et al.*, 1999) should be useful in determining whether increased lymphatic endothelial cell proliferation is indeed the mechanism that leads to jugular hypervascularization in *Vezf1*$^{+/-}$ embryos. Finally, it will be interesting to examine whether *Vezf1* is expressed in the recently described lymphangioblasts and, if so, whether it plays a functional role in lymphangioblast differentiation and/or proliferation.

The edematous phenotype observed in E13.5 *Vezf1*$^{+/-}$ embryos is reminiscent of a human malformation syndrome, called cystic hygroma. Cystic hygromas are congenital malformations of the lymphatic system that occur at sites of lymphatic-venous connection, most commonly in the posterior neck (Gallagher *et al.*, 1999). Typically, cystic hygromas develop late in the first trimester either as a consequence of failure of the lymphatic vessels to connect to the venous system, which leads to the accumulation of fluid in dilated lymphatics and progressive lymphedema, or due to abnormal budding of lymphatic endothelium (Edwards and Graham, 1990). Rates as high as 1 in 100 unselected pregnancies have been reported for this syndrome. Although cystic hygromas are frequently associated with other malformation syndromes characterized by chromosomal abnormalities, for instance Turner syndrome or Trisomy 21, there are reports of fetal nuchal cystic hygromas with a normal karyotype (Marchese *et al.*, 1985). It will be important to examine if haploinsufficiency of the human *Vezf1* ortholog ZNF161 can be associated with this human developmental abnormality. Moreover, it will be of great interest to determine whether loss of VEZF1 function can be correlated with conditions, which are postulated to be the result of excessive proliferation of lymphatic endothelilal

cells, such as lymphangioma, lymphangiosarcoma and Kaposi's sarcoma (Witte *et al.*, 1997).

4.3.4 Vascular overexpression of *Vezf1*

The preliminary analysis of *Vezf1* function by overexpression in the blood vasculature appears to underscore the importance of *Vezf1* as a regulator of vascular development. Three independent Tie2VIL transgene expressing lines were identified that displayed hypervascularization (more and larger vessels) in snout, ears, skin and hindlimbs. Vascular expression of the Tie2VIL transgene was monitored by β-galactosidase (encoded by the *LacZ* reporter gene) staining of E12.5 F1 transgenic embryos. The three transgenic lines 1, 14 and 17 showed only weak expression of the *LacZ* reporter gene, which was nevertheless, consistent with the findings of (Schlaeger *et al.*, 1997), confined to the blood vasculature. Whether these low *LacZ* expression levels reflect the inherent weak promoter activity of the *Tie2* promoter/enhancer elements or, alternatively, are a result of the low efficiency of translation initiation mediated by the IRES element in endothelial cells, as reported by (Peng *et al.*, 2000), remains to be resolved.
Hypervascularization was observed in about 30% of the transgenic animals derived from F1 (heterozygous transgenic) intercrosses. This suggests that homozygosity of the transgene is necessary to elicit the vascular phenotype. This dose-dependency of *Vezf1* function in transgenic mice is consistent with findings for the inactivation of *Vezf1*. Careful quantitative expression analysis of the *Vezf1* transgene will be required to establish a correlation between the vascular phenotype and the ectopic expression levels of *Vezf1*. The problem of differentiating between endogenous and ectopic *Vezf1* in this analysis could be circumvented by utilizing a *LacZ* probe on a Northern blot, which would unequivocally detect the transgenic mRNA. Moreover, the generation of transgenic mice with regulatable vascular expression of *Vezf1* should be useful in addressing the dose-dependency of *Vezf1* function. In addition, detection of the ectopic VEZF1 protein by either Western blot or immunohistochemistry will be necessary to formally prove the overexpression of VEZF1.

As this analysis of vascular *Vezf1* overexpression is preliminary, several open questions remain. The cause of death of the F2 Tie2VIL transgenic mice is unclear. It may due to the internal bleeding observed in these animals. Furthermore, the underlying mechanism of the hypervascularization needs to be elucidated. The identification of *Vezf1* target genes

will be instrumental in this respect. Increased endothelial cell proliferation is one likely mechanism. This raises the intriguing possibility that *Vezf1* acts as negative regulator of proliferation in lymphatic endothelium, while it promotes proliferation of arterial endothelial cells. Alternatively, *Vezf1* may function in a regional or vascular bed-specific way, as hypervascularization is observed only in certain tissues or regions (provided that this is not a consequence of regional differences in expression levels). Future studies will hopefully address some of these important questions and improve our understanding of the function of *Vezf1* during vascular development.

5. REFERENCES

Abbott, B. D., and Buckalew, A. R. (2000). Placental defects in ARNT-knockout conceptus correlate with localized decreases in VEGF-R2, ang-1, and tie-2. *Dev Dyn* **219,** 526-38.

Adams, R. H., Wilkinson, G. A., Weiss, C., Diella, F., Gale, N. W., Deutsch, U., Risau, W., and Klein, R. (1999). Roles of ephrinB ligands and EphB receptors in cardiovascular development: demarcation of arterial/venous domains, vascular morphogenesis, and sprouting angiogenesis. *Genes & Dev.* **13,** 295-306.

Aitsebaomo, J., Kingsley-Kallesen, M. L., Wu, Y., Quertermous, T., and Patterson, C. (2001). Vezf1/DB1 is an endothelial cell-specific transcription factor that regulates expression of the endothelin-1 promoter. *J Biol Chem* **14,** 14.

Baldwin, H. S., Shen, H. M., Yan, H. C., DeLisser, H. M., Chung, A., Mickanin, C., Trask, T., Kirschbaum, N. E., Newman, P. J., Albelda, S. M., and et al. (1994). Platelet endothelial cell adhesion molecule-1 (PECAM-1/CD31): alternatively spliced, functionally distinct isoforms expressed during mammalian cardiovascular development. *Development* **120,** 2539-53.

Banerji, S., Ni, J., Wang, S. X., Clasper, S., Su, J., Tammi, R., Jones, M., and Jackson, D. G. (1999). LYVE-1, a new homologue of the CD44 glycoprotein, is a lymph-specific receptor for hyaluronan. *J Cell Biol* **144,** 789-801.

Bird, A. P. (1986). CpG-rich islands and the function of DNA methylation. *Nature* **321,** 209-13.

Brady, G., and Iscove, N. N. (1993). Construction of cDNA libraries from single cells. *Methods Enzymol* **225,** 611-23.

Breiteneder-Geleff, S., Soleiman, A., Kowalski, H., Horvat, R., Amann, G., Kriehuber, E., Diem, K., Weninger, W., Tschachler, E., Alitalo, K., and Kerjaschki, D. (1999). Angiosarcomas express mixed endothelial phenotypes of blood and lymphatic capillaries: podoplanin as a specific marker for lymphatic endothelium. *Am J Pathol* **154,** 385-94.

Brown, P. O., and Botstein, D. (1999). Exploring the new world of the genome with DNA microarrays. *Nat Genet* **21,** 33-7.

Bugge, T. H., Xiao, Q., Kombrinck, K. W., Flick, M. J., Holmback, K., Danton, M. J., Colbert, M. C., Witte, D. P., Fujikawa, K., Davie, E. W., and Degen, J. L. (1996). Fatal

embryonic bleeding events in mice lacking tissue factor, the cell- associated initiator of blood coagulation. *Proc Natl Acad Sci U S A* **93,** 6258-63.

Carmeliet, P. (2000). Mechanisms of angiogenesis and arteriogenesis. *Nat Med* **6,** 389-95.

Carmeliet, P., Ferreira, V., Breier, G., Pollefeyt, S., Kieckens, L., Gertsenstein, M., Fahrig, M., Vandenhoeck, A., Harpal, K., Eberhardt, C., Declercq, D., Pawling, J., Moons, L., Collen, D., Risau, W., and Nagy, A. (1996a). Abnormal blood vessel development and lethality in embryos lacking a single VEGF allele. *Nature* **380,** 435-439.

Carmeliet, P., and Jain, R. K. (2000). Angiogenesis in cancer and other diseases. *Nature* **407,** 249-57.

Carmeliet, P., Lampugnani, M. G., Moons, L., Breviario, F., Compernolle, V., Bono, F., Balconi, G., Spagnuolo, R., Oostuyse, B., Dewerchin, M., Zanetti, A., Angellilo, A., Mattot, V., Nuyens, D., Lutgens, E., Clotman, F., de Ruiter, M. C., Gittenberger-de Groot, A., Poelmann, R., Lupu, F., Herbert, J. M., Collen, D., and Dejana, E. (1999). Targeted deficiency or cytosolic truncation of the VE-cadherin gene in mice impairs VEGF-mediated endothelial survival and angiogenesis. *Cell* **98,** 147-57.

Carmeliet, P., Mackman, N., Moons, L., Luther, T., Gressens, P., Van Vlaenderen, I., Demunck, H., Kasper, M., Breier, G., Evrard, P., Muller, M., Risau, W., Edgington, T., and Collen, D. (1996b). Role of tissue factor in embryonic blood vessel development. *Nature* **383,** 73-5.

Chang, H., Huylebroeck, D., Verschueren, K., Guo, Q., Matzuk, M. M., and Zwijsen, A. (1999). Smad5 knockout mice die at mid-gestation due to multiple embryonic and extraembryonic defects. *Development* **126,** 1631-1642.

Chitnis, A., Henrique, D., Lewis, J., Ish-Horowicz, D., and Kintner, C. (1995). Primary neurogenesis in Xenopus embryos regulated by a homologue of the Drosophila neurogenic gene Delta. *Nature* **375,** 761-6.

Choi, K. (1998). Hemangioblast development and regulation. *Biochem Cell Biol* **76,** 947-56.

Choi, K., Kennedy, M., Kazarov, A., Papadimitriou, J. C., and G., K. (1998). A common precursor for hematopoietic and endothelial cells. *Development* **125,** 725-732.

Clark, E. L. (1912). General observations on early superficial lymphatics in living chick embryos. *Anat. Rec.* **6,** 247-251.

Coffin, D. a. P., TJ. (1988). Embryonic vascular development: immunohistochemical identification of the origin and subsequent morphogenesis of the major vessel primordia in quail embryos. *Development* **102,** 735-748.

Cross, S. H., and Bird, A. P. (1995). CpG islands and genes. *Curr Opin Genet Dev* **5,** 309-14.

Darland, D. C., and D'Amore, P. A. (1999). Blood vessel maturation: vascular development comes of age. *J Clin Invest* **103,** 157-8.

Dickson, M. C., Martin, J. S., Cousins, F. M., Kulkarni, A. B., Karlsson, S., and Akhurst, R. J. (1995). Defective hematopoiesis and vasculogenesis in transforming growth factor-1 knock out mice. *Development* **121,** 1845-1854.

Doetschman, T. C., Eistetter, H., Katz, M., Schmidt, W., and Kemler, R. (1985). The *in vitro* development of blastocyst- derived embryonic stem cell lines: formation of visceral yolk sac, blood islands and myocardium. *J. Embryol. Exp. Morph.* **87,** 27-45.

Drake, C., and Fleming, P. (2000). Vasculogenesis in the day 6.5 to 9.5 mouse embryo. *Hemostasis, Thrombosis, and Vascular Biology* **95,** 1671-1679.

Dube, A., Akbarali, Y., Sato, T. N., Libermann, T. A., and Oettgen, P. (1999). Role of the Ets transcription factors in the regulation of the vascular-specific Tie2 gene. *Circ Res* **84,** 1177-85.

Dube, A., Thai, S., Gaspar, J., Rudders, S., Libermann, T. A., Iruela-Arispe, L., and Oettgen, P. (2001). Elf-1 is a transcriptional regulator of the Tie2 gene during vascular development. *Circ Res* **88,** 237-44.

Dumont, D., Gradwohl, J. G., Fong, G.-H., Puri, M., Gertsenstein, M., Auerbach, A., and Breitman, M. L. (1994). Dominant-negative and targeted null mutations in the endothelial receptor kinase, tek, reveal a critical role in vasculogenesis of the embryo. *Genes Dev.* **8,** 1897-1909.

Dumont, D. J., Jussila, L., Taipale, J., Lymboussaki, A., Mustonen, T., Pajusola, K., Breitman, M., and Alitalo, K. (1998). Cardiovascular failure in mouse embryos deficient in VEGF receptor-3. *Science* **282,** 946-949.

Dumont, D. J., Yamaguchi, T. P., Conlon, R. A., Rossant, J., and Breitman, M. L. (1992). *tek*, a novel tyrosine kinase located on mouse chromosome 4, is expressed in endothelial cells and their presumptive precursors. *Oncogene* **7,** 1471-1480.

Edwards, M. J., and Graham, J. M., Jr. (1990). Posterior nuchal cystic hygroma. *Clin Perinatol* **17,** 611-40.

Era, T., Takahashi, T., Sakai, K., Kawamura, K., and Nakano, T. (1997). Thrombopoietin enhances proliferation and differentiation of murine yolk sac erythroid progenitors. *Blood* **89,** 1207-13.

Ezaki, T., Matsuno, K., Fujii, H., Hayashi, N., Miyakawa, K., Ohmori, J., and Kotani, M. (1990). A new approach for identification of rat lymphatic capillaries using a monoclonal antibody. *Arch Histol Cytol* **53,** 77-86.

Faloon, P., Arentson, E., Kazarov, A., Deng, C. X., Porcher, C., Orkin, S., and Choi, K. (2000). Basic fibroblast growth factor positively regulates hematopoietic development. *Development* **127,** 1931-41.

Ferrara, N., Carver-Moore, K., Chen, H., Dowd, M., Lu, L., O'Shea, K. S., Powell-Braxton, L., Hillan, K. J., and Moore, M. W. (1996). Heterozygous embryonic lethality induced by targeted inactivation of the VEGF gene. *Nature* **380,** 439-442.

Fina, L., Molgaard, H., Robertson, D., Bradley, N., Monaghan, P., Sutherland, D., Baker, M., and Greaves, M. (1990). Expression of the CD34 gine in vascular endothelial cells. *Blood* **75,** 2417-2426.

Fong, G.-H., Rossant, J., Gertsenstein, M., and Breitman, M. (1995). Role of the Flt-1 receptor tyrosine kinase in regulating the assembly of vascular endothelium. *Nature* **376**.

Fong, G.-H., Zhang, L., Bryce, D.-M., and Peng, J. (1999). Increased hemangioblast commitment, not vascular disorganization, is the primary defect in *flt-1* knock-out mice. *Development* **126,** 3015-3025.

Gale, N. W., and Yancopoulos, G. D. (1999). Growth factors acting via endothelial cell-specific receptor tyrosine kinases: VEGFs, Angiopoietins, and ephrins in vascular development. *Genes & Dev*. **13,** 1055-1066.

Gallagher, P. G., Mahoney, M. J., and Gosche, J. R. (1999). Cystic hygroma in the fetus and newborn. *Semin Perinatol* **23,** 341-56.

Georgopoulos, K., Winandy, S., and Avitahl, N. (1997). The role of the Ikaros gene in lymphocyte development and homeostasis. *Annu Rev Immunol* **15,** 155-76.

Gerety, S. S., Wang, H. U., Chen, Z. F., and Anderson, D. J. (1999). Symmetrical mutant phenotypes of the receptor EphB4 and its specific transmembrane ligand ephrin-B2 in cardiovascular development. *Mol Cell* **4,** 403-14.

Gray, H. (1985). The lymphatic system. In Anatomy of the Human Body. *C.D. Celmente, ed. (Philadelphia: Lea and Febiger), pp. 866-932* .

Griffin, C. T., Srinivasan, Y., Zheng, Y. W., Huang, W., and Coughlin, S. R. (2001). A role for thrombin receptor signaling in endothelial cells during embryonic development. *Science* **293,** 1666-70.

Gumina, R. J., Kirschbaum, N. E., Piotrowski, K., and Newman, P. J. (1997). Characterization of the human platelet/endothelial cell adhesion molecule-1 promoter: identification of a GATA-2 binding element required for optimal transcriptional activity. *Blood* **89,** 1260-9.

Harland, R., and Gerhardt, J. (1997). Formation and function of Spemann's organizer. *AnnualRevCellDevBiol* **13,** 611-667.

Haub, O., and Goldfarb, M. (1991). Expression of the fibroblast growth factor-5 gene in the mouse embryo. *Development* **112,** 397-406.

Heikinheimo, M., Scandrett, J. M., and Wilson, D. B. (1994). Localization of transcription factor GATA-4 to regions of the mouse embryo involved in cardiac development. *Dev. Biol.* **164,** 361-373.

Hellstrom, M., Kal n, M., Lindahl, P., Abramsson, A., and Betsholtz, C. (1999). Role of PDGF-B and PDGFR-beta in recruitment of vascular smooth muscle cells and pericytes during embryonic blood vessel formation in the mouse. *Development* **126,** 3047-55.

Henderson, A. M., Wang, S. J., Taylor, A. C., Aitkenhead, M., and Hughes, C. C. (2001). The basic helix-loop-helix transcription factor HESR1 regulates endothelial cell tube formation. *J Biol Chem* **276,** 6169-76.

Herrmann, B. (1991). Expression pattern of the *Brachyury* gene in whole-mount T^{Wis}/T^{Wis} mutant embryos. *Development* **113,** 913-917.

Hirschi, K. K., Rohovsky, S. A., Beck, L. H., Smith, S. R., and D'Amore, P. A. (1999). Endothelial cells modulate the proliferation of mural cell precursors via platelet-derived growth factor-BB and heterotypic cell contact. *Circ Res* **84,** 298-305.

Hrabe de Angelis, M., McIntyre, J., 2nd, and Gossler, A. (1997). Maintenance of somite borders in mice requires the Delta homologue DII1. *Nature* **386,** 717-21.

Huntington, G. S. (1908). The genetic interpretation of the the development of the mammalian lymphatic system. *Anat. Rec.* **2,** 19-46.

Ihle, J. N. (2000). The challenges of translating knockout phenotypes into gene function. *Cell* **102,** 131-4.

Iljin, K., Dube, A., Kontusaari, S., Korhonen, J., Lahtinen, I., Oettgen, P., and Alitalo, K. (1999). Role of ets factors in the activity and endothelial cell specificity of the mouse Tie gene promoter. *Faseb J* **13,** 377-86.

Imagawa, M., Chiu, R., and Karin, M. (1987). Transcription factor AP-2 mediates induction by two different signal- transduction pathways: protein kinase C and cAMP. *Cell* **51,** 251-60.

Iyer, N. V., Kotch, L. E., Agani, F., Leung, S. W., Laughner, E., Wenger, R. H., Gassmann, M., Gearhart, J. D., Lawler, A. M., Yu, A. Y., and Semenza, G. L. (1998). Cellular and developmental control of O_2 homeostasis by hypoxia-inducible factor 1□. *Genes Dev*. **12,** 149-162.

Jaffredo, T., Gautier, R., Eichmann, A., and Dieterlen-Lievre, F. (1998). Intraaortic hemopoietic cells are derived from endothelial cells during ontogeny. *Development* **125,** 4575-4853.

Jain, S., Maltepe, E., Lu, M. M., Simon, C., and Bradfield, C. A. (1998). Expression of ARNT, ARNT2, HIF1 alpha, HIF2 alpha and Ah receptor mRNAs in the developing mouse. *Mech Dev* **73,** 117-23.

Javahery, R., Khachi, A., Lo, K., Zenzie-Gregory, B., and Smale, S. T. (1994). DNA sequence requirements for transcriptional initiator activity in mammalian cells. *Mol Cell Biol* **14,** 116-27.

Jeltsch, M., Kaipainen, A., Joukov, V., Meng, X., Lakso, M., Rauvala, H., Swartz, M., Fukumura, D., Jain, R. K., and Alitalo, K. (1997). Hyperplasia of lymphatic vessels in VEGF-C transgenic mice. *Science* **276,** 1423-5.

Jones, K. A., and Tjian, R. (1985). Sp1 binds to promoter sequences and activates herpes simplex virus 'immediate-early' gene transcription in vitro. *Nature* **317,** 179-82.

Kabrun, N., Buhring, H., Choi, K., Ullrich, A., Risau, W., and Keller, G. (1997). Flk-1 expression defines a population of early embryonic hematopoietic precursors. *Development* **124,** 2039-2048.

Kaipainen, A., Korhonen, J., Mustonen, T., van Hinsbergh, V. W., Fang, G. H., Dumont, D., Breitman, M., and Alitalo, K. (1995). Expression of the fms-like tyrosine kinase 4 gene becomes restricted to lymphatic endothelium during development. *Proc Natl Acad Sci U S A* **92,** 3566-70.

Kallianpur, A., Jordan, J., and Brandt, S. (1994). The SCL/TAL-1 gene is expressed in progenitors of both the hematopoietic and vascular systems during embryogenesis. *Blood* **83,** 1200-1208.

Kampmeier, O. F. (1912). The value of the injection method in the study of the lymphatic development. *Anat. Rec.* **6,** 223-233.

Kappel, A., Rönicke, V., Damert, A., Flamme, I., Risau, W., and Breier, G. (1999). Identification of vascular endothelial growth factor (VEGF) receptor-2 (*Flk-1*) promoter/enhancer sequences sufficient for angioblast and endothelial cell-specific transcription in transgenic mice. *Blood* **93,** 4284-4292.

Kappel, A., Schlaeger, T. M., Flamme, I., Orkin, S. H., Risau, W., and Breier, G. (2000). Role of SCL/Tal-1, GATA, and ets transcription factor binding sites for the regulation of flk-1 expression during murine vascular development. *Blood* **96,** 3078-85.

Kawana, M., Lee, M. E., Quertermous, E. E., and Quertermous, T. (1995). Cooperative interaction of GATA-2 and AP1 regulates transcription of the endothelin-1 gene. *Mol Cell Biol* **15,** 4225-31.

Keller, G., Kennedy, M., Papayannopoulou, T., and Wiles, M. V. (1993). Hemaptopoietic commitment during embryonic stem cell differentiation in culture. *Mol. Cell Biol.* **13,** 473-486.

Keller, G., Lacaud, G., and Robertson, S. (1999). Development of the hematopoietic system in the mouse. *Exp Hematol* **27,** 777-87.

Keller, G. M. (1995). *In vitro* differentiation of embryonic stem cells. *Curr. Opin. Cell Biol.* **7,** 862-869.

Kennedy, G. C., and Rutter, W. J. (1992). Pur-1, a zinc finger protein that binds to purine-rich sequences, transactivates an insulin promoter in heterologous cells. *Proc. Natl. Acad. Sci. USA* **89,** 11498-11502.

Kennedy, M., Firpo, M., Choi, K., Wall, C., Robertson, S., Kabrun, N., and Keller, G. (1997). A common precursor for primitive erythropoiesis and definitive haematopoiesis. *Nature* **386,** 488-493.

Khachigian, L. M., and Collins, T. (1997). Inducible expression of Egr-1-dependent genes. A paradigm of transcriptional activation in vascular endothelium. *Circ Res* **81,** 457-61.

Kimelman, D., and Griffin, J. (2000). Vertebrate mesendoderm induction and patterning. *Current Opinion in Genetics & Development* **10,** 350-356.

Kola, I., Brookes, S., Green, A. R., Garber, R., Tymms, M., Papas, T. S., and Seth, A. (1993). The Ets1 transcription factor is widely expressed during murine embryo development and is associated with mesodermal cells involved in morphogenetic processes such as organ formation. *Proc Natl Acad Sci U S A* **90,** 7588-92.

Koyano-Nakagawa, N., Nishida, J., Baldwin, D., Arai, K., and Yokota, T. (1994). Molecular cloning of a novel human cDNA encoding a zinc finger protein that binds to the interleukin-3 promoter. *Mol. Cell. Biol.* **14,** 5099-5107.

Kozak, M. (1987). At least six nucleotides preceding the AUG initiator codon enhance translation in mammalian cells. *J. Mol. Biol.* **196,** 947-950.

Kraut, N., Snider, L., Chen, C. M., Tapscott, S. J., and Groudine, M. (1998). Requirement of the mouse I-mfa gene for placental development and skeletal patterning. *Embo J* **17,** 6276-88.

Krebs, L. T., Xue, Y., Norton, C. R., Shutter, J. R., Maguire, M., Sundberg, J. P., Gallahan, D., Closson, V., Kitajewski, J., Callahan, R., Smith, G. H., Stark, K. L., and Gridley, T. (2000). Notch signaling is essential for vascular morphogenesis in mice. *Genes Dev* **14,** 1343-52.

Kubo, H., Fujiwara, T., Jussila, L., Hashi, H., Ogawa, M., Shimizu, K., Awane, M., Sakai, Y., Takabayashi, A., Alitalo, K., Yamaoka, Y., and Nishikawa, S. I. (2000). Involvement of vascular endothelial growth factor receptor-3 in maintenance of integrity of endothelial cell lining during tumor angiogenesis. *Blood* **96,** 546-53.

Kukk, E., Lymboussaki, A., Taira, S., Kaipainen, A., Jeltsch, M., Joukov, V., and Alitalo, K. (1996). VEGF-C receptor binding and pattern of expression with VEGFR-3 suggests a role in lymphatic vascular development. *Development* **122,** 3829-3837.

Kuo, C. T., Veselits, M. L., Barton, K. P., Lu, M. M., Clendenin, C., and Leiden, J. M. (1997). The LKLF transcription factor is required for normal tunica media formation and blood vessel stabilization during murine embryogenesis. *Genes Dev.* **11,** 2996-3006.

Kurihara, Y., Kurihara, H., Oda, H., Maemura, K., Nagai, R., Ishikawa, T., and Yazaki, Y. (1995). Aortic arch malformations and ventricular septal defect in mice deficient in endothelin-1. *J Clin Invest* **96,** 293-300.

Kurihara, Y., Kurihara, H., Suzuki, H., Kodama, T., Maemura, K., Nagai, R., Oda, H., Kuwaki, T., Cao, W. H., Kamada, N., and et al. (1994). Elevated blood pressure and craniofacial abnormalities in mice deficient in endothelin-1. *Nature* **368,** 703-10.

Larsson, J., Goumans, M. J., Sjostrand, L. J., van Rooijen, M. A., Ward, D., Leveen, P., Xu, X., ten Dijke, P., Mummery, C. L., and Karlsson, S. (2001). Abnormal angiogenesis but intact hematopoietic potential in TGF-beta type I receptor-deficient mice. *Embo J* **20,** 1663-73.

Lavia, P., Macleod, D., and Bird, A. (1987). Coincident start sites for divergent transcripts at a randomly selected CpG-rich island of mouse. *Embo J* **6,** 2773-9.

Leahy, A., Xiong, J.-W., Aufiero, B., Fallon, J. T., Taubman, M. B., and Stuhlmann, H. (2000). *Vezf1* is a novel marker for endothelial cells and is up-regulated in angiogenesis and arterial injury. *Submitted* .

Leahy, A., Xiong, J.-W., Aufiero, B., Fallon, J. T., Taubman, M. B., and Stuhlmann, H. (2001). *Vezf1* is a novel marker for endothelial cells and is up-regulated in angiogenesis and arterial injury. *Submitted* .

Leahy, A., Xiong, J.-W., Kuhnert, F., and Stuhlmann, H. (1999). Use of developmental marker genes to define temporal and spatial patterns of differentiation during embryoid body formation. *J. Exp. Zool.* **284**.

Lelievre, E., Lionneton, F., Soncin, F., and Vandenbunder, B. (2001). The Ets family contains transcriptional activators and repressors involved in angiogenesis. *Int J Biochem Cell Biol* **33,** 391-407.

Lenardo, M. J., and Baltimore, D. (1989). NF-kappa B: a pleiotropic mediator of inducible and tissue-specific gene control. *Cell* **58,** 227-9.

Lewis, F. (1905). The development of the lymphatic system in rabbits. *Am J Anat* **5,** 95-121.

Li, D. Y., Sorensen, L. K., Brooke, B. S., Urness, L. D., Davis, E. C., Taylor, D. G., Boak, B. B., and Wendel, D. P. (1999). Defective angiogenesis in mice lacking Endoglin. *Science* **284,** 1534-1537.

Liao, W., Bisgrove, B., Sawyer, H., Hug, B., Bell, B., Peters, K., Grunwld, D., and Stainier, D. (1997). The zebrafish gene cloche acts upstream of a flk-1 homologue to regulate endothelial cell differentiation. *Development* **124,** 381-389.

Lin, Q., Lu, J., Yanagisawa, H., Webb, R., Lyons, G. E., Richardson, J. A., and Olson, E. N. (1998). Requirement of the MADS-box transcription factor MEF2C for vascular development. *Development* **125,** 4565-4574.

Lindahl, P., Johansson, B. R., Leveen, P., and Betsholtz, C. (1997). Pericyte loss and microaneurysm formation in PDGF-B-deficient mice. *Science* **277,** 242-5.

Lindsay, E. A., Vitelli, F., Su, H., Morishima, M., Huynh, T., Pramparo, T., Jurecic, V., Ogunrinu, G., Sutherland, H. F., Scambler, P. J., Bradley, A., and Baldini, A. (2001). Tbx1 haploinsufficieny in the DiGeorge syndrome region causes aortic arch defects in mice. *Nature* **410,** 97-101.

Lints, T. J., Parsons, L. M., Hartley, L., Lyons, I., and Harvey, R. P. (1993). *Nkx-2.5*: a novel murine homeobox gene expressed in early heart progenitor cells and their myogenic descendants. *Development* **119,** 419-431.

Liu, Y., Wada, R., Yamashita, T., Mi, Y., Deng, C. X., Hobson, J. P., Rosenfeldt, H. M., Nava, V. E., Chae, S. S., Lee, M. J., Liu, C. H., Hla, T., Spiegel, S., and Proia, R. L. (2000). Edg-1, the G protein-coupled receptor for sphingosine-1-phosphate, is essential for vascular maturation. *J Clin Invest* **106,** 951-61.

Loughna, S., and Sato, T. N. (2001). A combinatorial role of angiopoietin-1 and orphan receptor TIE1 pathways in establishing vascular polarity during angiogenesis. *Mol Cell* **7,** 233-9.

Mackay, J. P., and Crossley, M. (1998). Zinc fingers are sticking together. *Trends Biochem Sci* **23,** 1-4.

Mahlapuu, M., Ormestad, M., Enerback, S., and Carlsson, P. (2001). The forkhead transcription factor Foxf1 is required for differentiation of extra-embryonic and lateral plate mesoderm. *Development* **128,** 155-166.

Maisonpierre, P. C., Suri, C., Jones, P. F., Bartunkova, S., Wiegand, S. J., Radziejewski, C., Compton, D., McClain, J., Aldrich, T. H., Papadopoulos, N., Daly, T. J., Davis, S., Sato, T. N., and Yancopoulos, G. D. (1997). Angiopoietin-2, a natural antagonist for Tie2 that disrupts in vivo angiogenesis. *Science* **277,** 55-60.

Makinen, T., Jussila, L., Veikkola, T., Karpanen, T., Kettunen, M. I., Pulkkanen, K. J., Kauppinen, R., Jackson, D. G., Kubo, H., Nishikawa, S., Yla-Herttuala, S., and Alitalo, K. (2001). Inhibition of lymphangiogenesis with resulting lymphedema in transgenic mice expressing soluble VEGF receptor-3. *Nat Med* **7,** 199-205.

Maltepe, E., Schmidt, J. V., Baunoch, D., Bradfield, C. A., and Simon, M. C. (1997). Abnormal angiogenesis and responses to glucose and oxygen deprivation in mice lacking the protein ARNT. *Nature* **386,** 403-407.

Marchese, C., Savin, E., Dragone, E., Carozzi, F., De Marchi, M., Campogrande, M., Dolfin, G. C., Pagliano, G., Viora, E., and Carbonara, A. (1985). Cystic hygroma: prenatal diagnosis and genetic counselling. *Prenat Diagn* **5,** 221-7.

Millauer, B., Wizigmann-Voos, S., Schnurch, H., Martinez, R., Moller, N. P. H., Risau, W., and Ullrich, A. (1993). High affinity VEGF binding and developmental expression suggest Flk-1 as a major regulator of vasculogenesis and angiogensis. *Cell* **72,** 835-846.

Miller, A. M. (1913). Histogenesis and morphogenesis of the thoracic duct in the chick; development of blood cells and their passage to the blood stream via the thoracic duct. *Am J Anat* **15,** 131-198.

Montarras, D., Chelly, J., Bober, E., Arnold, H., Ott, M. O., Gros, F., and Pinset, C. (1991). Developmental patterns in the expression of Myf5, MyoD, myogenin, and MRF4 during myogenesis. *New Biol* **3,** 592-600.

Morgan, B., Sun, L., Avitahl, N., Andrikopoulos, K., Ikeda, T., Gonzales, E., Wu, P., Neben, S., and Georgopoulos, K. (1997). Aiolos, a lymphoid restricted transcription factor that interacts with Ikaros to regulate lymphocyte differentiation. *Embo J* **16,** 2004-13.

Mortensen, R. M., Conner, D. A., Chao, S., Geisterfer-Lowrance, A. A., and Seidman, J. G. (1992). Production of homozygous mutant ES cells with a single targeting construct. *Mol Cell Biol* **12,** 2391-5.

Mucenski, M. L., McLain, K., Kier, A. B., Swerdlow, S. H., Schreiner, C. M., Miller, T. A., Pietryga, D. W., Scott, W. J., Jr., and Potter, S. S. (1991). A functional c-myb gene is required for normal murine fetal hepatic hematopoiesis. *Cell* **65,** 677-89.

Murray, P. (1932). The development in vitro of the blood of the early chick embryo. *Proc. Roy. Soc. London* **11,** 497-521.

Myers, C., Charboneau, A., and Boudreau, N. (2000). Homeobox B3 promotes capillary morphogenesis and angiogenesis. *J Cell Biol* **148,** 343-51.

Nagy, A., Gocza, E., Merentes Diaz, E., Prideaux, V. R., Ivanyi, E., Markkula, M., and Rossant, J. (1990). Embryonic stem cells alone are able to support fetal development in the mouse. *Development* **110,** 815-821.

Nakagawa, O., Nakagawa, M., Richardson, J. A., Olson, E. N., and Srivastava, D. (1999). HRT1, HRT2, and HRT3: a new subclass of bHLH transcription factors marking specific cardiac, somitic, and pharyngeal arch segments. *Dev Biol* **216,** 72-84.

Nishikawa, S. I., Fraser, S., Fujimoto, T., Endoh, M., Nishikawa, S., and Ogawa, M. (2000). All B cells are progeny of endothelial cells: a new perspective. *Immunol Rev* **175,** 112-9.

Nishikawa, S. I., Nishikawa, S., Hirashima, M., Matsuyoshi, N., and Kodama, H. (1998a). Progressive lineage analysis by cell sorting and culture identifies FLK1+VE-cadherin+

cells at a diverging point of endothelial and hemopoietic lineages. *Development* **125,** 1747-57.

Nishikawa, S. I., Nishikawa, S., Kawamoto, H., Yoshida, H., Kizumoto, M., Kataoka, H., and Katsura, Y. (1998b). In vitro generation of lymphohematopoietic cells from endothelial cells purified from murine embryos. *Immunity* **8,** 761-9.

O'Connell, K. A., and Edidin, M. (1990). A mouse lymphoid endothelial cell line immortalized by simian virus 40 binds lymphocytes and retains functional characteristics of normal endothelial cells. *J Immunol* **144,** 521-5.

Oda, N., Abe, M., and Sato, Y. (1999). ETS-1 converts endothelial cells to the angiogenic phenotype by inducing the expression of matrix metalloproteinases and integrin beta3. *J Cell Physiol* **178,** 121-32.

Ohara, O., Nagase, T., Ishikawa, K., Nakajima, D., Ohira, M., Seki, N., and Nomura, N. (1997). Construction and characterization of human brain cDNA libraries suitable for analysis of cDNA clones encoding relatively large proteins. *DNA Res* **4,** 53-9.

Oliver, G., Sosa-Pineda, B., Geisendorf, S., Spana, E. P., Doe, C. Q., and Gruss, P. (1993). Prox 1, a prospero-related homeobox gene expressed during mouse development. *Mech Dev* **44,** 3-16.

Orkin, S. H. (1992). GATA-binding transcription factors in hematopoietic cells. *Blood* **80,** 575-81.

Orlidge, A., and D'Amore, P. A. (1987). Inhibition of capillary endothelial cell growth by pericytes and smooth muscle cells. *J Cell Biol* **105,** 1455-62.

Oshima, M., Oshima, H., and Taketo, M. M. (1996). TGF-beta receptor type II deficiency results in defects of yolk sac hematopoiesis and vasculogenesis. *Dev. Biol.* **179,** 297-302.

Palis, J., Robertson, S., Kennedy, M., Wall, C., and Keller, G. (1999). Development of erythroid and myeloid progenitors in the yolk sac and embryo proper of the mouse. *Development* **126,** 5073-84.

Pardanaud, L., Luton, D., Prigent, M., Bourcheix, L., Catala, M., and Dieterlen-Lievre, J. (1996). Two distinct endothelial lineages in ontogeny, one of them related to hemopoiesis. *Development* **122,** 1363-1371.

Pardanaud, L. a. D.-L., F. (1999). Manipulation of the angiogenic/hematopoietic commitment in the avian embryo. *Development* **126,** 617-627.

Peng, J., Zhang, L., Drysdale, L., and Fong, G. H. (2000). The transcription factor EPAS-1/hypoxia-inducible factor 2alpha plays an important role in vascular remodeling. *Proc Natl Acad Sci U S A* **97,** 8386-91.

Pereira, F. A., Qiu, Y., Zhou, G., Tsai, M. J., and Tsai, S. Y. (1999). The orphan nuclear receptor COUP-TFII is required for angiogenesis and heart development. *Genes Dev* **13,** 1037-49.

Perkins, A. C., Sharpe, A. H., and Orkin, S. H. (1995). Lethal beta-thalassaemia in mice lacking the erythroid CACCC- transcription factor EKLF. *Nature* **375,** 318-22.

Perrotti, D., Melotti, P., Skorski, T., Casella, I., Peschle, C., and Calabretta, B. (1995). Overexpression of the zinc finger protein MZF1 inhibits hematopoietic development from embryonic stem cells: correlation with negative regulation of CD34 and c-myb promoter activity. *Mol Cell Biol* **15,** 6075-87.

Prevo, R., Banerji, S., Ferguson, D. J., Clasper, S., and Jackson, D. G. (2001). Mouse LYVE-1 is an endocytic receptor for hyaluronan in lymphatic endothelium. *J Biol Chem* **276,** 19420-30.

Puri, M. C., Rossant, J., Alitalo, K., Bernstein, A., and Partanen, J. (1995). The receptor tyrosine kinase TIE is required for integrity and survival of vascular endothelial cells. *EMBO J.* **14,** 5884-5891.

Quandt, K., Frech, K., Karas, H., Wingender, E., and Werner, T. (1995). MatInd and MatInspector: new fast and versatile tools for detection of consensus matches in nucleotide sequence data. *Nucleic Acids Res* **23,** 4878-84.

Quertermous, E. E., Hidai, H., Blanar, M. A., and Quertermous, T. (1994). Cloning and characterization of a basic helix-loop-helix protein expressed in early mesoderm and the developing somites. *Proc Natl Acad Sci U S A* **91,** 7066-70.

Risau, W. (1997). Mechanisms of angiogenesis. *Nature* **386,** 671-674.

Risau, W., and Flamme, I. (1995). Vasculogenesis. *Annu. Rev. Cell Dev biol.* **11,** 73-91.

Robertson, S. M., Kennedy, M., Shannon, J. M., and Keller, G. (2000). A transitional stage in the commitment of mesoderm to hematopoiesis requiring the transcription factor SCL/tal-1. *Development* **127,** 2447-59.

Robey, E. (1999). Regulation of T cell fate by Notch. *Annu Rev Immunol* **17,** 283-95.

Rogers, M. B., Hosler, B. A., and Gudas, L. J. (1991). Specific expression of a retinoic acid-regulated, zinc-finger gene, Rex- 1, in preimplantation embryos, trophoblast and spermatocytes. *Development* **113,** 815-24.

Ronicke, V., Risau, W., and Breier, G. (1996). Characterization of the endothelium-specific murine vascular endothelial growth factor receptor-2 (flk-1) promoter. *Circ. Res.* **79,** 277-285.

Rönicke, V., Risau, W., and Breier, G. (1996). Characterization of the endothelium-specific murine vascular endothelial growth factor receptor-2 (flk-1) promoter. *Circ. Res.* **79,** 277-285.

Ryan, H. E., Lo, J., and Johnson, R. S. (1998). HIF-1 alpha is required for solid tumor formation and embryonic vascularization. *Embo J* **17,** 3005-15.

Sabin, F. R. (1909). The lymphatic system in human embryos, with a consideration of the morphology of the system as a whole. *Am J Anat* **9,** 43-91.

Sambrook, J., Fritsch, E. F., and Maniatis, T. (1989). Molecular Cloning. *Cold Spring Harbor Laboratory Press* **2nd edition**.

Sato, T. M., Tozawa, Y., Deutsch, U., Wolburg-Buchholz, K., Fujiwara, Y., Gendron-Maguire, M., Gridley, T., Wolburg, H., Risau, W., and Qin, Y. (1995). Distinct roles of the receptor tyrosine kinases Tie-1 and Tie-2 in blood vessel formation. *Nature* **376,** 70-74.

Sato, T. N., Qin, Y., Kozak, C. A., and Audus, K. L. (1993). Tie-1 and tie-2 define another class of putative receptor tyrosine kinase genes expressed in early embryonic vascular system. *Proc Natl Acad Sci U S A* **90,** 9355-8.

Schaefer, B. C. (1995). Revolutions in rapid amplification of cDNA ends: new strategies for polymerase chain reaction cloning of full-length cDNA ends. *Anal Biochem* **227,** 255-73.

Schlaeger, T. M., Bartunkova, S., Lawitts, J. A., Teichmann, G., Risau, W., Deutsch, U., and Sato, T. N. (1997). Uniform vascular-endothelial-cell-specific gene expression in both embryonic and adult mice. *Proc. Natl. Acad. Sci. USA* **94,** 3058-3063.

Schlaeger, T. M., Qin, Y., Fujiwara, Y., Magram, J., and Sato, T. N. (1995). Vascular endothelial cell lineage-specific promoter in transgenic mice. *Development* **121,** 1089-1098.

Schneider, M., Othman-Hassan, K., Christ, B., and Wilting, J. (1999). Lymphangioblasts in the avian wing bud. *Dev Dyn* **216,** 311-9.

Schreiber, M., Wang, Z. Q., Jochum, W., Fetka, I., Elliott, C., and Wagner, E. F. (2000). Placental vascularisation requires the AP-1 component fra1. *Development* **127,** 4937-48.

Schuh, A. C., Faloon, P., Hu, Q. L., Bhimani, M., and Choi, K. (1999). In vitro hematopoietic and endothelial potential of flk-1(-/-) embryonic stem cells and embryos. *Proc Natl Acad Sci U S A* **96,** 2159-64.

Shalaby, F., Ho, J., Stanford, W. L., Fischer, K.-D., Schuh, A. C., Schwartz, L., Bernstein, A., and Rossant, J. (1997). A requirement for flk1 in primitive and definitive hematopoiesis and vasculogenesis. *Cell* **89,** 981-990.

Shalaby, F., Rossant, J., Yamaguchi, T. P., Gertsenstein, M., Wu, X., Breitman, M. L., and Schuh, A. C. (1995). Failure of blood-island formation and vasculogenesis in Flk-1-deficient mice. *Nature* **376,** 62-66.

Shirayoshi, Y., Yuasa, Y., Suzuki, T., Sugaya, K., Kawase, E., Ikemura, T., and Nakatsuji, N. (1997). Proto-oncogene of int-3, a mouse Notch homologue, is expressed in endothelial cells during early embryogenesis. *Genes Cells* **2,** 213-24.

Shivdasani, R., Mayer, E., and Orkin, S. (1995). Absence of blood formation in mice lacking the T-cell leukaemia oncoprotein tal-1/SCL. *Nature* **373,** 432-434.

Silverman, E. S., and Collins, T. (1999). Pathways of Egr-1-mediated gene transcription in vascular biology. *Am J Pathol* **154,** 665-70.

Sims, D. E. (1986). The pericyte--a review. *Tissue Cell* **18,** 153-74.

Smale, S. T. (1997). Transcription initiation from TATA-less promoters within eukaryotic protein-coding genes. *Biochim Biophys Acta* **1351,** 73-88.

Soker, S., Takashima, S., Miao, H. Q., Neufeld, G., and Klagsbrun, M. (1998). Neuropilin-1 is expressed by endothelial and tumor cells as an isoform- specific receptor for vascular endothelial growth factor. *Cell* **92,** 735-45.

Spyropoulos, D. D., Pharr, P. N., Lavenburg, K. R., Jackers, P., Papas, T. S., Ogawa, M., and Watson, D. K. (2000). Hemorrhage, impaired hematopoiesis, and lethality in mouse embryos carrying a targeted disruption of the Fli1 transcription factor. *Mol Cell Biol* **20,** 5643-52.

Steingrimsson, E., Tessarollo, L., Reid, S. W., Jenkins, N. A., and Copeland, N. G. (1998). The bHLH-Zip transcription factor Tfeb is essential for placental vascularization. *Development* **125,** 4607-16.

Sun, L., Liu, A., and Georgopoulos, K. (1996). Zinc finger-mediated protein interactions modulate Ikaros activity, a molecular control of lymphocyte development. *Embo J* **15,** 5358-69.

Sun, X., Xiong, J.-W., Lemons, D., English, M., Kuhnert, F., Licht, J., and Stuhlmann, H. (2001). VEZF1 is an endothelial transcription factor that binds to GC/CT-rich sequences in the IL-3, *flk-1* and *flt-1* promoter. *submitted to J.B.C* .

Suri, C., Jones, P. F., Patan, S., Barunkova, S., Maisonpierre, P. C., Davis, S., Sato, T. N., and Yancopoulos, G. D. (1996). Requisite role of angiopoietin-1, a ligand for the TIE2 receptor, during embryonic angiogensis. *Cell* **87,** 1171-1180.

Suri, C., McClain, J., Thurston, G., McDonald, D. M., Zhou, H., Oldmixon, E. H., Sato, T. N., and Yancopoulos, G. D. (1998). Increased vascularization in mice overexpressing Angiopoietin-1. *Science* **282,** 468-471.

Swiatek, P. J., Lindsell, C. E., del Amo, F. F., Weinmaster, G., and Gridley, T. (1994). Notch1 is essential for postimplantation development in mice. *Genes Dev* **8,** 707-19.

Takakura, N., Watanabe, T., Suenobu, S., Yamada, Y., Noda, T., Ito, Y., Satake, M., and Suda, T. (2000). A role for hematopoietic stem cells in promoting angiogenesis. *Cell* **102,** 199-209.

Tavian, M., Hallais, M., and Peault, B. (1999). Emergence of intraembryonic hematopoietic precursors in the pre-liver human embryo. *Development* **126,** 793-803.

Thomas, P. Q., Brown, A., and Beddington, R. S. P. (1998). *Hex*: a homeobox gene revealing peri-implantation asymmetry in the mouse embryo and an early transient marker of endothelial cell precursors. *Development* **125,** 85-94.

Threadgill, D. W., Dlugosz, A. A., Hansen, L. A., Tennenbaum, T., Lichti, U., Yee, D., LaMantia, C., Mourton, T., Herrup, K., Harris, R. C., and et al. (1995). Targeted disruption of mouse EGF receptor: effect of genetic background on mutant phenotype. *Science* **269,** 230-4.

Tian, H., Hammer, R. E., Matsumoto, A. M., Russell, D. W., and McKnight, S. L. (1998). The hypoxia-responsive transcription factor EPAS1 is essential for catecholamine homeostasis and protection against heart failure during embryonic development. *Genes Dev* **12,** 3320-4.

Tonegawa, A., Funayama, N., Ueno, N., and Takahashi, Y. (1997). Mesodermal subdivision along the mediolateral axis in chicken controlled by different concentrations of BMP-4. *Development* **124,** 1975-1984.

Tsai, F. Y., Keller, G., Kuo, F. C., Weiss, M., Chen, J., Rosenblatt, M., Alt, F. W., and Orkin, S. H. (1994). An early haematopoietic defect in mice lacking the transcription factor GATA-2. *Nature* **371,** 221-6.

Tupler, R., Perini, G., and Green, M. R. (2001). Expressing the human genome. *Nature* **409,** 832-3.

Urness, L. D., Sorensen, L. K., and Li, D. Y. (2000). Arteriovenous malformations in mice lacking activin receptor-like kinase-1. *Nat Genet* **26,** 328-31.

Uyttendaele, H., Ho, J., Rossant, J., and Kitajewski, J. (2001). Vascular patterning defects associated with expression of activated Notch4 in embryonic endothelium. *Proc Natl Acad Sci U S A* **98,** 5643-8.

Uyttendaele, H., Marazzi, G., Wu, G., Yan, Q., Sassoon, D., and Kitajewski, J. (1996). Notch4/int-3, a mammary proto-oncogene, is an endothelial cell-specific mammalian Notch gene. *Development* **122,** 2251-9.

van der Jagt, E. R. (1932). The origin and development of the anterior lymph sacs in the sea turtle (*Thalassochelys caretta*). *Q.J. Micr. Sci.* **75,** 151-165.

Veikkola, T., Jussila, L., Makinen, T., Karpanen, T., Jeltsch, M., Petrova, T. V., Kubo, H., Thurston, G., McDonald, D. M., Achen, M. G., Stacker, S. A., and Alitalo, K. (2001). Signalling via vascular endothelial growth factor receptor-3 is sufficient for lymphangiogenesis in transgenic mice. *Embo J* **20,** 1223-31.

Visvader, J. E., Fujiwara, Y., and Orkin, S. H. (1998). Unsuspetced role of for the T-cell leukemia protein SCL/tal-1 in vascular development. *Genes Dev.* **12,** 473-479.

Vittet, D., Prandini, M. H., Berthier, R., Schweitzer, A., Martin-Sisteron, H., Uzan, G., and Dejana, E. (1996). Embryonic stem cells differentiate in vitro to endothelial cells through successive maturation steps. *Blood* **88,** 3424-3421.

Vlaeminck-Guillem, V., Carrere, S., Dewitte, F., Stehelin, D., Desbiens, X., and Duterque-Coquillaud, M. (2000). The Ets family member Erg gene is expressed in mesodermal tissues and neural crests at fundamental steps during mouse embryogenesis. *Mech Dev* **91,** 331-5.

Wakiya, K., Begue, A., Stehelin, D., and Shibuya, M. (1996). A cAMP response element and an Ets motif are involved in the transcriptional regulation of flt-1 tyrosine kinase (vascular endothelial growth factor receptor 1) gene. *J Biol Chem* **271,** 30823-8.

Wang, H. U., Chen, Z.-F., and Anderson, D. J. (1998). Molecular distinction and angiogenic interaction between embryonic arteries and veins revealed by ephrin-B2 and its receptor Eph-B4. *Cell* **93,** 741-753.

Wang, L. C., Kuo, F., Fujiwara, Y., Gilliland, D. G., Golub, T. R., and Orkin, S. H. (1997). Yolk sac angiogenic defect and intra-embryonic apoptosis in mice lacking the Ets-related factor TEL. *EMBO J.* **16,** 4374-4383.

Wang, R., Clark, R., and Bautch, V. L. (1992). Embryonic stem cell-derived cystic embryoid bodies form vascular channels: an *in vitro* model of blood vessel development. *Development* **114,** 303-316.

Wang, W., and Lufkin, T. (2000). The murine Otp homeobox gene plays an essential role in the specification of neuronal cell lineages in the developing hypothalamus. *Dev Biol* **227,** 432-49.

Wigle, J. T., Chowdhury, K., Gruss, P., and Oliver, G. (1999). Prox1 function is crucial for mouse lens-fibre elongation. *Nat Genet* **21,** 318-22.

Wigle, J. T., and Oliver, G. (1999). Prox1 function is required for the development of the murine lymphatic system. *Cell* **98,** 769-78.

Wiles, M. V., and Keller, G. (1991). Multiple hematopoietic lineages develop from embryonic stem cells (ES) cells in culture. *Development* **111,** 259-267.

Wilting, J., and Christ, B. (1996). Embryonic angiogenesis: a review. *Naturwissenschaften* **83,** 158-163.

Wilting, J., Papoutsi, M., Othman-Hassan, K., Rodriguez-Niedenfuhr, M., Prols, F., Tomarev, S. I., and Eichmann, A. (2001). Development of the avian lymphatic system. *Microsc Res Tech* **55,** 81-91.

Witte, M. H., Way, D. L., Witte, C. L., and Bernas, M. (1997). Lymphangiogenesis: mechanisms, significance and clinical implications. *Exs* **79,** 65-112.

Xiong, J.-W., Battaglino, R., Leahy, A., and Stuhlmann, H. (1998). Large-scale screening for developmental genes in ES cells and embryoid bodies using retroviral entrapment vectors. *Dev. Dyn.* **212,** 181-197.

Xiong, J.-W., Leahy, A., Lee, H.-H., and Stuhlmann, H. (1999). *Vezf1*: a Zn finger transcription factor restricted to endothelial cells and their precursors. *Dev. Biol.* **206,** 123-141.

Xue, Y., Gao, X., Lindsell, C. E., Norton, C. R., Chang, B., Hicks, C., Gendron-Maguire, M., Rand, E. B., Weinmaster, G., and Gridley, T. (1999). Embryonic lethality and vascular defects in mice lacking the Notch ligand Jagged1. *Hum Mol Genet* **8,** 723-30.

Yamada, Y., Pannell, R., Forster, A., and Rabbitts, T. H. (2000). The oncogenic LIM-only transcription factor Lmo2 regulates angiogenesis but not vasculogenesis in mice. *Proc Natl Acad Sci U S A* **97,** 320-4.

Yamada, Y., Warren, A. J., Dobson, C., Forster, A., Pannell, R., and Rabbitts, T. H. (1998). The T cell leukemia LIM protein Lmo2 is necessary for adult mouse hematopoiesis. *Proc Natl Acad Sci U S A* **95,** 3890-5.

Yamagishi, H., Olson, E. N., and Srivastava, D. (2000). The basic helix-loop-helix transcription factor, dHAND, is required for vascular development. *J Clin Invest* **105,** 261-70.

Yamaguchi, T. P., Dumont, D. J., Conlon, R. A., Breitman, M. L., and Rossant, J. (1993). *flk-1*, an *flt*-related receptor tyrosine kinase is an early marker for endothelial cell precursors. *Development* **118,** 489-498.

Yamashita, J., Itoh, H., Hirashima, M., Ogawa, M., Nishikawa, S., Yurugi, T., Naito, M., and Nakao, K. (2000). Flk1-positive cells derived from embryonic stem cells serve as vascular progenitors. *Nature* **408,** 92-6.

Yancopoulos, G. D., Davis, S., Gale, N. W., Rudge, J. S., Wiegand, S. J., and Holash, J. (2000). Vascular-specific growth factors and blood vessel formation. *Nature* **407,** 242-8.

Yang, X., Castilla, L., Xu, X., Li, C., Gotay, J., Weinstein, M., Liu, P. P., and Deng, C.-X. (1999). Angiogenesis defects and mesenchymal apoptosis in mice lacking SMAD5. *Development* **126,** 1571-1580.

Yano, M., Iwama, A., Nishio, H., Suda, J., Takada, G., and Suda, T. (1997). Expression and function of murine receptor tyrosine kinases, TIE and TEK, in hamatopoietic stem cells. *Blood* **89,** 4317-4326.

Zhong, T. P., Childs, S., Leu, J. P., and Fishman, M. C. (2001). Gridlock signalling pathway fashions the first embryonic artery. *Nature* **414,** 216-20.

Zhong, T. P., Rosenberg, M., Mohideen, M. A., Weinstein, B., and Fishman, M. C. (2000). gridlock, an HLH gene required for assembly of the aorta in zebrafish. *Science* **287,** 1820-4.

Zhou, C., Tsai, S. Y., and Tsai, M. (2000). From apoptosis to angiogenesis: new insights into the roles of nuclear orphan receptors, chicken ovalbumin upstream promoter-transcription factors, during development. *Biochim Biophys Acta* **1470,** M63-8.

Zutter, M. M., Santoro, S. A., Painter, A. S., Tsung, Y. L., and Gafford, A. (1994). The human alpha 2 integrin gene promoter. Identification of positive and negative regulatory

elements important for cell-type and developmentally restricted gene expression. *J Biol Chem* **269,** 463-9.

6. APPENDIX

6.1 Abbreviations

A	adenine
Acvrl1	activin-receptor-like-kinase-1
Ang	angiopoietin
AP	alkaline phosphatase
dATP	deoxyadenosine-triphosphate
BAEC	bovine aortic endothelial cells
BFU-E	blast forming unit-erythroid
bHLH	basic helix-loop-helix
BMP	bone morphogenetic protein
bp	base pair
C	cytosine
C2H2	cysteine 2, histidine 2
CD	circular dichroism
cDNA	complementary DNA
cpm	counts per minute
dCTP	deoxycytidine-triphosphat
DAB	diaminobenzidine
Dll4	delta-like 4
DMEM	Dulbecco's modified Eagle medium
DNA	deoxyribonucleic acid
dpc	days post coitum
E	embryonic day
EB	embryoid body
EC	endothelial cell
EDTA	ethylenediaminetetraacetic acid
EKLF	erythroid Krüppel-like factor
ES cell	embryonic stem cell
EST	expressed sequence tag
FGF	fibroblast growth factor
FLK-1	fms-like kinase-1
G	guanine
GAPDH	glyceraldehydes-3-phosphate dehydrogenase
G-CSF	granulcyte colony stimulating factor
GM-CSF	granulocyte-macrophage colony stimulating factor
HBS	HEPES buffered saline
H+E	hematoxylin and eosin
HEPES	hydroxyethyl-piperazineethanesulfonic acid
HIF	hypoxia-inducible factor
IL-3	interleukin-3
IRES	internal ribosomal entry site
kb	kilobase
kDa	kilodalton
KL	c-kit ligand
KO	knock-out

LacZ	β-galactosidase gene
LIF	leukemia inhibitory factor
LKLF	lung Krüppel-like factor
Mac	macrophage
M-CSF	macrophage colony stimulating factor
MEF	myogenic enhancer factor
MMP	matrix metalloproteinase
mRNA	messenger RNA
NCBI	National Center for Biotechnology Information
neo	neomycin resistance gene
NR	non-redundant
nt	nucleotide
ORF	open reading frame
p	plasmid
P	phsophor
PBS	phosphate buffered saline
PC	pericyte
PCR	polymerase chain reaction
PDGF	platelet-derived growth factor
PDS	plasma-derived serum
PECAM	platelet-endothelial cell adhesion molecule
PFA	paraformaldehyde
PFHM-II	protein-free hybridoma medium
puro	puromycin resistance gene
RACE	rapid amplification of cDNA ends
RLM	RNA ligase mediated
RNA	ribonucleic acid
RT	reverse transcription
S	sulfur
SCL	stem cell leukemia
SDS	sodium dodecyl sulfate
SMβ-actin	smooth muscle β-actin
SSC	sodium saline citrate
SVEC	SV40-transformed endothelial cell line
T	thymine
TGF-β	transforming growth factor β
dUTP	deoxyuridine-triphosphate
UTR	untranscribed region
VEGF	vascular endothelial growth factor
VEGFR	vascular endothelial growth factor receptor
VEZF	vascular endothelia zinc finger
VSMC	vascular smooth muscle cells
wt	wild type
ZNF	zinc finger protein

6.2 Curriculum vitae

Persona data

Dipl. Biol. Frank Kuhnert

E-mail: fkuhnert@stanford.edu

Date of birth: 01.04.1969

Citizenship: German

Marital Status: single

Education

1975-1979	**Grundschule Benninghausen**
1979-1988	**Evangelisches Gymnasium Lippstadt**, Allgemeine Hochschulreife
1988-1989	**Military Service**
1989-1991	**University of Muenster**, Germany Undergraduate studies
1991-1995	**University of Braunschweig**, Germany Diploma in Biochemistry, Genetics, Microbiology Thesis Titel: Elimination of replication competent retroviruses by sequence specific recombination
1996-2001	**Mount Sinai School of Medicine,** New York Brookdale Center for Developmental Biology **The Scripps Research Institute,** La Jolla Department of Vascular Biology Ph.D. student in Dr. Heidi Stuhlmann's laboratory Thesis project: Functional Analysis of *Vezf1* during mouse development
2001-present	**Stanford University,** Department of Hematology, Research Associate in Dr. Calvin Kuo's laboratory

Training and Courses

1996	**Jackson Laboratory**, Bar Harbor, Maine Graduate Course in Experimental Mouse Genetics

Academic Awards

1995	DAAD Fellowship

6.3 Presentations and publications

Oral Presentations

Kuhnert, F., Campagnolo, L., and Stuhlmann, H. (2001). Functional Analysis of *Vezf1* during mouse development. Young Investigators Forum of the American Heart Association, Los Angeles

Abstracts

Kuhnert, F., Leahy, A., and Stuhlmann, H. (1997). Mis-expression analysis of *oct-3* during mammalian development. Mouse Molecular Genetics Meeting, EMBL Heidelberg

Leahy, A., Kuhnert, F., Xiong, J.-W., and Stuhlmann, H. (1998). Identification of developmental genes by *in vitro* pre-selection. Mouse Molecular Genetics Meeting, Cold Spring Harbor Laboratory, Cold Spring Harbor, New York

Kuhnert, F., Xiong, J.-W., Sun X, Leahy, A., Fallon J., Taubman M., Keller G., and Stuhlmann H. (2000). Vezf1: a novel endothelial-specific Zn finger gene that is required for fetal survival at birth. Keystone Symposium: Molecular Biology of the Cardiovascular System, Snowbird, Utah

Publications

Klehr-Wirth, D., Kuhnert, F., Unsinger, J. and Hauser, H. (1997). Generation of mammalian cells with conditional expression of *cre* recombinase, Elsevier Trends Journals Technical Tips Online. T40067.

Leahy, A., Xiong, J.-W., Kuhnert, F., and Stuhlmann, H. (1999). Use of developmental marker genes to define temporal and spatial patterns of differentiation during embryoid body formation. J. Exp. Zoology 284:67-81.

Kuhnert, F., Xiong, J.-W., Campagnolo, L., Lemons, D., and Stuhlmann, H. (2001). Vascular Malformations and loss of vessel integrity in mouse embryos deficient for *Vezf1*. Manuscript in preparation.

Kuhnert, F., LeVine, W., and Stuhlmann, H. (2001). Overexpression of *Vezf1* in the vascular endothelium induces hypervascularization, vascular malformations and CNS defects. Manuscript in preparation